ISSN 0494-7304 0132-053x

TARTU ÜLIKOOLI

TOIMETISED

УЧЕНЫЕ ЗАПИСКИ ТАРТУСКОГО УНИВЕРСИТЕТА

ACTA ET COMMENTATIONES UNIVERSITATIS TARTUENSIS

939

ON THE DESIGN OF NONELASTIC CONSTRUCT

Mehaanika-alaseid töid

TARTU 1992

TARTU ÜLIKOOLI TOIMETISED
ACTA ET COMMENTATIONES UNIVERSITATIS TARTUENSIS
Alustatud 1893.a. VIHIK 939

ON THE DESIGN OF NONELASTIC CONSTRUCT

Mehaanika-alaseid töid

TARTU 1992

Tartu Ülikooli toimetised.
Vihik 939.
ON THE DESIGN OF NONELASTIC CONSTRUCT.
Mehaanika-alaseid töid.
Tartu Ülikool.
EE2400 Tartu, Ülikooli 18.
Vastutav toimetaja K. Soonets.
Korrektor R. Valla.
T.07.7.75.T.233.300.
Hind rbl. 21.
TÜ trükikoda, EE2400 Tartu, Tiigi 78.

Acta Et Commentationes Universitatis Tartuensis. 939. 1992.

EDITORIAL

ON THE OCCASION OF PROFESSOR LEPIK'S 70th BIRTHDAY

Professor Ülo Lepik, an outstanding scientist in the theory of plasticity, plastic analysis of structures and optimization of non-elastic plates and shells, who was born on July 11, 1921 in Tartu, celebrated his 70th birthday last year.

Ülo Lepik attended the Hugo Treffner High School in Tartu and graduated from Tartu University in 1948. Still being a student of the university he delivered lectures for the younger students.

Ülo Lepik's scientific activity began at the end of the 1940 s. He defended the doctoral degree (Candidate of Physical and Mathematical Sciences) in 1952. In 1959 he received the higher doctoral degree (Doctor of Phys. and Math. Sc.) for a work devoted to the large deflections of elastic-plastic structures. The supervisor of his doctoral thesis was professor A.A. Iljushin from Moscow, well-known for his works in the theory of plasticity.

The academic career of Ülo Lepik is connected with Tartu University. Here he was made assistant professor in 1948, associate professor in 1954 and full professor in 1960. In 1959 - 1990 he was the head of the department of theoretical mechanics of Tartu University. During that period the department of theoretical mechanics organized seven conferences (summer-schools) for researchers of the Soviet Union on the optimization and non-elastic analysis of structures.

Professor Ülo Lepik's research is related to the plastic analysis of structures including the stability and dynamic analysis of elastic-plastic beams, plates and shells as well as large deflection analysis of rigid-plastic plates and shells. He has obtained many valuable results in the investigation of the dynamic behaviour of plastic structures. During last decades he has studied the optimization of non-elastic structures. Professor Lepik's results in the application of the Pontryagin's maximum principle for optimal design of rigid-plastic plates and shells has won a wide recognition. His monograph-book on optimal design of plastic structures subjected to the dynamic loading was published in 1982. Although the book was written in Russian, it is familiar to scientific circles.

So far, Professor Ü. Lepik has published more than 150 papers (excluding the abstracts of numerous reports of all-union and international conferences). He has supervised 12 scientists. One of his students has gained the higher doctoral degree.

Professor Ülo Lepik is a member of numerous scientific councils. He is a member of the Editorial Board of the journal "Structural Optimization". The lectures delivered by Professor Lepik on theoretical mechanics, mechanics of continuous media and higher mathematics are appreciated by the students. Students and colleagues consider his text-book on theoretical mechanics (co-authored with L. Roots) an excellent Estonian text-book.

Although he is very busy with teaching, research and many international cooperation projects Professor Ülo Lepik is a devoted husband, father and grandfather. He spends many weekends with his wife Aino at their summer house near Elva. Often his daughter Pila, sons Rein and Toivo join them.

On behalf of Professor Ülo Lepik's students, colleagues and friends from all over the world we wish him good health and many fruitful years.

Acta Et Commentationes Universitatis Tartuensis. 939. 1992.

OPTIMAL DESIGN OF DYNAMICALLY LOADED ANNULAR PLATES, CONSIDERING THE HARDENING OF MATERIAL

Juri Kirs
Tallinn Technical University

Abstract. In this paper the optimal design of annular plates considering the hardening of material is studied. Tresca yield condition and the associated deformation law are used. A number of cases are studied on the occasion of different cross-sections and different functions of thickness.

1. Introduction

The paper [1] was one of the first, where optimal design of circular plates was studied considering the hardening of material. A simply supported plate is subjected to uniform dynamic pressure load. This load rapidly decreases in the course of time according to exponential function. The Mises yield condition is used.

In paper [2] the full solution of optimal design of simply supported circular plates considering the hardening of material is presented. The Mises yield condition is used. A plate is subjected to uniform dynamic pressure load, which is varying in time according to the law of triangular impulse.

In paper [3] analogical problem in the case of a clamped circular plates is solved by the use of two different methods.

In paper [4] the piecewise-linear yield conditions have been used to solve the problem of optimal design of circular plates considering the hardening of material. Tresca yield condition is accompanied by the non-associated deformation law; the rhombwise yield condition – by the associated deformation law.

2. Formulation of the problem and derivation of basic equation

Let us consider an annular plate of inner radius r_a, outer radius R and thickness $2H$. Outer boundary is simply supported, inner is free. A plate is subjected to uniform dynamic pressure load p, which is monotonously decreasing in time according to the law of triangular impulse, it means

$$p = \begin{cases} p_0(1 - \tau/\tau_1), & \text{if } 0 \leqslant \tau \leqslant \tau_1, \\ 0, & \text{if } \tau_1 \leqslant \tau \leqslant \tau_f, \end{cases} \qquad (2.1)$$

where τ – time, p_0 – prescribed constant.

The motion of the plate is divided into two phases, in general. During the first phase the plate is loaded with dynamic pressure load p, which is decreasing in time by the linear law (2.1) till the moment of time τ_1, when the load p will be equal to zero. Further movement of the plate takes place during the second phase $\tau > \tau_1$ because of inertia. The movement of the plate will stop at the moment $\tau = \tau_f$. However, the movement can stop already during the first phase, if $0 \leqslant \tau \leqslant \tau_1$.

The purpose is to determine the thickness of the plate $2H$ (depending upon radial coordinate r) in such a way, that the residual deflections by the inner boundary were as small as possible. Here we must take into consideration a preliminary condition – the whole volume of the plate V_0 is prescribed. A lot of different projects are compared and 4 groups of plates are studied: 1) thickness of the plate is limited from below $H \geqslant H_0$; 2) thickness is limited from above $H \leqslant H_m$; 3) thickness is limited from both sides $H_0 \leqslant H \leqslant H_m$; 4) thickness of the plate is not limited at all. In these cases H_0 and H_m are prescribed constants.

We shall use the cylindrical coordinates r, φ and z. The starting point of the coordinates is in the center of the plate on the prolongation of the median surface. Axis Oz is directed downwards. We shall denote $\sigma_r = \sigma_1$ and $\sigma_\varphi = \sigma_2$. We shall take into consideration only plastic deformations and confine ourselves to small deflections. Besides – we shall assume, that displacement along r–axis $u = 0$.

The basic equation for isotropic hardening in the case of piecewise–linear yield conditions is deduced in paper [4]. The starting point in that paper is the following interrelation between the plastic work A_p and intensity of shift stresses T, namely

$$A_p = \frac{T^2}{B_p \sigma_{so}} + C_0, \qquad (2.2)$$

where B_p – prescribed constant, describing the hardening of the material, σ_{so} – the yield–point of the material at the

beginning, C_0 – constant, which will be determined by means of initial conditions. From the yield condition can be deduced in general

$$\sigma_2 = c_1\sigma_1 + c_2\sigma_s \operatorname{sign} z, \tag{2.3}$$

where σ_s – the yield-point of material at an arbitrary moment of time, c_1 and c_2 – prescribed constants. The rate of plastic work is

$$\dot{A}_p = \sigma_1\dot{e}_1 + \sigma_2\dot{e}_2, \tag{2.4}$$

where $\dot{e}_1$ and $\dot{e}_2$ are rates of strain components. In this equation we substitute stress σ_2 from the formula (2.3) taking into consideration, that $\dot{e}_1 = z\dot{\varkappa}_1$ and $\dot{e}_2 = z\dot{\varkappa}_2$, where $\dot{\varkappa}_1$ and $\dot{\varkappa}_2$ are the rates of curvatures. Now it is not difficult to deduce from formulae (2.2) and (2.4) a differential equation. After solving it one obtains

$$\sigma_s = \sigma_{so}\left\{1 + 2B_p z\left[G(\varkappa_1 + c_1\varkappa_2) + c_2\varkappa_2\right]\operatorname{sign} z\right\}. \tag{2.5}$$

This is the basic equation for isotropic hardening, where the function $G(r)$ is defined by the formula

$$\sigma_1 = G\sigma_s \operatorname{sign} z. \tag{2.6}$$

From equation (2.5) one easily obtains

$$M_s = \sigma_{so}H^2 + \tfrac{4}{3}B_p\sigma_{so}H^3\left\{G(\varkappa_1 + c_1\varkappa_2) + c_2\varkappa_2\right\}, \tag{2.7}$$

where M_s is the maximum value for bending yield moments. One can learn about it more thoroughly in paper [4].

3. System of equations of the problem

According to Tresca yield condition in this case we have $M_2 = M_s$ and therefore in formulae (2.3), (2.5) and (2.7) must $c_1 = 0$ and $c_2 = 1$. From the associated deformation law one can conclude, that $\varkappa_1 = 0$. Taking these circumstances into account the limit bending moment for annular plate is

$$M_s = \sigma_{so}H^2\left[1 + \tfrac{4}{3}B_pH\varkappa_2\right]. \tag{3.1}$$

Let us remind, that in this case the inner boundary of the plate is free and outer is simply supported.

To solve the problem of optimal design the method of mode motions is used. According to this the deflection W is

$$W = F_1(r)\,\Phi_1(\tau). \tag{3.2}$$

From the associated deformation law follows

$$r_1 = \frac{R - r}{R - r_a}. \tag{3.3}$$

It is convenient to use following dimensionless quantities:

$$h = \frac{H}{H_0}, \qquad x = \frac{r}{R}, \qquad a = \frac{r_a}{R}, \qquad t = \frac{\tau}{\tau_1},$$

$$m_{1,2} = \frac{M_{1,2}}{\sigma_{s0}H_0^2}, \qquad m_s = \frac{M_s}{\sigma_{s0}H_0^2}, \qquad n_q = \frac{Q_1 R}{\sigma_{s0}H_0^2}, \tag{3.4}$$

$$q = \frac{pR^2}{\sigma_{s0}H_0^2}, \qquad \nu_{1,2} = \frac{\varkappa_{1,2}R^2}{H_0\,\varphi}, \qquad V = \frac{V_0}{2\pi R^2 H_0},$$

$$w = \frac{W}{H_0}, \qquad \alpha = \frac{4B_D H_0^2}{3R^2}, \qquad k = \frac{\mu R^2}{\sigma_{s0}\tau_1^2},$$

where $2H_0$ – either prescribed minimal admissible thickness of the plate or simply some sort of prescribed characteristic thickness; τ_1 – moment of time when the load becomes equal to zero (see formula 1.1); $M_{1,2}$ – bending moments in the radial and circumferential directions; Q_1 – shear force; $\nu_{1,2}$ – non-dimensional curvatures; V_0 – prescribed whole volume of the plate; μ – density; α – parameter describing the degree of hardening; k – non-dimensional parameter of the plate.

Now equations of motions take the form

$$\left(xm_1\right)' = m_2 + xn_q, \qquad xn_q = \int_a^x (2k\bar{\varphi}hf - q)x\,dx. \tag{3.5}$$

Here and later on dots denote differentiation with respect to non-dimensional time t, apostrophe denote differentiation with respect to x.

Non-dimensional deflection is

$$w = f(x)\,\varphi(t), \tag{3.6}$$

$$f(x) = \frac{1 - x}{1 - a}. \tag{3.7}$$

Yield condition takes the form

$$m_2 = m_s, \tag{3.8}$$

$$m_s = h^2\left[1 + \alpha\varphi h\nu_2\right] = h^2 + \frac{\alpha\varphi h^3}{x(1 - a)}. \tag{3.9}$$

Finally – non-dimensional load is

$$q = q_0(1 - t). \tag{3.10}$$

To equations (3.5)–(3.10) one must add additional condition

dictated by prescribed volume of the plate. From it proceeds

$$V = 2\int_a^1 xh\,dx. \qquad (3.11)$$

Formulae (3.5)–(3.11) form the system of basic equations of this problem. It remains to define the thickness of the plate h as a function of coordinate x in such a way, that it should consist unknown parameters. These parameters are determined after solving the system (3.5)–(3.11) through minimization of residual deflection by the inner boundary of the plate. As follows from formulae (3.6) and (3.7) the function one must minimize is

$$F_m = w\left[x = a, t = t_f\right] = \varphi(t_f). \qquad (3.12)$$

4.Choice of function h(x) and solving of basic system of equations

Let us consider annular plates of 6 different shapes.

1.shape(Fig.1.1). Thickness of the plate h(x) is defined by the following equation

$$h = b_0 + b_1x + b_2x^2 + b_3x^3, \qquad (4.1)$$

where $a \leqslant x \leqslant 1$. In this case thickness h(x) is limited from below, it means $h \geqslant 1$ all over the plate. No limit from above exists, therefore thickness by the inner boundary of plate $h_a = h(a)$ is not limited from above.

Between 4 parameters b_0, b_1, b_2 and b_3 we have only one interrelation, it follows from the equation (3.11). Consequently there are 3 independent parameters. But in practice it is more convenient to do the calculations using the parameters $h_a = h(a)$, $h_1 = h(1)$ and b_3 as independent ones. It follows from the calculations at once, that in the case of optimal project (minimal residual deflections) we have always $h_1 = 1$. So, actually, there are only 2 independent parameters – h_a and b_3. Computer determined them minimizing the function F_m (3.12). The profile of the plate in this case is depicted in Fig.1 under number 1.

2.shape(Fig.1.2). Thickness of the plate is

$$h = c + \frac{b}{x} \qquad (4.2)$$

and it is valid all over the plate. There are no limits to the thickness of the plate, nor from above neither from below. The only restriction is $h \geqslant 0$. Between 2 parameters c

and b there is only 1 interrelation (3.11). Therefore we have

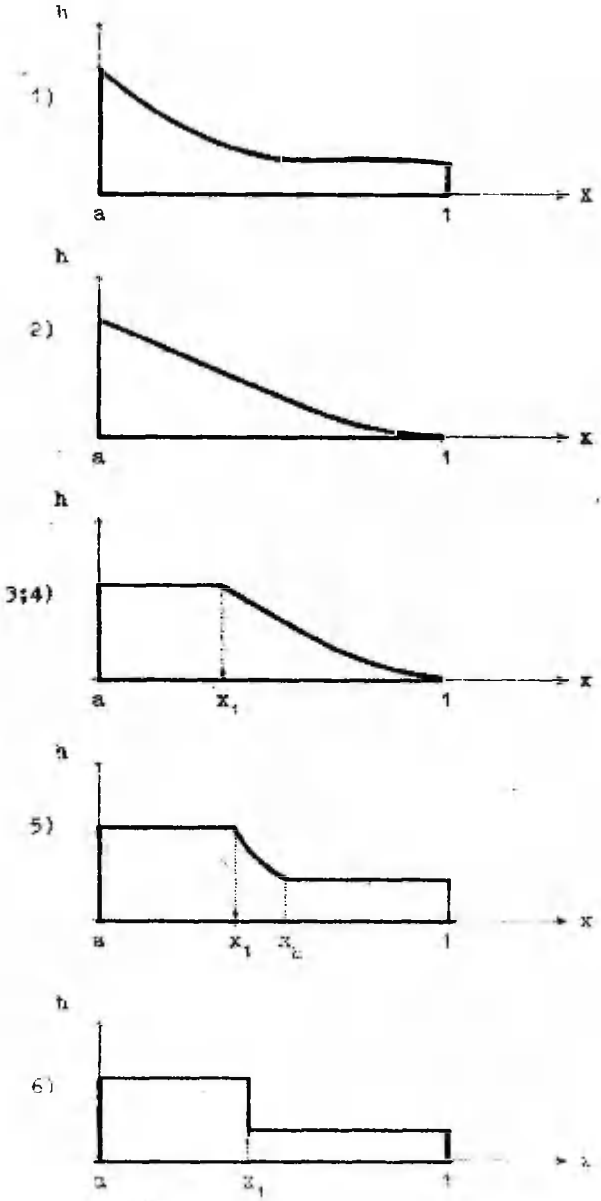

Fig. 1

here only 1 independent parameter. It is expedient to use h_1 as independent one. It followed from calculations, that in the case of optimal project $h_1 = 0$. The profile of this plate is depicted in Fig. 1 under number 2.

3.shape(Fig.1.3). Thickness of the plate is

$$h = \begin{cases} h_m = h_{max}, & \text{if } a \leqslant x \leqslant x_1, \\ c + \dfrac{b}{x}, & \text{if } x_1 \leqslant x \leqslant 1. \end{cases} \tag{4.3}$$

In this case the thickness of the plate is limited from above, it means $h \leqslant h_m$ all over the plate, where h_m is prescribed constant. From below we have $h \geqslant 0$. For 3 parameters x_1, b and c here there are 2 equations: 1) condition (3.11) and 2) interrelation $h_m = c + b/x_1$. Independent parameter is h_1. Again – in the case of optimal project $h_1 = 0$. The profile of the plate is depicted in Fig. 1 under number 3.

4.shape(Fig.1.4). Thickness of the plate is

$$h = \begin{cases} h_m = h_{max}, & \text{if } a \leqslant x \leqslant x_1, \\ b_0 + b_1 x + b_2 x^2, & \text{if } x_1 \leqslant x \leqslant 1. \end{cases} \tag{4.4}$$

Function h(x) must here satisfy inequalities $0 \leqslant h \leqslant h_m$. Between parameters b_0, b_1, b_2 and x_1 three interrelations exist: 1) constraint (3.11); 2) condition $h_m = b_0 + b_1 x_1 + b_2 x_1^2$ and 3) $h_1 = 0$. Here the last condition is prescribed, otherwise thickness h in some intermediate point will be zero. An independent parameter is x_1. This shape of the plate is in Fig. 1.4.

5.shape(Fig.1.5). Thickness of the plate is

$$h = \begin{cases} h_m = h_{max}, & \text{if } a \leqslant x \leqslant x_1, \\ b_0 + b_1 x + b_2 x^2, & \text{if } x_1 \leqslant x \leqslant x_2, \\ 1, & \text{if } x_2 \leqslant x \leqslant 1. \end{cases} \tag{4.5}$$

Thickness h(x) must satisfy condition $1 \leqslant h \leqslant h_m$. Between 5 parameters b_0, b_1, b_2, x_1 and x_2 we have 3 interrelations: 1) $h_m = b_0 + b_1 x_1 + b_2 x_1^2$; 2) $1 = b_0 + b_1 x_2 + b_2 x_2^2$; 3) condition (3.11). Independent parameters are x_1 and x_2. The profile of the plate in this case is depicted in Fig. 1.5. As followed from the calculations, the intermediate interval $(x_1; x_2)$ is very small. The results should become better if $x_2 \to x_1$. The circumstance, that nevertheless $x_1 \neq x_2$ is due to

calculating procedure, rounding of values and specification of the computer.

6.shape (Fig.1.6). Thickness of the plate is

$$h = \begin{cases} h_m, & \text{if } a \leq x \leq x_1, \\ 1, & \text{if } x_1 \leq x \leq 1. \end{cases} \tag{4.6}$$

Function $h(x)$ must here satisfy condition $1 \leq h \leq h_m$. We don't have here an independent parameter, because $h_1 = 1$ is prescribed. This shape of plate is depicted in Fig. 1.6.

Now solving of the system (3.5)–(3.11) follows. Let us start from the equations (3.5) and substitute there function $f(x)$ from (3.7), expression of bending moment m_2 from (3.8) and (3.9), and from formula (3.10) the load $q(t)$. After this we take necessary expression of thickness $h(x)$ from among equations (4.1)–(4.6) and integrate equations obtained. So we get expression of bending moment m_1. Constant of integration can be determined from condition $m_1(a) = 0$. If the plate is divided into different regions as regard thickness, then by going from one region to another the continuity conditions must be satisfied. From the expression obtained proceeds by the aid of condition $m_1(1) = 0$ differential equation for determination of function $\varphi(t)$. All this process must be gone through 6 times, using in turn all the formulae of thickness (4.1)–(4.6). There is nothing difficult in principle in this process, only the amount of technical work is great. All these transformations and equations take so many place that to write it all down here is impossible.

So resuming all this – we obtain 6 differential equations for determination of functions $\varphi(t)$. Yet all of them are quite alike. General form of these differential equations is

$$\ddot{\varphi} + A^2\varphi = B + Q(1 - t). \tag{4.7}$$

Differences are only in constants A,B and Q, which actually are long expressions. In solving this quite simple differential equation we use initial conditions $\varphi(0)=\dot{\varphi}(0)=0$ and the conditions of continuity. Outcomes in all 6 cases are similar :

During the I phase if $0 \leq t \leq 1$ and $q \neq 0$:

$$\varphi_1 = \frac{Q}{A^2}\left\{L(1 - \cos At) + \frac{1}{A}(\sin At - At)\right\}, \tag{4.8}$$

$$\dot{\varphi}_1 = \frac{Q}{A^2}\left\{AL\ \sin At + \cos At - 1\right\}, \qquad (4.9)$$

where

$$L = 1 + \frac{B}{Q}. \qquad (4.10)$$

During the II phase if $1 \leq t \leq t_f$ and $q = 0$ (then $Q = 0$):

$$\varphi_2 = \frac{Q}{A^3}\left\{AL(1 - \cos At) + \sin(A - At) + \sin At - A\right\}, \qquad (4.11)$$

$$\dot{\varphi}_2 = \frac{Q}{A^2}\left\{AL\ \sin At + \cos At - \cos(A - At)\right\}. \qquad (4.12)$$

From formulae (4.8)–(4.11) it is easy to derive expressions of final time t_f and minimizing function $F_m = \varphi(t_f)$. So one obtains:

a) if movement of the plate will end already during the I phase, then

$$t_f = \frac{2}{A}\arctan(AL), \qquad (4.13) \qquad F_m = \frac{Q}{A^2}(2L - t_f), \qquad (4.14)$$

where $t_f \leq 1$;

b) if movement of the plate will end during the II phase:

$$t_f = \begin{cases} \frac{1}{A}\arctan N, & \text{if } N > 0, \\ \frac{1}{A}(\pi + \arctan N), & \text{if } N < 0, \end{cases} \qquad (4.15)$$

where

$$N = \frac{1 - \cos A}{\sin A - AL} \qquad (4.16)$$

and where $t_f > 1$. If in the second case the final time t_f is determined by the formula (4.15), then the value of minimizing function F_m one can easily calculate from equation (4.11) because here $F_m = \varphi(t_f)$.

It only remains to give formulae for the coefficients A,B, and Q for each shape of the plate. To spare the room the corresponding equations only for shape 2 and 3 are written down here.

In the case of shape 2:

$$A^2 = \frac{6\alpha A_1}{kA_2 s^3}, \qquad B = \frac{6A_3}{kA_2 s^2}, \qquad Q = \frac{q_0(1 + 2a)}{kA_2},$$

where

$$A_1 = 3bc^2u_1 - c^3\ln(a) + 1.5b^2cu_2 + \frac{b^3u_3}{3},$$

$$A_2 = c(1 + 3a) + 4b,$$

$$A_3 = 2bc\ \ln(a) - b^2u_1 - c^2s,$$

$$s = 1 - a, \qquad u_1 = -1 + \frac{1}{a}, \qquad u_2 = -1 + \frac{1}{a^2},$$

$$u_3 = -1 + \frac{1}{a^3}, \qquad b = \frac{V - (1 - a^2)h_1}{(1 - a)^2}, \qquad c = h_1 - b.$$

In the case of shape 3:

$$k^2 = \frac{\alpha(A_1 + A_2)}{k(A_5 + A_6)}, \qquad B = \frac{B_1(1 - a)}{k(A_5 + A_6)}, \qquad Q = \frac{B_2q_0(1 - a)}{6k(A_5 + A_6)},$$

where

$$A_1 = h_m^3\ \ln(x_1/a) - c^3\ln(x_1),$$

$$A_2 = 3bc\left\{\frac{cu_1}{x_1} + \frac{b_2}{2x_1^2}\right\} + \frac{b^3u_3}{3x_1^3},$$

$$A_3 = 3(x_1 + a) - 2(x_1^2 + ax_1 + a^2),$$

$$A_4 = 2(1 - a)(x_1 + 2a) - v(x_1 + a),$$

$$A_5 = \frac{vh_m}{3}\left[u_1A_3 + 0.5\ A_4v\right] + \frac{c}{6}\left[4au_1 - u_4\right],$$

$$A_6 = b(u_2 - 2au_1) + \frac{1}{3}(c - b)\left[u_3 - 3a^2u_1\right],$$

$$B_1 = 2bc\ \ln(x_1)\ \frac{b^2u_1}{x_1} - h_m^2v - c^2u_1,$$

$$B_2 = u_3 - 3a^2u_1 + v^2(x_1 + 2a),$$

$$u_1 = 1 - x_1, \quad u_2 = 1 - x_1^2, \quad u_3 = 1 - x_1^3,$$

$$u_4 = 1 - x_1^4, \quad v = x_1 - a, \quad b = h_1 - c,$$

$$x_1 = \frac{V + h_ma^2 - h_1}{h_m - h_1}, \qquad c = \frac{h_1 - h_mx_1}{1 - x_1},$$

Corresponding equations are very long for shapes 1,4 and 5.

4.Discussion

To illustrate the theory a lot of numerical examples were solved. A program was made where prescribed parameters are V,

k, q_0, a, α and for the shapes 3–6 h_m also. The program consists loops, where the values of free parameters are changed in prescribed limits by prescribed steps. For example in the case of shape 1 we have a triple loop: b_3 (the outer one), h_a and h_i. In every single case the values of final time t_f and function F_m are calculated. In the calculating process the computer remembers all necessary quantities, which correspond to the value of function F_m, minimal by that time.

Let us consider the annular plate where $V = 1.25$; $q_0 = 120$; $k = 5$; $a = 0.4$. In Fig. 2 the dependence of minimizing function F_m upon the parameter α for all 6 shapes of the plate is depicted. To remind – α is a parameter describing the amount of hardening of material. In these calculations in the case of shapes 3–6 $h_m = 2.5$. The numbers in the Fig. 2 indicate the number of shape of the plate (see Fig.1). Some conclusions and remarks as follows:

a)As we see in Fig. 2 – the minimal values of function F_m we have in the case of shape 2. Shapes 1 and 2 (see Fig.1 – 1 and 2) are similar due to the fact that thickness by inner boundary h(a) is not limited. As we see – the shape 2 is much better than shape 1. This conclusion is valid for all calculations. Besides – to derive necessary equations in the case of shape 2 is much easier. Therefore – we should always prefer the shape 2 to the shape 1.

b)Shapes 3 and 4 are very similar (Fig.1 – 3 and 4). The difference between them is only in region $x_1 \leq x \leq 1$ and it is very small. More precisely – in this region we have in the case of shape 3: $h = c + b/x$ and shape 4: $h = b_0 + b_1 x + b_2 x^2$. In both cases thickness is limited only from above. Here we can also draw a conclusion that hyperbolical shape 3 is much better than polynomial shape 4.

c)Shapes 5 and 6 (see Fig.1 – 5 and 6) almost coincide, while shape 6 is a little better than shape 5. But if one takes into consideration a great deal of technical work one has to do to derive the equations of shape 5, then the conclusion is – shape 6 is much better than shape 5.

d)Comparing shapes 2 and 3 – as we see in Fig. 2, the shape 2 is better than shape 3 (the values of function F_m in the case of shape 2 are smaller). But on the other hand – thickness at inner boundary h(a) in the case of shape 2 is not limited. It has quite a great value and might have more

if, for example, to enlarge the value of parameter $\bar{V}$ a little. Thickness h(a) is often too great and such details in mechanisms are very troublesome. Therefore we should prefer shape 3 to shape 2.

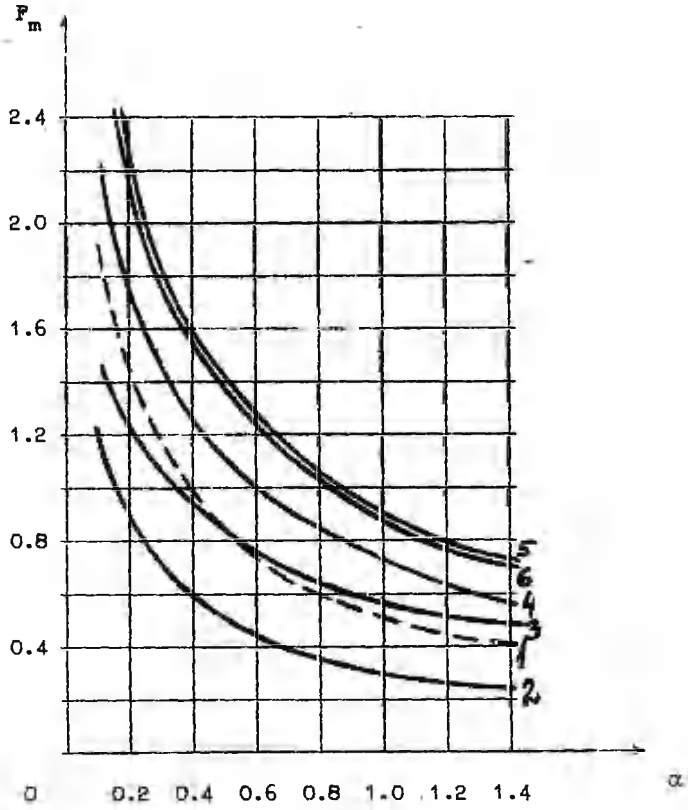

Fig. 2

e)Optimal design of annular plates is also studied in paper [5]. Although the formulation of the problem there is quite different, the results are very interesting. For example – as follows by Fig. 1 (page 44 in paper [5]) the shape of the plate in case 1 is quite similar to the shapes 3 and 4 in this paper.

f)In table 1 for $\bar{V} = 1.25$, $k = 5$, $q = 120$, $a = 0.4$, $\alpha = 0.2$ the results of calculations of following quantities are presented: function F_m, final time t_f, maximum thickness h_m

and parameters h(a), h_1, x_1 for all cases of shapes of the plate. In tables 2 and 3 the values of coefficients of thickness-function h(x) are presented in this numerical example.

Table 1

	shape 1	shape 2	shape 3	shape 4	shape 5	shape 6
F_m	1.4560	0.8601	1.2086	1.7565	2.1970	2.1713
t_f	1.0840	0.9619	1.5543	1.2300	1.3040	1.2958
h_m	——	——	2.5	2.5	2.5	2.5
h(a)	4.8100	5.2083	h_m	h_m	h_m	h_m
h_1	1	0	0	0	1	1
x_1	——	——	0.6600	0.7130	x_1 0.635 x_2 0.680	0.6580

Table 2

	shape 2	shape 3
c	-3.472222	-4.852942
b	3.472222	4.852942

Table 3

	shape 1	shape 4	shape 5
b_0	27.68465	29.95973	4.17182
b_1	-95.02524	-59.76189	51.44577
b_2	112.10061	29.80216	-64.47083
b_3	-43.76000	—	—

g)In table 4 for V = 1.25, k = 5, q_0= 120, a = 0.4, h_1= 0 the values of function F_m depending on the parameters α and h_m in the case of shape 3 are presented. Let it be reminded that when we use non-dimensional quantities (see formulae (3.4)) then H_0 is some prescribed characteristic thickness of plate. In the case of shape 3 it is not a maximum thickness H_m, but some sort of fictitious thickness. Let us assume that H_0 has equal values in all shapes.

The calculations have shown that the deflections and the value of function F_m will decrease if to enlarge the maximum thickness h_m. So by increasing h_m shape 3 will near shape 2. Which value of maximum thickness h_m one has to choose exactly – it depends upon the purpose and character of the detail.

3

Table 4

α	F_m * shape 3		
	h_m= 2.0	h_m= 2.5	h_m= 3.0
0.1	1.9758	1.5044	1.2662
0.2	1.5968	1.2086	1.0061
0.3	1.3791	1.0376	0.8556
0.4	1.2308	0.9205	0.7523
0.5	1.1204	0.8330	0.6749
0.6	1.0335	0.7639	0.6137
0.7	0.9626	0.7072	0.5636
0.8	0.9031	0.6596	0.5216
0.9	0.8521	0.6186	0.4859
1.0	0.8077	0.5828	0.4551
x_1	0.7850	0.6600	0.57667
c	-7.30233	-4.85294	-4.08661
b	7.30233	4.85294	4.08661

h)In table 5 for V = 1.25, k = 5, q_0 = 120, h_m = 3, h_1 = 0, α = 0.5 the values of function F_m, parameter x_1 and coefficients b and c are presented depending on the size of the aperture of the plate in the case of shape 3.

Table 5

a	shape 3			
	F_m	x_1	b	c
0.2	0.6616	0.45667	2.521472	
0.3	0.7175	0.50667	3.081081	
0.4	0.6749	0.57667	4.086614	c = -b
0.5	0.5339	0.66667	6.000000	
0.6	0.3276	0.77667	10.432837	

1)In table 6 for V = 1.25, k = 5, q_0 = 120, h_1 = 0, α = 0.5 the analogical values in the case of shape 2 are presented.

To investigate this problem very many numerical examples were solved, but because of the lack of paper we confine ourselves to above-given ones.

In conclusion - in the case of annular plates it turns out that the hyperbolical thickness-function h(x) is the most effective, both in sense of optimality and simplicity of

derivation of equations.

Table 6

a	shape 2			
	F_m	h(a)	b	c
0.2	0.2072	7.8125	1.953125	
0.3	0.4164	5.9524	2.551020	
0.4	0.4978	5.2083	3.472222	c = -b
0.5	0.4163	5.0000	5.000000	
0.6	0.2266	5.2083	7.812500	

References

1. Кирс Ю., Кенк К., Оптимальное проектирование равномерно нагруженной круговой пластины. Уч. зап. Тартуск. ун-та, 1985, 721, 83-87.
2. Кирс Ю., Оптимальная форма упрочняющейся круговой пластины при динамическом нагружении. Прикладные проблемы прочности и пластичности, Горький, 1988, 72-79.
3. Кирс Ю., Оптимальное проектирование круговых упрочняющихся пластин, заделанных по краю. Уч. зап. Тартуск. ун-та, 1988, 799, 97-120.
4. Кирс Ю., Оптимизация динамически нагруженных упрочняющихся пластин в случае некоторых кусочно-линейных условий пластичности. Уч. зап. Тартуск. ун-та, 1989, 853, 118-136.
5. Леллеп Я., Маяк Ю., Оптимальное проектирование жёстко пластических кольцевых пластин при условий пластичности Мизеса. Уч. зап. Тартуск. ун-та, 1989, 853, 38-48.

ОПТИМАЛЬНОЕ ПРОЕКТИРОВАНИЕ ДИНАМИЧЕСКИ НАГРУЖЕННЫХ КОЛЬЦЕВЫХ УПРОЧНЯЮЩИХСЯ ПЛАСТИН

Юрий Кирс

Таллинский технический университет

Резюме

Решается задача оптимального проектирования кольцевых пластин учитывая изотропное упрочнение материала пластины. Пластина шарнирно закреплена по внешней границе и свободная по внутренней. Используется условие пластичности Треска и ассоциированный закон течения. Найдена толщина пластины в зависимости от радиальной координаты таким образом, чтобы конечные прогибы пластины были минимальными. Учитывается и добавочное условие - так как объем пластины задан. Рассматривается 6 типов пластины.

Acta Et Commentationes Universitatis Tartuensis, 939, 1992

OPTIMAL DESIGN OF DYNAMICALLY LOADED RIGID-PLASTIC STEPPED CIRCULAR PLATES

Andrus Salupere
Tallinn Technical University

Abstract. Rigid-plastic stepped circular plates under dynamic pressure load are considered. Tresca yield condition is used. An exact solution for calculating final deflections is worked out. Such plate dimensions are sought for which the plate of constant volume attains the minimal final deflection.

Notation

a, R, h_1, h_2 - plate dimensions (Fig.1)
Q^* - shear force
Q - dimensionless shear force
M_r^* - radial bending moment
M_1 - dimenslonless radial bending moment
M_t^* - circumferential bending moment
M_2 - dimensionless circumferential bending moment
M_k - maximum value of bending moments in the rigid region
p^* - uniform pressure load
p - dimenslonless uniform pressure load
r - radial coordinate
x - dimenslonless radial coordinate
α, γ - dimenslonless parameters for plate (6)
V - plate volume
Δ - dimensionless plate volume
M_0^* - yield moment
σ_0 - yield stress
p_0^* - load carrying capacity
w^* - deflection
w - dimensionless deflection
w_f - dimenslonless final deflection
$\dot{w}^*$ - deflection rate
v, $\dot{w}$ - dimensionless deflection rate
$\ddot{w}^*$ - acceleration
$\dot{v}$, $\ddot{w}$ - dimenslonless acceleration
α^0, γ^0 - optimal parameters, which correspond to the minimum value of the w_f

s_i - radius of circle between different plastic stages

ρ - density

μ - $\rho V/\pi R^2$

$(')$ - $\frac{\partial}{\partial x}$

$(\dot{})$ - $\frac{\partial}{\partial \tau}$

1. Introduction

The problem of dynamically loaded uniform circular plates was first studied by Hopkins and Prager [1]. Youngdahl [4] found an exact solution for a uniform plate in case of the pressure load function having general shape. He examined the influence of the pulse shape on the final deflections. Mazalov and Nemirovski [4] considered circular plates with rigid central part. Soonets and Vainikko [5] solved dynamic problems for stepped circular plates under medium pressure load, which has a constant value in interval (0,t). Lepik and Mróz [2] and Lepik [3] considered impulsively loaded stepped circular plates.

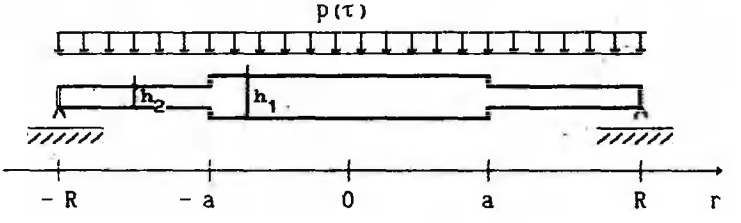

Fig. 1

The aim of this paper is to find the exact solution for the problem of dynamically loaded simply supported two-stepped circular plates. The pressure load function $p(\tau)$ has a general shape (Fig.3). Assuming the plate has a constant volume, optimal parameters for which the final central deflection has the minimum value are to be found.

2. The method of solution

We shall consider rigid-plastic simply supported thin circular plates with piecewise constant thickness (Fig.1). The yield condition is assumed in the form of Tresca hexagon (Fig.2). The associated flow rule is used. The yield moments

(Fig.2) are

$$M^*_{01} = \frac{\sigma_0 h_1^2}{4}, \qquad (1) \qquad M^*_{02} = \frac{\sigma_0 h_2^2}{4}. \qquad (2)$$

The plate equations have the form

$$\frac{\partial(rQ^*)}{\partial r} = -\left(rp^* - \mu\frac{\partial^2 w^*}{\partial t^2}\right), \qquad (3) \qquad \frac{\partial(rM_r^*)}{\partial r} = M_t^* + rQ^*. \qquad (4)$$

A dynamic load varies in time by the rule

$$p^* = \begin{cases} b\, e^{-ct}\sin \omega t, & \text{for } 0 \le t \le T, \\ 0, & \text{for } t > T. \end{cases} \qquad (5)$$

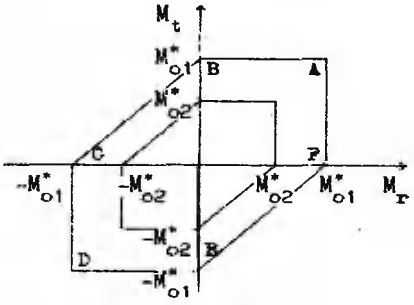

Fig. 2

Now we shall introduce the following dimensionless quantities

$$x = \frac{r}{R}, \quad \alpha = \frac{a}{R}, \quad \gamma = \frac{h_2}{h_1}, \quad M = \frac{4M^*}{\sigma_0 h_1^2}, \quad Q = \frac{4RQ^*}{\sigma_0 h_1^2},$$

$$w = \frac{2\pi\rho R^4 w^*}{3\sigma_0 VT^2}, \quad p = \frac{2\pi^2 R^6 p^*}{3\sigma_0 V^2}, \quad \Delta = \gamma + \alpha^2(1-\gamma), \quad \tau = \frac{t}{T}, \qquad (6)$$

where

$$V = \pi R^2 h_1 \Delta. \qquad (7)$$

Since the volume V is specified, we have

$$h_1 = \frac{V}{\pi R^2 \Delta}, \qquad h_2 = \frac{V\gamma}{\pi R^2 \Delta}. \qquad (8)$$

Making use of (6) and (7), formulas (3) and (4) acquire the following form:

$$(xQ)' = -6x\,(\Delta^2 p - h(x)\Delta\ddot{w}), \qquad (9)$$

$$(xM_1)' = M_2 + xQ, \qquad (10)$$

where

$$h(x) = \begin{cases} 1 & \text{for } 0 \le x < \alpha, \\ \gamma & \text{for } \alpha \le x \le 1, \end{cases} \tag{11}$$

and yield moment

$$M_0 = \begin{cases} 1 & \text{for } 0 \le x < \alpha, \\ \gamma^2 & \text{for } \alpha < x \le 1. \end{cases} \tag{12}$$

After transition to the dimensionless time τ constants b, c and ω in (5) acquire the concrete content:

$$b = p^*_{max} \frac{\exp\left[\dfrac{\pi\tau_*}{\tan(\pi\tau_*)}\right]}{\sin(\pi\tau_*)}, \tag{13}$$

$$c = \frac{\pi}{\tan(\pi\tau_*)}, \qquad \omega = \pi, \tag{14}$$

where τ_* corresponds to p^*_{max} and according to experiment $\tau_* = 0.2$. Thus (5) takes the form

$$p^* = \begin{cases} b\, e^{-c\tau} \sin \pi\tau, & \text{for } 0 \le \tau \le 1, \\ 0, & \text{for } \tau > 1. \end{cases} \tag{15}$$

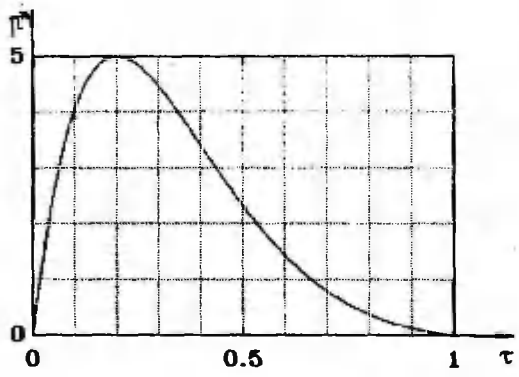

Fig. 3

In Fig.3 the pressure load function is represented for $p^*_{max} = 5$.

As we know, for $p < p_0$ the plate is rigid, but if $p \ge p_0$, the plastic flow starts and $n - 1$ circular and annular regions originate there, each in different plastic stage. Let us denote by s_i the radius of the circle between different plastic stages ($s_1 = 0, \ldots, s_n = 1$). A side or a vertex of the Tresca hexagon corresponds to each region. Any regions

may stay in the rigid stage. For rigid regions moments M_1 and M_2 are located inside the Tresca hexagon. Circles s_1 may be stationary, i.e., $\dot{s}_1 = 0$, or unstationary, i.e., $\dot{s}_1 \neq 0$. Some of circles s_1 are plastic hinges. Below possible combinations of the plastic stages are named as cases. Formulas for accelerations, lower boundary p^l and upper boundary p^u for each case are found. The case can take place if $p^l \leq p \leq p^u$. Deflections can be obtained by integrating the acceleration formulas twice.

Case 1. A stationary plastic hinge is in the center of the plate (Fig.4). For acceleration we have the formula

$$\ddot{w} = \dot{v}_1 (1 - x). \tag{16}$$

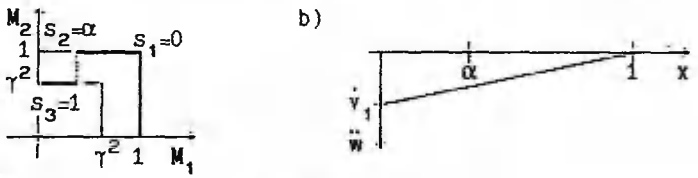

Fig. 4

Now we shall integrate (9) and (10), making use of (16). The boundary condition $M_1(1) = 0$ gives

$$\dot{v}_1 = \frac{\Delta^2 p - \alpha - \gamma^2(1 - \alpha)}{\Delta A1}, \tag{17}$$

where

$$A1 = \alpha^2(3 - 4\alpha + 1.5\alpha^2)(1 - \gamma) + 0.5\gamma. \tag{18}$$

We must have $M_1(\alpha) \leq \gamma^2$ (Fig.4). From this condition we have

$$p_a = \frac{[\alpha + \gamma^2(1 - \alpha)]\alpha^2(1 - 0.5\alpha) - (1 - \gamma^2)A1}{\Delta^2\alpha^2(1 - 0.5\alpha - A1)}. \tag{19}$$

If $p = p_a$, a stationary plastic hinge will originate in the section $s_2 = \alpha$.

The bending moment M_1 must attain the maximum value, if $x = 0$. Therefore we must have $M_1(0) = 0$ and $\dot{M}_1(0) \leq 0$. We have $M_1(0) \equiv 0$, and the condition $\dot{M}_1(0) = 0$ gives

$$p_m = \frac{\alpha + \gamma^2(1 - \alpha)}{\Delta^2(1 - A1)}. \tag{20}$$

If $p = p_m$, the stationary hinge s_1 becomes into unstationary. The lower boundary p_1^l for case 1 is the load carrying capacity p_0, if $\tau \leq 0.2$ and $p_1^l = 0$, if $\tau > 0.2$. The upper boundary

$$p_1^u = \min(p_a, p_m). \tag{21}$$

Case 2. A stationary plastic hinge is in the section $x = \alpha$. The central part of the plate is in the rigid stage (Fig.5). Now we have for acceleration the following expression:

$$\ddot{w} = \begin{cases} \dot{v}_1 & \text{for } 0 \le x \le \alpha, \\ \dot{v}_1 \dfrac{1-x}{1-\alpha} & \text{for } \alpha \le x \le 1. \end{cases} \tag{22}$$

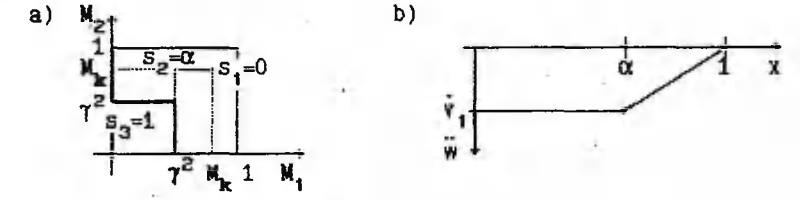

Fig. 5

Let us integrate (9) and (10) using (22). From the boundary conditions $M_1(\alpha) = \gamma^2$ and $M_1(1) = 0$ we get

$$\dot{v}_1 = \frac{\Delta^2 p(1-\alpha^3) - \gamma^2}{A2}, \tag{23}$$

where

$$A2 = \Delta(1-\alpha)[3\alpha^2 + 0.5\gamma(1-\alpha)(1+3\alpha)], \tag{24}$$

$$M_k = \gamma^2 + (\Delta p - \dot{v}_1)\Delta\alpha^2. \tag{25}$$

For case 2 we have conditions $\gamma^2 \le M_k \le 1$ and $M_1'(\alpha_+) \ge 0$. It appears that conditions $M_k = \gamma^2$ and $M_1'(\alpha_+) = 0$ coincide and they give the upper boundary

$$p_2^u = \frac{\gamma^2}{\Delta^2(1-\alpha)^2[1+2\alpha-0.5\gamma(1+3\alpha)]} \tag{26}$$

for case 2. For the lower boundary we have the condition $M_k = 1$ and

$$p_2^l = \frac{\Delta\alpha^2\gamma^2 - (1-\gamma^2)A2}{\Delta^2(1-\alpha^2-\alpha^3)}. \tag{27}$$

If $p = p_2^l$, a stationary hinge in the section $x = 0$ originates, but if $p = p_2^u$, the stationary hinge in the section $x = \alpha$ becomes unstationary.

Case 3. There are stationary hinges in the sections $x = 0$ and $x = \alpha$ (Fig.6). In this case the acceleration field has the form

$$\ddot{w} = \begin{cases} \dfrac{\dot{v}_1(\alpha - x) + \dot{v}_2 x}{\alpha} & \text{for } 0 \le x \le \alpha, \\ \dot{v}_2 \dfrac{1 - x}{1 - \alpha} & \text{for } \alpha \le x \le 1. \end{cases} \tag{28}$$

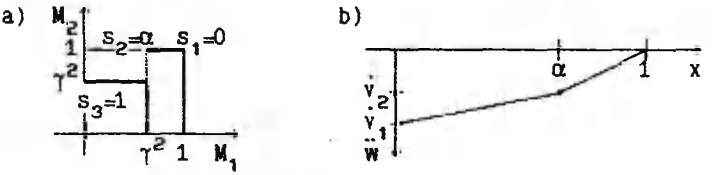

Fig. 6

To get expressions for $\dot{v}_1$ and $\dot{v}_2$ we have to substitute (28) into (9) and (10) and integrate them. The boundary conditions $M_1(\alpha) = \gamma^2$ and $M_1(1) = 0$ give

$$\dot{v}_2 = pA4 + A5, \tag{29}$$

$$\dot{v}_1 = pA6 + A7, \tag{30}$$

where

$$A3 = \Delta(1 - \alpha)[\alpha^2 + 0.5\gamma(1 - \alpha)(1 + 3\alpha)], \tag{31}$$

$$A4 = \Delta^2(1 - 2\alpha^2 + \alpha^3)/A3, \tag{32}$$

$$A5 = [2(1 - \alpha + \alpha\gamma^2) - 3\gamma^2]/A3, \tag{33}$$

$$A6 = 2\Delta - A4, \tag{34}$$

$$A7 = -2(1 - \gamma^2)/\Delta\alpha^2 - A5. \tag{35}$$

For case 3 the condition of the deflection rate field having to be convex applies. By checking this condition for each value of p, we get the lower and the upper boundaries.

Case 4 can take place after case 1 and only if $p_m < p_a$. If $p(\tau_4) = p_1^u$, a unstationary hinge $0 < s_2 < \alpha$ will originate. Here τ_4 is the starting moment of case 4. Distribution of moments and deflection rate for this case are shown in Fig.7. The vertex A of the Tresca hexagon corresponds to $s_1 \le x < s_2$. Thus $Q(x) = 0$ and

$$\ddot{w} = \Delta p. \tag{36}$$

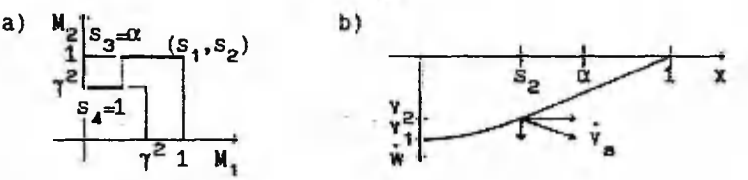

Fig. 7

For $s_2 < x \le 1$ the deflection rate field is expressed as

$$\dot{w} = v_2 \frac{1 - x}{1 - s_2}. \tag{37}$$

After differentiation we have

$$\ddot{w} = \dot{v}_s(1 - x), \tag{38}$$

where

$$\dot{v}_s = \frac{d}{d\tau}\left[\frac{v_2}{1 - s_2}\right]. \tag{39}$$

We shall integrate (9) and (10) by making use (39). From the boundary condition $M_1(1) = 0$ we get

$$\dot{v}_s = \frac{\Delta^2 p(1 - s_2^2 + 2s_2^3) - \alpha - \gamma^2(1 - \alpha)}{A9}, \tag{40}$$

where

$$A9 = \Delta[\alpha^2(3 - 4\alpha + 1.5\alpha^2)(1 - \gamma) +$$

$$+ 0.5\gamma - s_2^2(3 - 4s_2 + 1.5s_2^2)].$$

In the region $s_2 \le x \le 1$, the moment M_1 must have the maximum value, if $x = s_2$. Since $M_1(s_2) \equiv 0$, we use the condition $\dot{M}_1(s_2) = 0$ and we get

$$\dot{v}_s\,(1 - s_2) - \Delta p = 0. \tag{41}$$

Using (40) the above expression gives us the equation

$$\Delta^2 p[(1 - s_2)^3(1 + 2s_2) - \alpha^2(3 - 4\alpha + 1.5\alpha^2)(1 - \gamma) - \tag{42}$$

$$- 0.5\gamma + s_2^2(3 - 4s_2 + 1.5s_2^2)] - (1 - s_2)[\alpha + \gamma^2(1 - \alpha)] = 0$$

for calculation s_2.

According to (36), for $0 \le x < s_2$,

$$\dot{w}(x,\tau) = \Delta\int_{\tau_4}^{\tau} p(\tau)d\tau + \Phi(x). \tag{43}$$

Function $\Phi(x)$ can be found from the condition of continuity for deflection rate, i.e.,

$$\dot{w}(s_2-) = \dot{w}(s_2+). \tag{44}$$

Taking into account (39) and (41), we get

$$v_2(\tau) = [1 - s_2(\tau)]\left[\dot{w}(0,\tau_4) + \Delta\int_{\tau_4}^{\tau} \frac{p(\tau)}{1 - s_2(\tau)}d\tau\right]. \tag{45}$$

If we take $x = s_2$ for (43), then $\dot{w}(s_2,\tau) = v_2(\tau)$ and

$$\Phi(s_2) = [1 - s_2(\tau)]\left[\dot{w}(0,\tau_4) + \Delta\int_{\tau_4}^{\tau(s_2)} \frac{p(\tau)}{1 - s_2(\tau)}d\tau\right] -$$
$$- \Delta\int_{\tau_4}^{\tau(s_2)} p(\tau)d\tau, \qquad (46)$$

where $\tau(s_2)$ is the moment when the radius of the plastic hinge is s_2. It is possible to demonstrate, proceeding from (42), that $\dot{s}_2$ and $\dot{p}$ have the same sign. Therefore $\dot{s}_2 > 0$ for $\tau < 0.2$ and $\dot{s}_2 < 0$ for $\tau > 0.2$. Hence we have to use formulas (42)-(46) for $\tau \le 0.2$. If $\tau > 0.2$, the plastic hinge moves into the region, which corresponds to the vertex A of the Tresca hexagon and we have got (40) for calculating $\dot{v}$ and formula

$$\dot{s}_2 = \frac{(1 - s_2)[\dot{v}_s(1 - s_2) - \Delta p]}{\Delta\int_{\tau_2}^{\tau} p(\tau)d\tau + \Phi(s_2)}, \qquad (47)$$

for calculating velocity of the plastic hinge. It is easy to solve the system of differential equations (40),(47) by the Runge-Kutta method. This case disappears, when $s_2 = 0$ again.

Case 5 can start after case 2, if we have $p(\tau) > p_2^{II}$. In Fig.8 the distribution of moments and deflection rate are represented. It is possible to demonstrate that we can not construct feasible distribution of moments M_1 and M_2, which does not include side FA of the Tresca hexagon.

For $0 \le x < \alpha$, the plate is in the rigid stage and $\dot{w}(0) = \dot{w}(\alpha)$. Region $\alpha \le x \le s_3$ corresponds to the side FA of the Tresca hexagon and $\dot{w}' = 0$ in this region, according to the associated flow rule. Therefore we have $\dot{w}(0) = \dot{w}(s_3)$ and also $\ddot{w}(0) = \ddot{w}(s_3)$. For M_1 (25) is valid as in the case 2. Equations (9) and (10) with the boundary condition $M_2(s_3) = \gamma^2$ give

$$\dot{v}_1 = \frac{\Delta p s_3^2}{\alpha^2(1 - \gamma) + \gamma s_3^2}. \qquad (48)$$

For $s_3 \le x \le 1$ we get for deflection rate and accelerations the following expressions

$$\dot{w} = v_1\frac{1 - x}{1 - s_3} \qquad (49), \qquad \ddot{w} = \dot{v}_s(1 - x), \qquad (50)$$

where

$$\dot{v}_s = \frac{d}{d\tau}\left(\frac{v_1}{1 - s_3}\right). \qquad (51)$$

After integrating (9) and (10) by using (51), we find from the boundary condition $M_1(1) = 0$, that

$$\dot{v}_s = \frac{2[\Delta^2 p(1 - s_3)^2(1 + 2s_3) - \gamma^2]}{\Delta\gamma(1 - s_3)^3(1 + 3\,s_3)}. \tag{52}$$

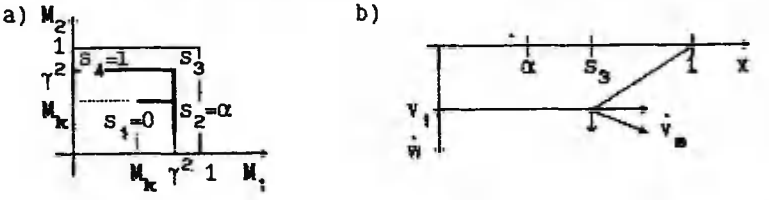

Fig. 8

In the observed region moment M_1 must attain the maximum value if $x = s_3$. It appears that we have $M_1(s_3) \equiv 0$ and $M_1'(s_3) < 0$ for each $s_3 > \alpha$. Thus we do not get an algebraic equation for s_3 as in the case 4. Now we shall find from (51) after differentiation

$$\dot{s}_3 = \frac{1 - s_3}{v_1}[\dot{v}_s(1 - s_3) - \dot{v}_1]. \tag{53}$$

The system of differential equations (48),(52),(53) is solved by the Runge-Kutta method.

By the plate continuity condition, moment M_2 may have discontinuity in the section $x = \alpha$, but by the rule of plastic flow the distribution of moments M_1 and M_2 must be dislocated inside or on sides and vertexes of the Tresca hexagon. Therefore, we have the condition $M_2(\alpha) \geq 0$ and we have to check it for each value of p. If we have $M_2(\alpha) < 0$, then the current case is not valid and we must consider distribution of moments M_1 and M_2 which includes the side EF of the Tresca hexagon.

3. Numerical results

The problem is solved for four values of the parameter p_{max} : 2, 3, 5 and 10. Ranges for parameters α and γ are the following: $0 \leq \alpha \leq 1$ and $0.1 \leq \gamma \leq 1$. Values $\alpha = 0$, $\alpha = 1$ and $\gamma = 1$ correspond to the uniform plate.

In Table 1, the optimal parameters α^0 and γ^0, corresponding to the minimum value of the final central deflection w_f^0, the final central deflection for a uniform plate and ratio w_f^u / w_f^0 are given for four values of p_{max}.

Table 1

p_{max}	α^o	γ^o	w_f^o	w_f^u	w_f^u / w_f^o
2	0.84	0.600	0.099	0.282	2.85
3	0.85	0.583	0.423	0.958	2.26
5	0.90	0.483	1.649	3.214	1.95
10	0.90	0.483	7.915	13.96	1.76

In Fig.9 and Fig.10 one can find in which region, which cases and in which order are realized. Numbers of the regions have the following meaning : region 1 - only case 1, region 2 - cases 1->3->1, region 3 - cases 1->3->2->3->1, region 4 - cases 2->3->1, region 5 - only case 2, region 6 - cases 1->4->1, region 7 - cases 2->5->2, region 8 - there are no solution because in case 5 $M_2(\alpha) < 0$. For $p_{max}= 5$ and $p_{max}= 10$ we can get analogical figures, only regions 6, 7 and 8 are wider and the other regions are narrower. For $p_{max}= 10$ we can establish three new very narrow regions : 9. for cases 1->3->2->5->2->3->1, 10. for cases 1->3->2->5->3->1 and 11. for cases 2->5->3->1. Therefore, there are at least 11 different solutions for two-stepped circular plates. It appears that the final deflection has the minimum value on the bound between regions 3 and 4.

In Fig.11-14 we can find the optimal parameters α^o and γ^o, i.e., the values for parameters α and γ which correspond to the minimum value of the final deflection w_f. In Fig.11 and 13 regions where the final central deflection for stepped plates w_f^s is less than the final central deflection for uniform plates w_f^u are represented. Step between isolines is

$$\Delta w = 0.2(w_f^u - w_f^o), \tag{54}$$

where

$$w_f^o = \min_{\alpha,\gamma} (w_f^s). \tag{55}$$

In Fig.12 and 14 regions, where

$$w_f^o \le w_f^s \le 1.05 w_f^o \tag{56}$$

are represented. For $p_{max} = 2$ and $p_{max} = 5$ we can get analogical figures.

4. Conclusions

An exact solution for calculating the final deflections for dynamically loaded simply supported two-stepped circular plates is worked out. Numerical data for the optimal parameters are given. It follows from this data that the final

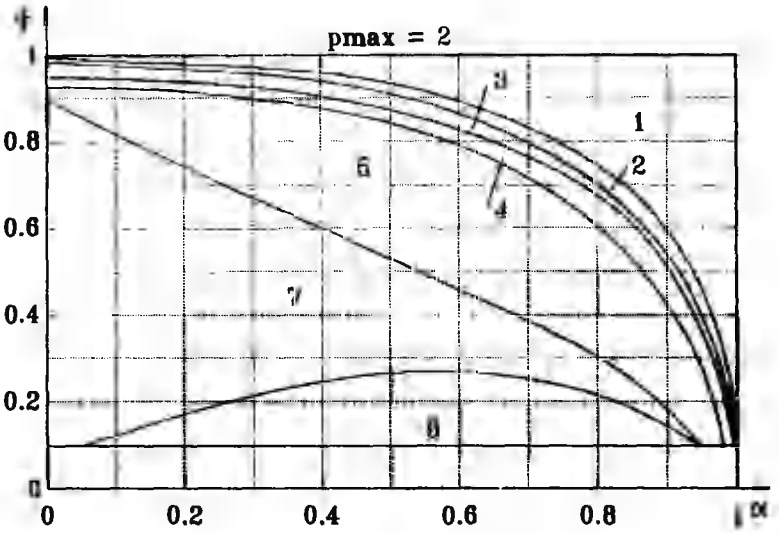

Fig. 9

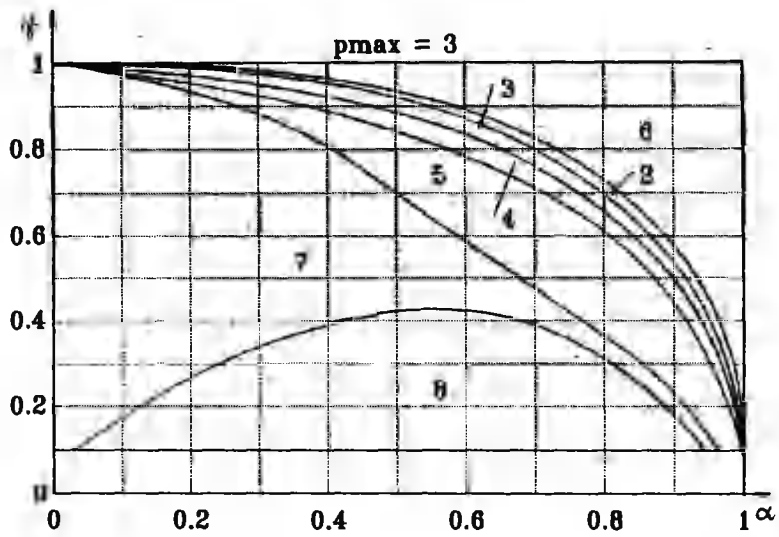

Fig. 10

central deflection for two-stepped circular plate can be decreased 1.76 to 2.85 times, comparing with the plate of uniform thickness. If p_{max} Increases, the percentage of economy decreases.

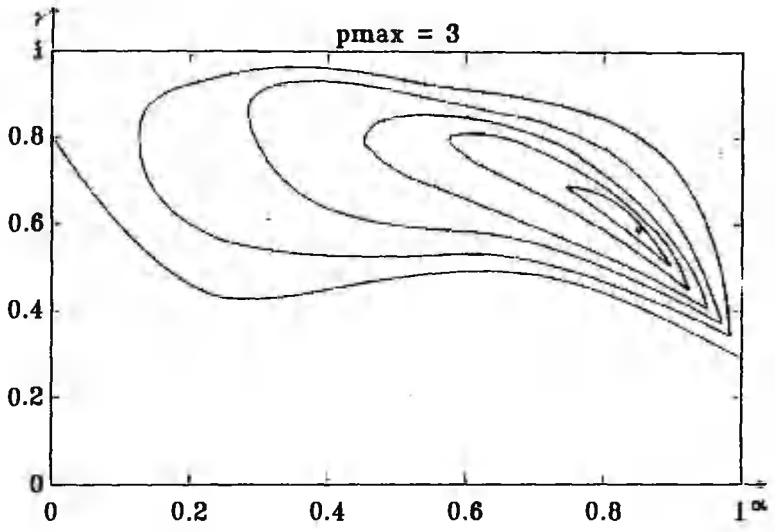

Fig. 11

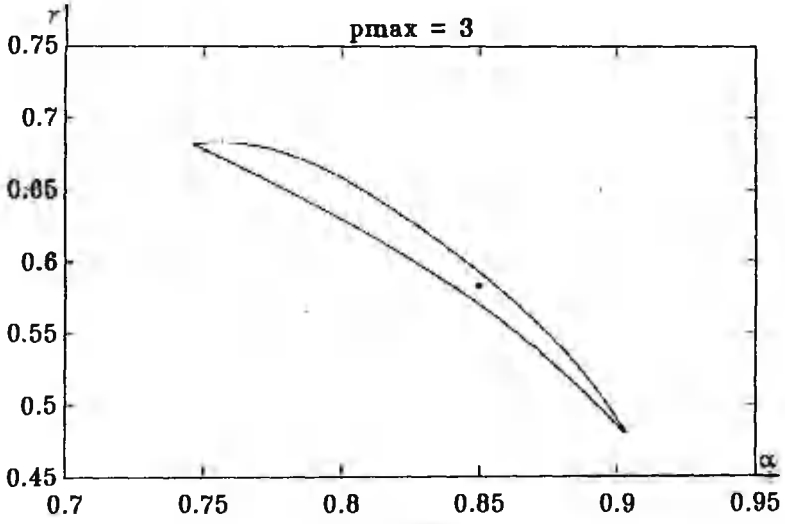

Fig. 12

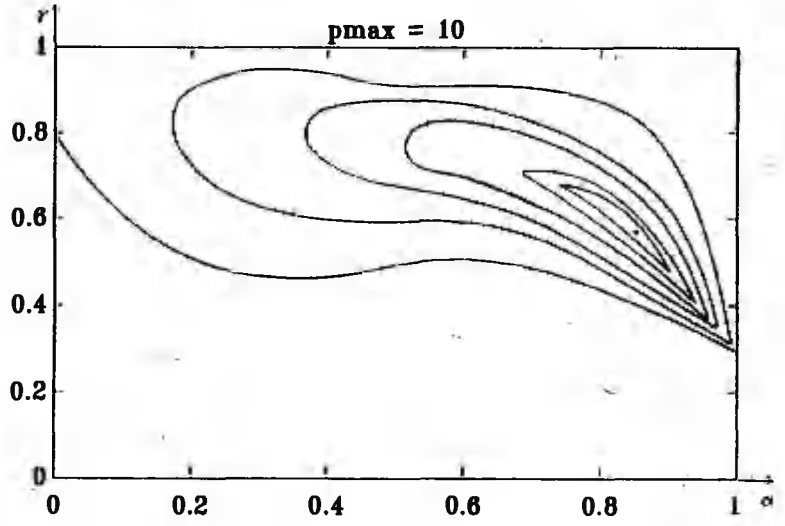
pmax = 10
r
1
0.8
0.6
0.4
0.2
0
0
0.2
0.4
0.6
0.8
1
α

Fig. 13

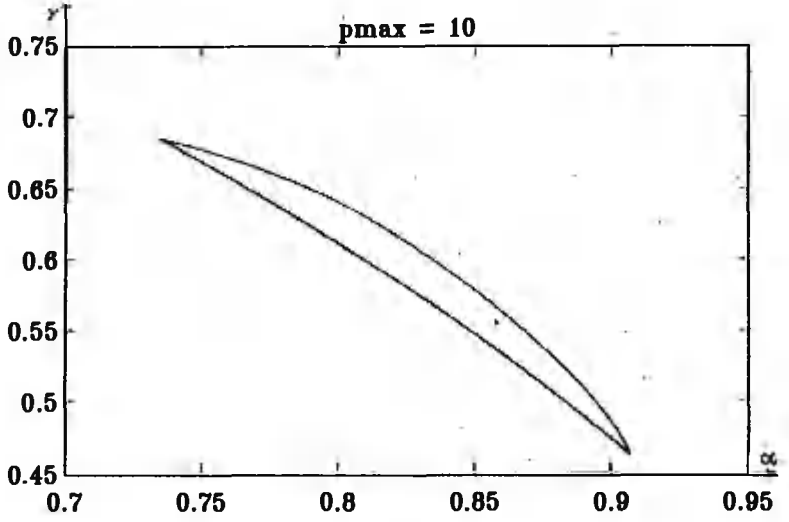
pmax = 10
r
0.75
0.7
0.65
0.6
0.55
0.5
0.45
0.7
0.75
0.8
0.85
0.9
0.95
α

Fig. 14

References

1.Hopkins H.G and Prager W., On the dynamics of plastic circular plates. ZAMP., 1954, 5, 317-330.

2.Lepik Ü, Mróz Z., Optimal design of plastic structures under impulsive and dynamic pressure loading. Int. J. Solids and Struct., 1977, 13(7), 657-674.

3.Лепик Ю., Оптимальное проектирование неупругих конструкций в случае динамического нагружения. Таллинн, "Валгус". 1982, 69-74.

4.Мазалов В.Н. и Немировский Ю.В., Динамика тонкостенных пластических конструкций. Сб. Механика, 1975, 5, 155-248.

5.Соонетс К., Вайникко И., О динамическом изгибе жестко-пластических круглых пластинок. Уч. зап. Тартуского ун-та., 1977, 430, 123-131.

6.Youngdahl C., Influence of pulse shape on the final plastic deformation of a circular plate. Int. J. Solids and Struct., 1971, 7, 1127-1142.

ОПТИМАЛЬНОЕ ПРОЕКТИРОВАНИЕ ЖЕСТКОПЛАСТИЧЕСКИХ СТУПЕНЧАТЫХ КРУГЛЫХ ПЛАСТИНОК ПРИ ДИНАМИЧЕСКОЙ НАГРУЗКЕ

Андрус Салупере

Таллиннский технический университет

Резюме

Исследуются жесткопластические ступенчатые свободно опертые круглые пластинки (фиг. 1). Используется условие текучести Треска (фиг. 2). На пластинку действует нормальная динамическая нагрузка (фиг. 1 и 3), которая имеет вид (5). Ищутся такие значения для параметров α и γ (6), при которых остаточный прогиб имеет минимальное значение. Изучаются пять режимов движения (фиг. 4,8), которые реализуются в различных последовательностях (фиг. 9 и 10). Оптимальные значения для параметров α^0 и γ^0, соответствующий остаточный прогиб w_1^0 и остаточный прогиб однородной пластинки w_1^u приведены в таблице 1. На фиг. 11 и 13 представлены области, где остаточный прогиб для ступенчатой пластинки w_1^s меньше чем остаточный прогиб для однородной пластинки w_1^u. На фиг. 11 и 13 представлены области, где остаточный прогиб для ступенчатой пластинки до 5 процентов больше чем оптимальное значение w_1^0.

Acta Et Commentationes Universitatis Tartuensis. 939, 1992

A COMPARISON OF THE TRESCA AND MISES YIELD CONDITIONS IN CASE OF DYNAMICALLY LOADED CYLINDRICAL SHELLS

Toomas Lepikult
Tartu University

Abstract. The problem of dynamic behavior of rigid-plastic cylindrical shells was touched in [1]. The systems of equations and inequalities for both the Tresca and Mises yield conditions were derived. The general methods and strategy of numerical solution of the problem were proposed in that article.

The results of computing of the maximal residual deflections in both cases will be compared in this report.

1. Formulation of the problem

Let us consider a rigid-plastic cylindrical sandwich-shell. The general thickness of the wall is assumed to be piecewise constant. The thicknesses of layers varies proportionally. The ends of the shell can be clamped, supported, or free. There is no hindrance to the displacements in the direction of the axis of the shell, therefore no axial forces appear. During a certain time-interval the shell is loaded with the internal pressure that exceeds the load-carrying capacity. After the load-carrying capacity is exhausted, either the entire shell or some regions of it transfer into the plastic state and obtain any kinetic energy. The plastic zones can either enlarge or narrow down during the motion, new plastic zones can appear, and the old ones can disappear.

Afterwards, when the pressure is taken off (or, at least, decreased under the limit load) the kinetic energy of the motion dissipate into the plastic work. After the motion has stopped, the walls of the shell will have obtained certain residual deflections, whose shapes and sizes depend upon boundary and load conditions, material constants and on the shape of the shell.

In the following formulas ξ and τ denote the undimensioned coordinate and time, respectively, apostrophe ($'$) and dot ($\cdot$) stand for differentiation according to ξ and τ. The symbols m, n and w denote the bending moment along the axis of the shell, circumferential force, and deflection. Parameter

$c^2 = \frac{4l^2}{Rh_м} > 0$ (l - half of the length of the shell, R - radii, $h_м$ - medium thickness of the wall) characterizes the slenderness of the shell.

From the mathematical point of view, three functions $w(\xi,\tau)$, $n(\xi,\tau)$, and $m(\xi,\tau)$ are searched. These must satisfy the following conditions:

a) the equation of the motion $\quad m' + c^2(n - p + \gamma\ddot{w}) = 0;$

b) the yield condition $\quad \Phi(m,n) \le 0;$

c) the associated yield law

$$\varkappa = \frac{\dot{w}'}{c^2} = \lambda \frac{\partial\Phi}{\partial m}, \qquad \dot{\varepsilon} = \dot{w} = \lambda \frac{\partial\Phi}{\partial n},$$

where

$\lambda = 0$, in case of $\Phi(m,n) < 0$ or

$$\Phi(m,n)=0, \quad \frac{\partial\Phi}{\partial m}\dot{m} + \frac{\partial\Phi}{\partial n}\dot{n} < 0;$$

$\lambda \ge 0$, in case of $\Phi(m,n) = 0$:

d) initial conditions $\quad \dot{w}(0,\xi) = w(0,\xi) = 0;$

e) boundary conditions for m and $\dot{w}$:

1) at supported edges $\xi^* = 0$ or $\xi^* = 2$:

$$m(\xi^*,\tau) = \dot{w}(\xi^*,\tau) = 0;$$

2) at free edges $\quad m(\xi^*,\tau) = m'(\xi^*,\tau) = 0;$

3) at clamped edges $\quad \dot{w}(\xi^*,\tau) = 0$ and

$$\dot{w}'(\xi^*,\tau) = 0 \quad \text{or} \quad m(\xi^*,\tau) = \gamma^2;$$

f) the capacity of plastic dissipation must be non-negative: $m\varkappa + n\dot{\varepsilon} \ge 0$ or

$$m(\dot{w}'(\xi^*+,\tau) - \dot{w}'(\xi^*-,\tau)) \ge 0,$$

when $\dot{w}'$ is undetermined in cross-section ξ^*.

The function Φ describes the yield surface. The most common yield surfaces are presented in Fig. 1. The hexagon 1 is described by the Tresca yield condition, the ellipse 2 by that of Mises. Quite often the exact yield surface is approximated by rectangle 3.

2. Numerical results

The methods for solving of the problem described above are presented in [1] for both the Tresca and Mises yield criterions. Now we shall make an attempt to compare the numerical results for both criterions.

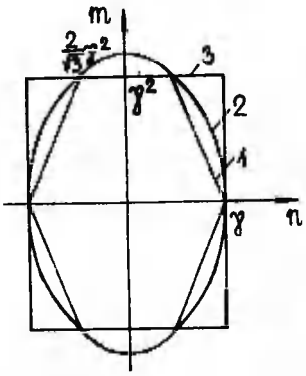

Fig. 1

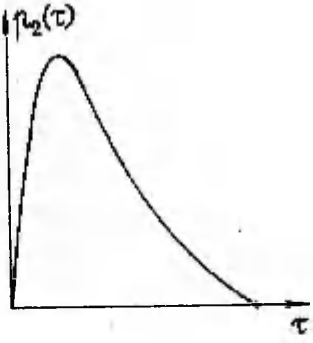

Fig. 2

The pressure was taken in the form

$$p(\xi,\tau) = p_1(\xi)p_2(\tau),$$

where

$$p_2(\tau) = \begin{cases} \exp\left\{-\dfrac{\pi(\tau - 0.2)}{\tan(0.2\pi)}\right\} \dfrac{\sin(\pi\tau)}{\sin(0.2\pi)}, & \text{if } \tau \le 1, \\ 0, & \text{if } \tau > 1 . \end{cases}$$

The function $p_2(\tau)$ is presented on Fig.2.

The calculations were carried out for three combinations of loads and shapes of the shell. For every combination the results are presented for three different values of parameter c^2. The distribution of the function $p_1(\xi)$ is displayed on Fig. 3a), 4a), and 5a). The shapes of the wall are demonstrated on Fig. 3b), 4b), 5b). The residual deflections in the case of the Tresca condition are marked with solid lines, in the case of the Mises condition with dotted lines (parts c - e on Fig. 3 - 5).

From the results of computing. We can make some interesting conclusions.

The differences in results decrease with increasing of parameter c^2. The differences are more obvious at the ends of the beam and near the cross-sections, where the thickness of the wall varies. The differences also seem to decrease, if the relation $\dfrac{p_2(\xi)}{\gamma(\xi)}$ decreases.

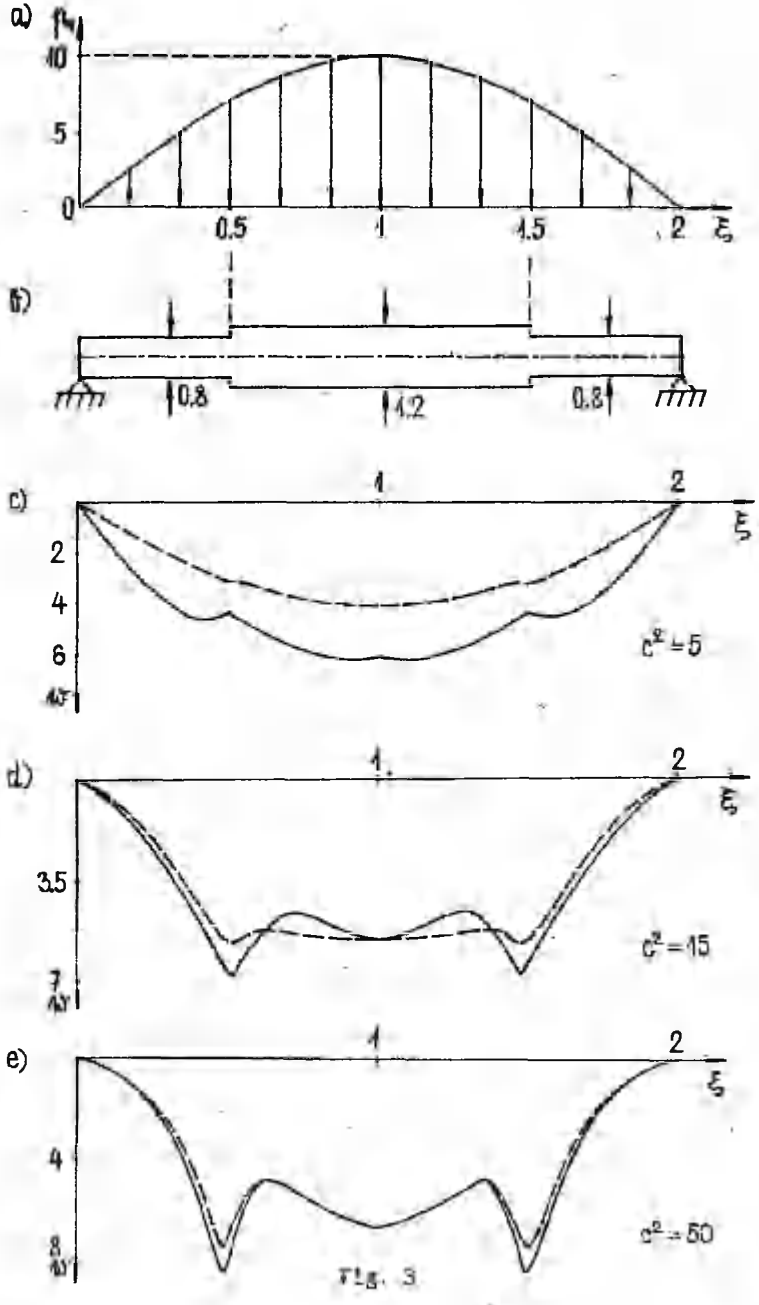
a)
10
5
0
0.5
1
1.5
2
ξ
b)
0.8
1.2
0.8
c)
1
2
ξ
2
4
6
c² = 5
d)
1
2
ξ
3.5
7
c² = 15
e)
1
2
ξ
4
8
c² = 50

Fig. 3

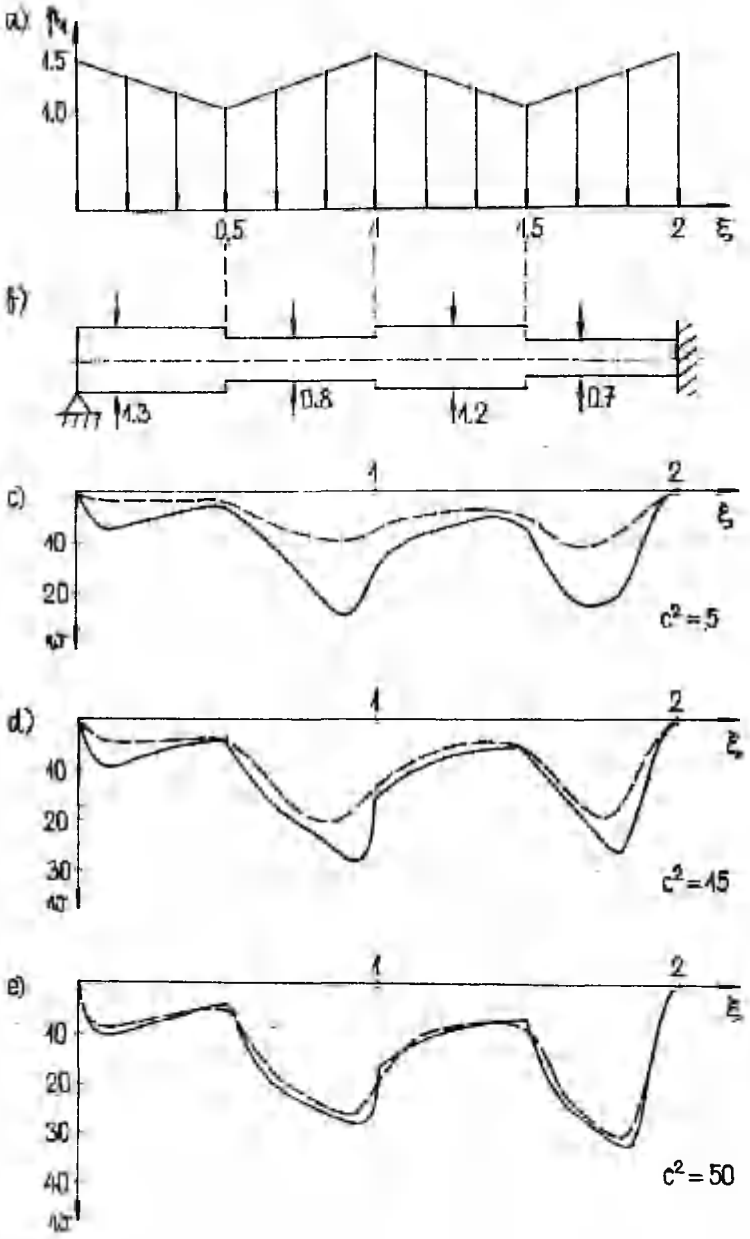
a)
1.5
1.0
0.5
1
1.5
2
ξ
b)
1.3
0.8
1.2
0.7
c)
1
2
ξ
10
20
$c^2=5$
d)
1
2
ξ
10
20
30
$c^2=15$
e)
1
2
ξ
10
20
30
40
$c^2=50$

Fig. 4

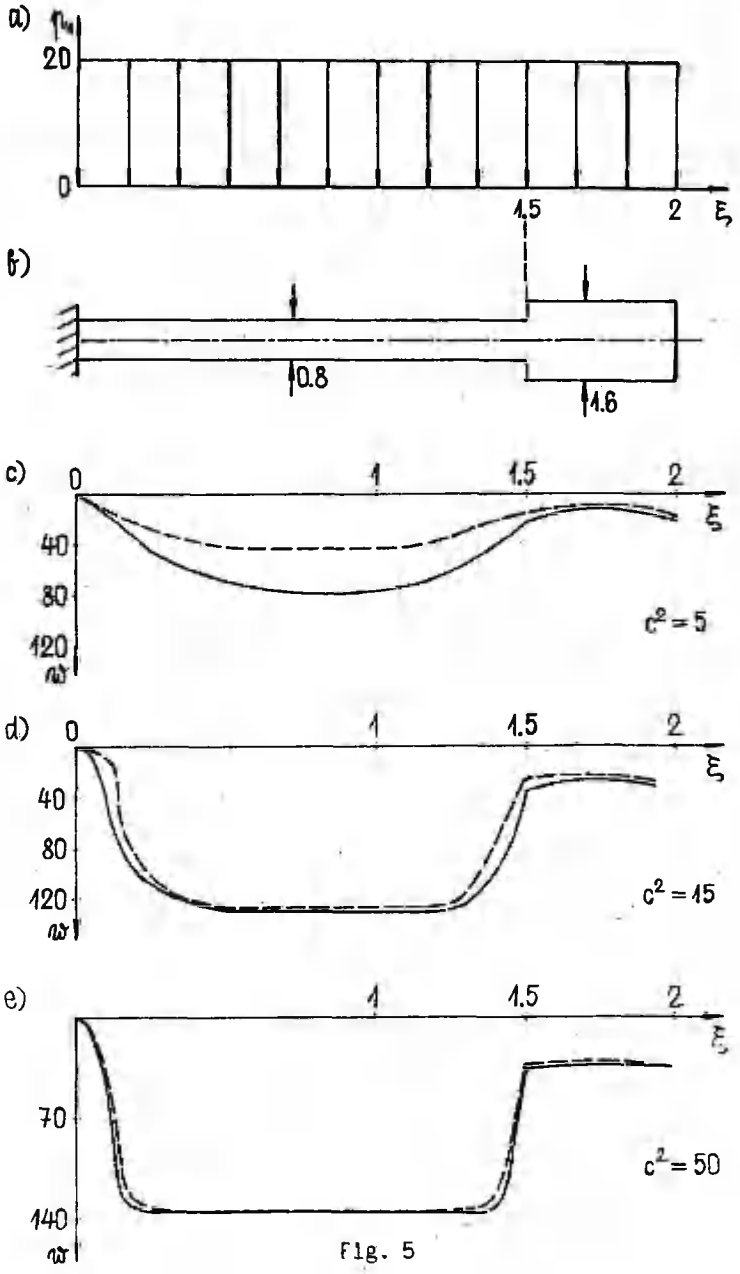
a)
20
0
1.5
2
ξ
b)
0.8
1.6
c)
0
1
1.5
2
ξ
40
80
120
w
$c^2 = 5$
d)
0
1
1.5
2
ξ
40
80
120
w
$c^2 = 15$
e)
1
1.5
2
ξ
70
140
w
$c^2 = 50$

Fig. 5

References

1. Лепикулт Т., Автоматизированный расчет динамики жесткопластических цилиндрических оболочек. Tartu Ülik Toim., 1988, 799, 33-63.

DÜNAAMILISELT KOORMATUD JAIKPLASTSETE SILINDRILISTE KOORIKUTE VÕRDLEMINE TRESCA JA MISESE VOOLAVUSTINGIMUSTE KORRAL

Toomas Lepikult
Tartu Ülikool

Resümee

Artiklis vaadeldakse jäikplastseid silindrilisi koorikuid. Teatud ajavahemiku vältel on koorikule rakendatud siserõhk. Eeldades, et koormus ületab staatilise piirkoormuse, leitakse kooriku jääkläbipainded liikumise lõpul. Kasutatakse nii Tresca kui Misese voolavustinglmusi. Esitatakse tulemuste võrdlus kummagi voolavustingimuse korral.

Acta Et Commentationes Universitatis Tartuensis. 939. 1992

MINIMUM WEIGHT DESIGN OF PLASTIC CYLINDRICAL SHELLS ACCOUNTING FOR LARGE DEFLECTIONS

Jaan Lellep and Jüri Majak
Tartu University

Abstract. The minimum weight problem is studied in the case of circular cylindrical shells. Material of the shells obeys the Von Mises yield condition and the associated deformation law. Moderately large deflections are taken into account. Numerical results are presented for the shells with pinned edges.

Introduction

Considerable progress has been made in the optimal design of rigid-plastic plates and shells after establishing the theorem of constant energy dissipation by Drucker and Shield [2]. Particular problems solved by means of the Drucker-Shield criterion are reviewed by Save and Prager [12], by Zyczkowski and Kruzelecki [13], Lellep and Lepik [8]. However, the theorem of constant energy dissipation is related to the initial collapse mode of the structure and thus it is not applicable in the range of large deflections.

Another approach to the minimum weight problems is related to the use of variational methods. The pioneers of this direction are Freiberger [3], Reiss and Megarefs [10]. Their studies are devoted to the cylindrical shells operating in the limit state.

Optimal design of rigid-plastic cylindrical shells accounting for large deflections was studied in [7,9] using piece-wise linear yield conditions, and in [14,15] in the case of the Von Mises yield condition assuming that the loading consisted of the lateral pressure and edge tension. In the present paper the attention is focused on the shells with pinned edges assuming the material to obeys the Von Mises yield condition.

1. Problem formulation

Let us consider a rigid-plastic circular cylindrical shell of radii R which is subjected to the uniform internal pressure of intensity P. The length of the tube is marked by 2l. For the sake of symmetry, only the right-hand part of the shell will be considered, e.g. $x \in (0,l)$, the origin of

coordinates lying in the central cross-section. Let us assume that the shell wall has the sandwich form and the thickness of carrying layers h(x) is variable, whereas the wall thickness H is a constant.

The post-yield behaviour of the shell will be studied under the requirement that the radial and axial displacements W and U do not exceed the order of the shell wall thickness. Thus, the Von Karman equations may be employed in order to prescribe the plastic behaviour of the shell under consideration.

In the present paper a such shell is sought in the case of which the weight (volume) of carrying layers

$$J = \int_0^1 h \, dx \tag{1.1}$$

reaches its minimum under the condition that the maximal deflection W_0 coincides with the central deflection of the corresponding shell of constant thickness h_*. We shall confine our attention to comparatively short shells. In this case deflection attains its maximal value at the center of the shell.

2. Basic equations and assumptions

The equilibrium equations of a shell element have the form

$$\frac{d^2M_1}{dx^2} - N_1 \frac{d^2W}{dx^2} + \frac{N_2}{R} - p = 0 \tag{2.1}$$

in the shell theory which accounts for moderately large deflections [5]. In (2.1) N_1 and N_2 stand for the axial and hoop membrane forces, respectively, whereas M_1 is the bending moment.

Geometrical relations may be presented as

$$\varepsilon_1 = \frac{dU}{dx} + \frac{1}{2}\left(\frac{dW}{dx}\right)^2, \quad \varepsilon_2 = \frac{W}{R}, \quad \varkappa_1 = -\frac{d^2W}{dx^2}, \quad \varkappa_2 = 0 \tag{2.2}$$

provided the stress-strain state is axisymmetric.

The concept of a rigid-plastic body will be used assuming the material obeys the Von Mises yield condition. Since the exact yield surface in the space of stress resultants has quite an intricate form, it is reasonable to introduce simpler approximations of this surface. One of the widely used approximations is [4, 11]

$$p_{11}^2 + p_{12}^2 = 1, \tag{2.3}$$

where

$$p_n^2 = \frac{1}{N_0^2}\left(N_1^2 - N_1N_2 + N_2^2 \right),\quad p_m^2 = \frac{1}{M_0^2}\left(M_1^2 - M_1M_2 + M_2^2 \right). \quad (2.4)$$

Here M_2 is the hoop moment.

In (2.3) and (2.4) N_0 and M_0 stand for the limit load and moment, respectively. In the case of a "sandwich" shell wall, $N_0 = 2\sigma_0 h$, $M_0 = \sigma_0 hH$, where σ_0 stands for the yield stress.

A deformation-type theory of plasticity will be used in the present study. According to the associated deformation law and (2.3), (2.4) we obtain

$$\varepsilon_1 = \frac{\lambda^2}{N_0^2}(2N_1 - N_2),\quad \varepsilon_2 = \frac{\lambda^2}{N_0^2}(2N_2 - N_1),$$
$$\varkappa_1 = \frac{\lambda^2}{M_0^2}(2M_1 - M_2),\quad \varkappa_2 = \frac{\lambda^2}{M_0^2}(2M_2 - M_1), \quad (2.5)$$

where λ^2 stands for an unknown non-negative multiplier.

It follows from relations (2.2) and (2.5) that

$$M_2 = 0.5M_1. \quad (2.6)$$

Making use of (2.6) we can give the equation of the yield surface (2.3), (2.4) in the form

$$\frac{1}{N_0^2}(N_1^2 + N_2^2 - N_1N_2) + \frac{3}{4}\frac{M^2}{M_0^2} - 1 = 0. \quad (2.7)$$

The both ends of the shell under consideration are assumed to be hinged. Thus, the boundary conditions may be presented as

$$W(0) = W_0, \frac{dW(0)}{dx} = \frac{dM(0)}{dx} = U(0) = M(1) = W(1) = U(1) = 0. \quad (2.8)$$

3. Optimality conditions

It will be convenient to use the following non-dimensional quantities

$$\xi = \frac{x}{l},\quad m = \frac{M_1}{M_*},\quad n_{1,2} = \frac{N_{1,2}}{N_*},\quad v = \frac{h}{h_*},$$
$$p = \frac{pR}{N_*},\quad w = \frac{N_*W}{M_*},\quad u = \frac{lN_*U}{M_*},\quad \alpha = \frac{N_*l^2}{RM_*}, \quad (3.1)$$

where N_* and M_* stand for the yield force and yield moment of a shell whose carrying layers have thickness h_*.

Introducing the quantity $q = m'$ and making use of (3.1) one can cast the equilibrium equations (2.1) into the form

$$n_1' = 0, \qquad m' = q, \qquad q' = \frac{3\alpha w n_1 m}{2(2n_2 - n_1)} + \alpha\,(p - n_2), \tag{3.2}$$

where primes denote differentiation with respect to the coordinate ξ.

Eliminating the deformation components ε_1, ε_2, $\varkappa_1$, $\varkappa_2$ from the associated deformation law (2.5) making use of (2.2) and (3.1) one obtains

$$w' = z, \qquad z' = \frac{3\alpha w m}{2(2n_2 - n_1)},$$
$$u' = -\frac{1}{2} z^2 + \frac{\alpha w(2n_1 \quad n_2)}{2n_2 - n_1}, \tag{3.3}$$

where z should be interpreted as an additional variable. According to (2.7) non-dimensional quantities satisfy the equation

$$n_1^2 - n_1 n_2 + n_2^2 + \frac{3}{4} m^2 - v^2 = 0. \tag{3.4}$$

In order to establish necessary optimality conditions, let us introduce the augmented functional

$$J_* = \int_0^1 \Big\{ v + \Phi_0 n_1' + \Phi_1 (m' - q) + \Phi_2 (q' - \frac{3\alpha w m n_1}{2(2n_2 - n_1)} -$$
$$- \alpha\,(p - n_2)) + \Phi_3 (w' - z) + \Phi_4 (z' - \frac{3\alpha w m}{2(2n_2 - n_1)} + -$$
$$+ \Phi_5 \,(u' + \tfrac{1}{2} z^2 - \frac{\alpha w(2n_1 - n_2)}{2n_2 - n_1} + \varphi(n_1^2 - n_1 n_2 +$$
$$+ n_2^2 + \frac{3}{4} m^2 - v^2)\Big\}\, d\xi. \tag{3.5}$$

In (3.5) Φ_0 to Φ_5 stand for adjoint variables, φ being the non-constant Lagrange multiplier. The variables n_1, m, q, w, z, u are referred to as state variables, whereas v and n_2 have been put into the role of control variables.

The functional (3.5) has to be differentiated in the space of continuous state variables and piece-wise continuous control variables. Variation of (3.5) leads to the adjoint set

$$\Phi_0' = -\frac{\partial L}{\partial n_1}, \qquad \Phi_1' = -\frac{\partial L}{\partial m}, \qquad \Phi_2' = -\frac{\partial L}{\partial q},$$
$$\Phi_3' = -\frac{\partial L}{\partial w}, \qquad \Phi_4' = -\frac{\partial L}{\partial z}, \qquad \Phi_5' = -\frac{\partial L}{\partial u} \tag{3.6}$$

and to the conditions

$$\frac{\partial L}{\partial n_2} = \frac{\partial L}{\partial v} = 0. \tag{3.7}$$

Here L stands for the Lagrangelan function

$$L = - v + \psi_1 q + \psi_2 \left(\frac{3\alpha w m n_1}{2(2n_2 - n_1)} + \alpha(p - n_2) \right) + \psi_3 z +$$

$$+ \psi_4 \frac{3\alpha w m}{2(2n_2 - n_1)} + \psi_5 \left(- \frac{z^2}{2} + \frac{\alpha w}{2n_2 - n_1} (2n_1 - n_2) \right) +$$

$$+ \varphi(v^2 - n_1^2 + n_1 n_2 - n_2^2 - \frac{3}{4} m^2). \tag{3.8}$$

Taking into account the boundary conditions for state variables (2.8) one obtains the following transversallty conditions

$$\psi_0(0) = \psi_1(0) = \psi_0(1) = \psi_2(1) = \psi_4(1) = 0. \tag{3.9}$$

After substitution of (3.8) and calculation of derivatives equations (3.7) may be converted into

$$v = (2\varphi)^{-1} \tag{3.10}$$

and

$$\varphi = \frac{-1}{(2n_2 - n_1)^3} \left\{ \alpha \Psi_2 (2n_2 - n_1)^2 + 3\alpha w [m(n_1 \Psi_2 + \Psi_4) + n_1 \Psi_5] \right\} \tag{3.11}$$

Substituting the quantity v according to (3.10), (3.11) into (3.4) one obtains the equation

$$4\alpha^2 [3wm (n_1 \Psi_2 + \Psi_4) + 3w n_1 \Psi_5 + \Psi_2 (2n_2 - n_1)^2]^2 (n_1^2 -$$

$$- n_1 n_2 + n_2^2 + \frac{3}{4} m^2 - (2n_2 - n_1)^6 = 0, \tag{3.12}$$

which should be referred to as an equation for determination of the control variable n_2 at each node point of the mesh.

4. Numerical solution

Employing the necessary optimality conditions one can transform the posed problem into a boundary value problem. It consists in the integration of equations (3.2), (3.3), (3.6) making use of (3.10)-(3.12) accounting for the boundary requirements (2.8) and (3.9). The method of type adjoint operators is accommodated for solving the two-point boundary value problem.

The solution algorithm slightly differs from the one which

was used in the case of the shell subjected to the transverse pressure and tension applied at the edges of the shell [14,15]. In order to start with the numerical procedure one has to determine the load-deflexion relation for the associated shell of constant thickness. This in its turn demands the information about the load carrying capacity of the shell of a constant thickness. For determination of the limit load of the shell the lower bound theorem of limit analysis is employed. This leads to the integration of the set (3.2) where $w = 0$ accounting for suitable boundary conditions and performing maximization with respect to the loading parameter.

For numerical integration of the set (3.2), (3.3), (3.6) the fourth order Runge-Kutta method is used. The integration is accomplished from the left to the right in the region (0,1), preliminarily assigning certain values to $n_1(0)$, $m(0)$, $\Psi_2(0)$, $\Psi_3(0)$, $\Psi_4(0)$, $\Psi_5(0)$. Increments to these boundary values are calculated by means of complementary variables x_j which satisfy the equations

$$x_j' = -\sum_{k=1}^{12} \frac{\partial f_k}{\partial y_j} x_k; \qquad j = 1,\ldots,12. \tag{4.1}$$

The complementary system (4.1) is integrated 6 times at each step of iteration from the right to the left using the boundary conditions $x_j(1) = 1$ and $x_1(1) = 0$, where $1 \neq j$, respectively.

In (4.1) f_k ($k = 1,\ldots,12$) stand for the right-hand sides of equations (3.2), (3.3) and (3.6), whereas y_j ($j = 1,\ldots,12$) denote the set of state and adjoint variables. Improvements of the boundary values of $y_j(0)$ for $j \in I_0$ are calculated from the system of algebraic equations

$$\sum_{j \in I_0} x_j^i(0)\delta y_j(0) = -z_i(1); \qquad i \in I_1, \tag{4.2}$$

where the set I_1 is specified by the indexes of state variables fixed at $\xi = 1$ according to (2.8) and (3.9). The quantities $z_i(1)$ in the right-hand side of (4.2) stand for the discrepancies of the calculated boundary values and the exact ones given by (2.8) and (3.9).

5. Discussion

The results of numerical calculations are presented in

Fig.1-6 and in Tables 1,2. The curves 1,2 and 3 in Fig.1-5 correspond to the values of the load intensity p = 1,34; p = 1,63 and p = 2,04, respectively (here $\alpha = 4$).

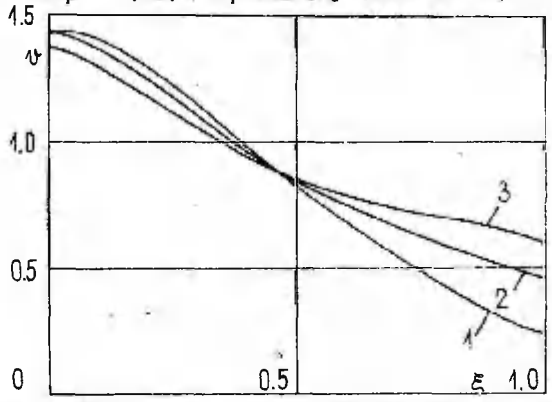

Fig. 1

The optimal thickness distribution of carrying layers is presented in Fig.1. It appears that the optimal thickness remarkably depends upon the load intensity. In the case of the shells subjected to the transverse pressure and to the constant edge loading this effect was not observed [14]. Consequently, the optimal thickness distribution hardly depends upon the membrane forces which have been generated as the reactions of the supports in the present case.

The economy of an established design may be evaluated by the ratio

$$e = \frac{1}{h_*} \int_0^1 h \, dx, \qquad (5.1)$$

where h_* stands for the constant thickness of an associated shell with the same load-deflection diagram. It means that under given pressure p, the shells of optimal thickness h and of the constant thickness h_*, respectively, have the same maximal deflexion w_0. The values of the economy coefficient e as well as the maximal deflexion w_0 and the membrane force n_1 are presented in Tables 1 and 2. Table 1 corresponds to the case $\alpha = 2$, Table 2 - $\alpha = 4$.

In Tables 1 and 2 n_* denotes the membrane force in the corresponding shell of a constant thickness. It is worth mentioning that the tension in a shell of an optimal shape is smaller than in the associated shell of a constant thickness. It appears that the maximal amount of material saving may be achieved in the limit state. In the case $\alpha = 2$, one can save

up 19,1% of the material, provided the shell operates in the limit state. Naturally, by increasing load intensity the membrane forces as well as the economy coefficient increase.

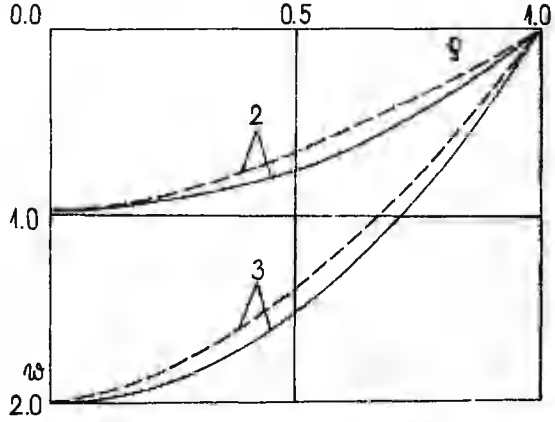

Fig. 2

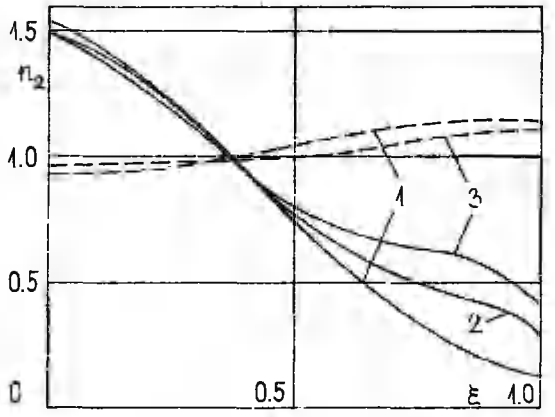

Fig. 3

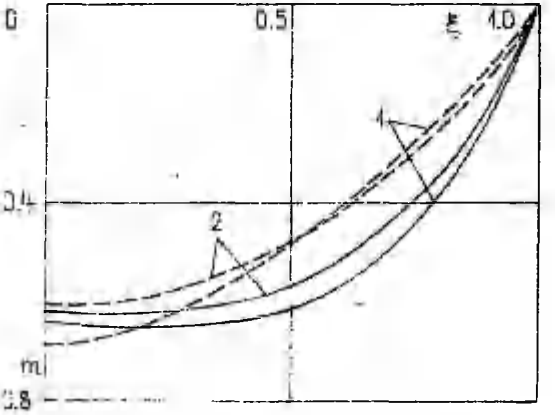

Fig. 4

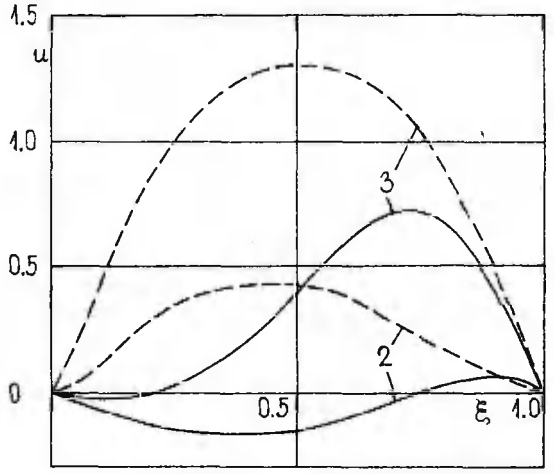

Fig. 5

In Figs 2–5 the lateral deflection, hoop force, bending moment and axial deflexion are presented. The continuous lines in Figs. 2–5 correspond to the shell of optimal shape, whereas the dotted lines are associated with the shell of constant thickness.

With reference to Figs. 2–5, it can be seen that the transverse displacement and bending moment of the shell with optimal thickness only slightly differ from those corresponding to the shell of constant thickness. However, the hoop forces and axial displacements are essentially different in these cases. Calculations show that the difference between the corresponding moment distributions increases when the geometrical parameter α increases. On the other hand, the moment distribution is not very sensitive to the changes in the load intensity. This was also observed in the case of the shells loaded by the lateral pressure and axial tension [14,15].

The results presented in Figs. 1–5 correspond to the so-called short shells, hinged at both ends. There are various reasons why the calculations become more complicated for long shells. One of them is related to the behaviour of the bending moment distribution - its minimum (maximum of the absolute value) is withdrawn from the central cross-section of the shell. Moreover, the convergence of the calculation process will change unfavourably if the parameter α increases. The shells clamped at both ends have been studied in [14].

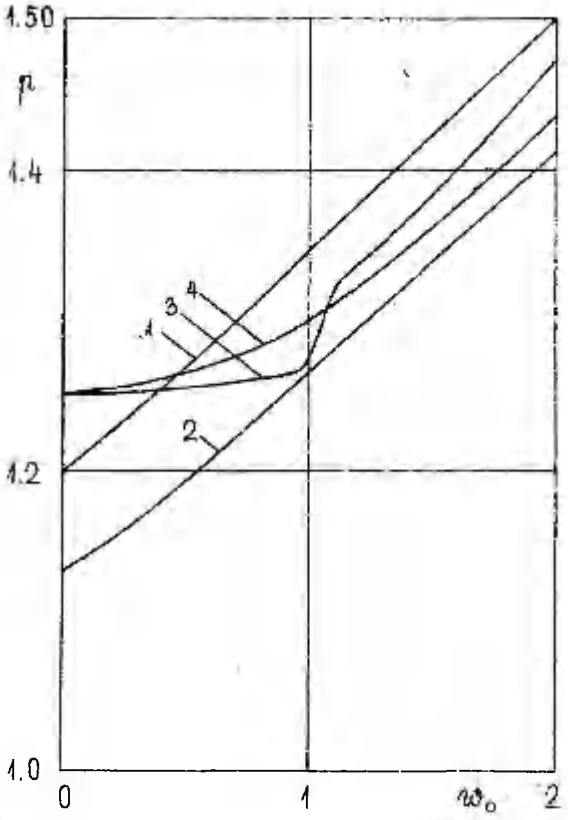

Fig. 6

It should be emphasized that the optimal solutions of the posed problem have been obtained for the given values of the load intensity p. One can check if the design obtained for $p = p_*$ is able to carry the loads for which $p < p_*$. In this case the maximal deflection of a shell of variable thickness is smaller than that of the associated shell of constant thickness. But its load carrying capacity (limit load) is greater than the limit load for the shell with a constant thickness.

The load-deflection relations for shells of constant thickness are presented in Fig. 6. Here $\alpha = 8$. Line 1 corresponds to the present solution, whereas 2,3 and 4 are associated with the Tresca yield condition. Diagram 2 was obtained by Lepik [16], line 3 by Duszek [1] and 4 by Lance and Soechting [6]. It should be noted that the differences between the re-

sults are not large,although the solutions have been obtained by using of different approximations of yield conditions.

Table 1

p	w_0	e	n_1	n_w
1,765	0	0,809	0,186	0,378
1,85	0,209	0,827	0,262	0,443
2,00	0,502	0,850	0,373	0,526
2,15	0,747	0,867	0,454	0,589
2,30	0,966	0,880	0,517	0,640
2,45	1,167	0,891	0,569	0,682
2,60	1,355	0,900	0,612	0,718
2,82	1,616	0,910	0,665	0,762

Table 2

p	w_0	e	n_1	n
1,34	0	0,844	0,260	0,498
1,45	0,413	0,869	0,388	0,573
1,51	0,611	0,878	0,439	0,606
1,63	0,969	0,894	0,519	0,662
1,71	1,188	0,902	0,563	0,692
1,76	1,320	0,906	0,587	0,710
1,82	1,473	0,911	0,613	0,729
1,88	1,621	0,915	0,637	0,747
1,91	1,694	0,917	0,648	0,755
2,04	2,000	0,925	0,692	0,789

References

1.Duszek M., Geometrycznie nielinniowa teoria konstrukcji sztywno-plastycznych. Warszawa, IPPT PAN, 1975.

2.Drucker D.C., Shield R.T., Design for minimum weight. Proc. 9th Int. Congr. Appl. Mech. (Brussels, 1956), 1957, 5, 212-222.

3.Freiberger W., On the minimum weight design problem for cylindrical sandwich shells. J. Aeron. Scl., 1957, 24(11), 847-848.

4.Haydl H.M., Sherbourne A.N., Some approximations to the Ilyushin yield surface for circular plates and cylindrical shells. Z. angew. Math. und Mech., 1979, 59(2), 131-132.

5.Jones N., Consistent equations for the large deflections of structures. Bull. Mech. Eng. Educ., 1971, 10(1), 9-20.

6.Lance R.H., Soechting I.E., A displacement bounding principle in finite plasticity. Int. J. Solids and Struct.,

1970, 6, 1103-1118.
7.Lellep J., Parametrical optimization of plastic cylindrical shells in the post-yield range. Int. J. Eng. Sci., 1985, 23(12), 1289-1303.
8.Lellep J., Lepik Ü., Analytical methods in plastic structural design. Eng. Optimiz., 1984, 7(3), 209-239.
9.Lellep J., Sawczuk A., Optimal design of rigid-plastic cylindrical shells in the post-yield range. Int. J. Solids and Struct., 1987, 23(5), 651-664.
10.Reiss R., Megarefs G.J., Minimal design of sandwich axisymmetric cylindrical shells obeying Mises' criterion. Acta Mech., 1969, 7(1), 72-98.
11.Robinson M., A comparison of yield surfaces for thin shells. Int. J. Mech. Sci., 1971, 13(4), 345-354.
12.Save M., Prager W., Optimality criteria. Structural optimization. Vol.I. Plenum Press, New York, 1985.
13.Życzkowski M., Kruželecki J., Aktualne kierunki rozwoju kształtowania wytrzymałościowego powłok. Zesz. Nauk. Wyż. Szkoły Inżyn. W Opolu, 1984, 90, 57-97.
14.Леллеп Я., Маяк Ю., Оптимизация жесткопластических геометрически нелинейных цилиндрических оболочек. Уч. зап. Тартуск. ун-та, 1988, 799, 27-36.
15.Леллеп Я.А., Маяк Ю.П., Оптимальное проектирование геометрически нелинейных пластических цилиндрических оболочек. Изв. АН СССР. Мех. тверд. тела, 1990, 1, 118-122.
16.Лепик Ю.Р., Большие прогибы жестко-пластической цилиндрической оболочки под действием внутреннего и внешнего давления. Тр. VI Всес. конф. по теории оболочек (Баку, 1966). М., Наука, 1966, 534-541.

МИНИМИЗАЦИЯ ВЕСА ПЛАСТИЧЕСКИХ ЦИЛИНДРИЧЕСКИХ ОБОЛОЧЕК С УЧЕТОМ БОЛЬШИХ ПРОГИБОВ

Яан Леллеп, Юрий Маяк
Тартуский университет

Резюме

Представлена методика решения задач минимизации веса жесткопластических круговых цилиндрических оболочек, материал которых подчиняется условию пластичности Мизеса и ассоциированному закону деформирования. Учитываются умеренно большие перемещения. С помощью вариационных методов теории оптимального управления задача сводится к нелинейной краевой задаче, которая решается численно методом типа сопряженных уравнений.

Acta Et Commentationes Universitatis Tartuensis, 939, 1992

AN APPROXIMATE ANALYSIS OF LARGE PLASTIC DEFORMATIONS OF CIRCULAR AND ANNULAR PLATES

Jaan Lellep and Helle Hein
Tartu University

Abstract. In the present paper an approximate method of investigation of large deflections of circular and annular plates is developed. The analysis is based on the yield line method of Sawczuk [6], which was also applied by Kondo and Pian [3,4]. The method is illustrated by a study of circular and annular plates of piece-wise constant thickness.

Introduction

Geometrically non-linear problems of plastic plates and shells have become problems of practical interest. Some of these ways of their application in engineering are related to design of pressure vessels as well as ship and aircraft structures. Large deflections of plastic circular plates, the material of which obeys the piece-wise linear yield condition have been investigated by Onat and Haythornthwalte [5], Lepik [9], Jones [2], Kondo and Pian [3] and others. An efficient solution was obtained by Calladine [1], considering the plate to be a three-dimensional body.

1. Governing equations

Let us consider an annular plate of outer radii R and of inner radii a which is subjected to the uniformly distributed transverse pressure of intensity P. The outer edge of the plate is assumed to be hinged, whereas the inner one is completely free.

In this paper large deflections of circular and annular plates will be studied. The plates of constant thickness h as well as piece-wise constant thickness will be analyzed. In the latter case $h = h_j$ for $r \in (a_j, a_{j+1})$ where $j=0,\ldots,n$ and $a_0 = a$, $a_{n+1} = R$. Here $a_j (j=1,\ldots,n)$ stand for the values of the radii where the thickness varies rapidly. The quantities h_j as well as a_j are assumed to be given constants in the present study.

Taking into account the post-yield behaviour of plastic plates the membrane forces N_r, N_φ and bending moments M_r, M_φ will be used in order to predict the stress state of the

plate under consideration. Let U and W denote the in-plane and transverse displacement of the plate, respectively.

Assuming that the displacements do not exceed the order of the plate thickness the equations of Von Karman theory are applicable. Thus, the equilibrium equations have the form

$$(\rho n_1)' = n_2,$$
$$[(\rho m_1)' - m_2 + \rho n_1 w']' + 2p\rho = 0, \tag{1.1}$$

whereas the deformation components may be written as

$$\varepsilon_1 = \frac{M_*^2}{R^2 N_*^2}(u' + \frac{1}{2}w'^2), \qquad \varepsilon_2 = \frac{M_*^2}{R^2 N_*^2}\frac{u}{\rho},$$
$$\varkappa_1 = \frac{M_*}{N_* R^2}w'', \qquad \varkappa_2 = -\frac{M_*}{N_* R^2}\frac{w'}{\rho}, \tag{1.2}$$

where primes denote the differentiation with respect to the non-dimensional quantity ρ. Here N_* and M_* stand for the limit load and limit moment, respectively. In the case of homogeneous cross-section one has $N_* = \sigma_0 h_*$, $M_* = \sigma_0 h_*^2/4$, σ_0 being the yield stress and h_* the thickness of the plate.

Dimensional and non-dimensional quantities are related by

$$\rho = \frac{r}{R}, \quad n_{1,2} = \frac{N_{r,\varphi}}{N_*}, \quad m_{1,2} = \frac{M_{r,\varphi}}{M_*}, \quad \tau_j = \frac{h_j}{h_*},$$
$$w = \frac{N_*}{M_*}W, \quad u = \frac{RN_*^2}{M_*^2}U, \qquad p = \frac{R^2 P}{2M_*}, \quad \alpha_j = \frac{a_j}{R}. \tag{1.3}$$

Material of the plate is assumed to be an ideal rigid-plastic one (without strain-hardening) obeying the Tresca yield condition. A simplified analysis will be presented in this paper. The simplifications (in comparison with the exact theory of plastic plates) consist in the following. Firstly, the exact yield surface is replaced by an approximate surface using the concept of the "limited interaction between forces and moments". This concept was widely used in the limit analysis as well as in the large deflection theory of plastic plates and shells [6,7]. The second simplification is related to the use of the yield-line theory [3,4,6] which states the existence of a system of hinge circles in the plates. Among these hinges the plates take the forms of truncated cones.

Such an approximation of the exact yield surface associated

with the Tresca yield condition will be used, which may be presented as (Fig.1)

$$n_1^2 + |m_1| \le \gamma_j^2, \quad n_2^2 + |m_2| \le \gamma_j^2, \quad j = 0,\ldots,n \qquad (1.4)$$

for the region $\rho \in D_j$, where D_j stands for the interval (α_j,α_{j+1}). The approximation of the yield surface (Fig.1) should be handled as the further simplification of the method of limited interaction (couple of hexagons on the planes of forces and moments, respectively). It was employed by Kondo and Pian [3,4].

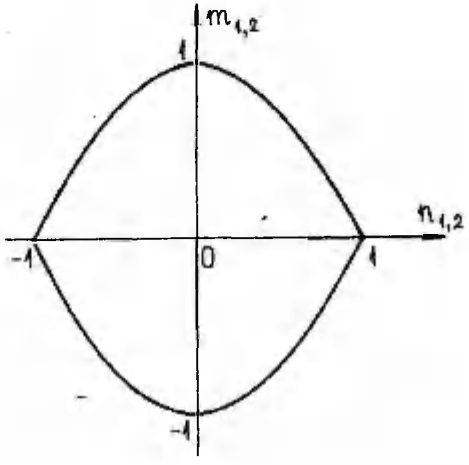

Fig. 1

The relations between the stresses and strain components (1.2) will be stated by the associated deformation law. A deformation-type theory of plasticity is used in the present study. It is assumed that the vector of strain components (1.2) is directed along the outward normal to the yield surface prescribed by (1.4), if the corresponding stress point lies on the surface. If this condition is not satisfied, e.g. the stress point lies in the internal region of the surface, the strain vector must vanish. This associated deformation law may be interpreted in the present case as follows. Applying the gradient law with respect to the configuration on the m_1-n_1 plane the vector of deformation components contains the components ε_1 and $\varkappa_1$. Similarly, on the m_2-n_2 plane the deformation components ε_2 and $\varkappa_2$ will be used.

Since the outer edge of the plate is hinged the boundary

conditions may be expressed as

$$m_1(1) = w(1) = u(1) = 0. \tag{1.5}$$

In the case of an annular plate at the free inner edge one has

$$m_1(\alpha) = n_1(\alpha) = q(\alpha) = 0, \tag{1.6}$$

where q stands for the non-dimensional shear force. At the center of the circular plate the symmetry considerations lead to the following conditions

$$m_1(0) = m_2(0), \quad n_1(0) = n_2(0). \tag{1.7}$$

2. Large deflections of circular plates

The post-yield behaviour of a simply supported circular plate of constant thickness will be examined now ($\gamma_1 = 1$). Let us assume that the plastic behaviour of the plate can be quite adequately simulated by the mechanism shown in Fig.2. Thus, at the positions $\rho = \alpha_j$ ($j = 0,\ldots,n$) will form the plastic hinge circles. Corresponding deflections are marked by w_j. The aim of the paper is the determination of the quantities w_j ($j = 0,\ldots,n$) for each value of the intensity of lateral loading $p \geq p_0$, p_0 being the load carrying capacity of the plate.

The deflection distrubution among plastic hinge circles is linear with respect to the radii ρ, therefore

$$w' = \varphi_j \tag{2.1}$$

for $\rho \in D_j$; $j = 0,\ldots,n$. In (2.1)

$$\varphi_j = \frac{w_{j+1} - w_j}{\alpha_{j+1} - \alpha_j}; \quad j = 0,\ldots,n, \tag{2.2}$$

where one has to take into account that $\alpha_0 = 0$, $\alpha_{n+1} = 1$, $w_{n+1} = 0$.

Integration of the equations (2.1) leads to the relations

$$w = \varphi_j (\rho - A_j) \tag{2.3}$$

for $\rho \in D_j$; $j = 0,\ldots,n$. The integration constants A_j can be satisfied taking into account the boundary conditions (1.5) and continuity requirements of the deflection w at $\rho = \alpha_j$. Thus, one has $A_n = 1$ and

$$A_{j-1} = \frac{\alpha_j (\varphi_{j-1} - \varphi_j)}{\varphi_{j-1}} + \frac{\varphi_j}{\varphi_{j-1}} A_j, \tag{2.4}$$

where $j = n,n-1,\ldots,1$.

It is worth emphasizing that in conformity with (1.2) and

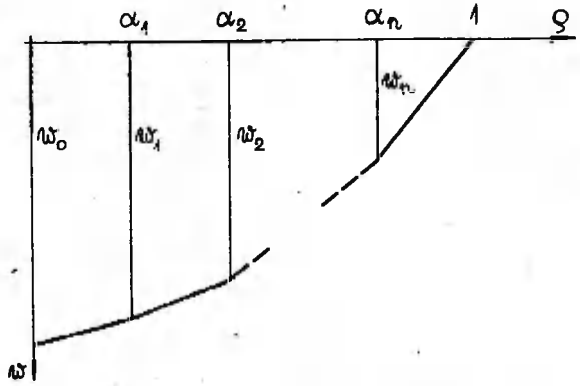

Fig. 2

(2.1) the deformation component $\varkappa_1$ always vanishes. Thus, the associated deformation law yields $\varepsilon_1 = 0$, or

$$u' = -\frac{1}{2} w'^2, \tag{2.5}$$

which holds good in each region D_j $(j = 0,\ldots,n)$, except at the boundaries $\rho = \alpha_j$ $(j = 0,\ldots,n)$. At the hinge circles $\rho = \alpha_j$ the corresponding stress point reaches the yield curve on the $m_1 - n_1$ plane (Fig.1). Thus, according to (1.4)

$$m_1(\alpha_j) = 1 - n_1^2(\alpha_j), \quad j = 0,\ldots,n \tag{2.6}$$

since the bending moment is assumed to be non-negative.

The associated deformation law applied to the configuration on the $m_2 - n_2$ plane (Fig.1) furnishes the relation

$$\frac{\varepsilon_2}{\varkappa_2} = 2n_2 \frac{M_*}{N_*} \tag{2.7}$$

under the condition that the corresponding stress point lies on the yield curve on the $m_2 - n_2$ plane. Substitution of (1.2) into (2.7) leads to the equation

$$n_2 = -\frac{1}{2} \frac{u}{w'}, \tag{2.8}$$

which holds good almost everywhere.

In order to determine the in-plane displacement u one has to integrate the equation (2.5) in each region D_j making use of (2.1), (2.2). Satisfying the boundary condition $u(1) = 0$ and continuity conditions at $\rho = \alpha_j$ one obtains

$$u = -\frac{\varphi_j^2}{2}(\rho - \alpha_{j+1}) - \frac{1}{2}\sum_{i=j+1}^{T}\varphi_i^2(\alpha_i - \alpha_{i+1}) \qquad (2.9)$$

for $\rho \in D_j$; $j = 0,\ldots,n-1$ and for $\rho \in D_n$

$$u = -\frac{1}{2}\varphi_n^2(\rho - 1). \qquad (2.10)$$

Substitution of (2.1), (2.9), (2.10) into (2.8) gives

$$n_2 = \frac{\varphi_j}{4}(\rho - \alpha_{j+1}) + R_j \qquad (2.11)$$

for $\rho \in D_j$; $j = 0,\ldots,n$. Here R_j stand for the following expressions

$$R_j = \frac{1}{4\varphi_j}\sum_{i=j+1}^{T}\varphi_i^2(\alpha_i - \alpha_{i+1});\ j = 0,\ldots,n-1;\ R_n = 0. \qquad (2.12)$$

As above, we assume herein that $\alpha_0 = 0$; $\alpha_{n+1} = 1$. Since the stress state corresponds to the parabola on the $m_2 - n_2$ plane (Fig.1) making use of (2.11), one obtains

$$m_2 = 1 - \frac{\varphi_j^2}{16}(\rho - \alpha_{j+1})^2 - \frac{\varphi_j}{2}R_j(\rho - \alpha_{j+1}) - R_j^2 \qquad (2.13)$$

for $\rho \in D_j$; $j = 0,\ldots,n$.

Taking into account the expression (2.11)-(2.13) for stress resultants m_2, n_2 as well as the displacement field (2.1)-(2.4) one can solve the equilibrium equations (1.1). The first of them after substitution (2.11) yields

$$n_1 = \frac{\varphi_j}{4}\left[\frac{\rho}{2} - \alpha_{j+1}\right] + R_j + \frac{B_j}{\rho} \qquad (2.14)$$

for $\rho \in D_j$; $j = 0,\ldots,n$, where B_j stand for integration constants. They may be presented in the form

$$B_0 = 0,$$
$$B_j = B_{j-1} - \frac{\alpha_j^2}{8}(\varphi_j + \varphi_{j-1}) + \frac{\varphi_j}{4}\alpha_j\alpha_{j+1} + \alpha_j(R_{j-1} - R_j), \qquad (2.15)$$

where $j = 1,\ldots,n$; provided n_1 is continuous and the second symmetry condition in (1.7) is satisfied.

The second equation in the set (1.1) after substitutions of the quantities m_2, n_1, w' according to (2.1), (2.13), (2.14) gives

$$m_i = 1 - \frac{\varphi_i^2}{480}(\rho - \alpha_{j+1})^3 - \frac{\varphi_i R_i}{40}(\rho - \alpha_{j+1})^2 - \frac{\varphi_i^2}{8}\left(\frac{\rho^2}{3} - \rho\alpha_{j+1}\right) - R_j^2 - R_j\varphi_j\frac{\rho}{2} - \frac{p}{3}\rho^2 - B_j\varphi_j + \frac{C_j}{\rho} \tag{2.16}$$

for $\rho \in D_j$; $j = 0,\ldots,n$. Here C_j stand for the previously unknown constants which may be determined according to continuity requirements and symmetry condition (1.7) as follows:

$$C_0 = 0,$$

$$C_j = C_{j-1} + \frac{\varphi_i^2}{48}(\alpha_j - \alpha_{j+1})^3 + \frac{\varphi_i R_i}{4}(\alpha_j - \alpha_{j+1})^2 + \alpha_j(R_j^2 - R_{j-1}^2) + \frac{\varphi_i^2}{8}\alpha_j^2\left(\frac{\alpha_j}{3} - \alpha_{j+1}\right) + \frac{\varphi_{i-1}^2}{12}\alpha_j^3 + \frac{\alpha_j^2}{2}(\varphi_j R_j - \varphi_{j-1}R_{j-1}) + \alpha_j(\varphi_j B_j - \varphi_{j-1}B_{j-1}), \tag{2.17}$$

where $j = 1,\ldots,n$.

It is worth noting that neither the boundary condition $m_1(1) = 0$ in (1.5) nor the requirements (2.6) are used in derivation of relations (2.16), (2.17). Satisfying these conditions with the help of (2.16) and (2.14) one obtains the following set of non-linear equations

$$1 + \frac{\varphi_n^2}{12} - B_n\varphi_n + C_n - \frac{p}{3} = 0,$$

$$\frac{\varphi_j\alpha_{j+1}}{12}(\varphi_j\alpha_{j+1} - 6R_j) - R_j^2 - B_j\varphi_j - \frac{p}{3}\alpha_{j+1}^2 + \frac{C_j}{\alpha_{j+1}} + \left(\frac{B_j}{\alpha_{j+1}} + R_j - \frac{\varphi_j\alpha_{j+1}}{8}\right)^2 = 0, \tag{2.18}$$

where $j = 0,\ldots,n-1$. After substitution of quantities φ_j, R_j, B_j, C_j the equations (2.18) serve for determination of parameters w_j $(j = 0,\ldots,n)$.

3. Large deflections of annular plates

Let us consider now an annular plate hinged at the outer edge and free at the inner edge. Let the innner radii be $\alpha_0 = \alpha$.

Using the same technique as in the previous paragraph, one can obtain a result showing that the relations (2.1)–(2.14) remain valid. By integration of the first one of the equilibrium equations (1.1) one gets (2.14) where the integration constant B_0 takes the form of

$$B_0 = -\frac{\varphi_0}{4}\left(\frac{\alpha^2}{2} - \alpha_1\alpha\right) - R_0\alpha, \qquad (3.1)$$

provided that $m_1(\alpha) = 0$. The recurrent relation in (2.15) which connects the integration constants B_j, B_{j-1} ($j = 1,\ldots,n$) remains valid. Integrating (1.1) and taking into account the boundary condition (1.6) we can obtain the expression for bending moment

$$m_1 = 1 - \frac{\varphi_j^2}{48\rho}(\rho - \alpha_{j+1})^3 - \frac{\varphi_j R_j}{48\rho}(\rho - \alpha_{j+1})^2 - \qquad (3.2)$$

$$\frac{\varphi_j^2}{8}\left(\frac{\rho^2}{3} - \rho\alpha_{j+1}\right) - R_j^2 - R_j\varphi_j\frac{\rho}{2} - \frac{p}{3}\rho^2 + p\alpha^2 - B_j\varphi_j + \frac{C_j}{\rho},$$

where $j = 0,\ldots,n$ and

$$C_0 = -\alpha + \frac{\varphi_0^2}{48}(\alpha - \alpha_1)^3 + \frac{\varphi_0 R_0}{4}(\alpha - \alpha_1)^2 + \frac{\varphi_0^2\alpha}{8}\left(\frac{\alpha^2}{3} -\right.$$

$$\left. - \alpha\alpha_1\right) + R_0^2\alpha + \varphi_0 R_0\frac{\alpha^2}{2} - \frac{2}{3}p\alpha^3 + \varphi_0 B_0\alpha. \qquad (3.3)$$

The quantities $C_1,\ldots,C_n$ can be calculated by means of (2.17).

The plasticity condition (2.6) at the plastic hinges α_j ($j = 1,\ldots,n$) and the boundary condition $m_1(1)=0$ give a set of nonlinear algebraic equations for determination parameters w_i ($i = 0,\ldots,n$):

$$\begin{aligned}
&1 + \frac{\varphi_n^2}{12} - \varphi_n B_n + C_n - \frac{p}{3} + p\alpha^2 = 0,\\
&\frac{\varphi_j\alpha_{j+1}}{12}(\varphi_j\alpha_{j+1} - 6R_j) - R_j^2 - B_j\varphi_j - \frac{p}{3}\alpha_{j+1}^2 +\\
&+ \frac{C_j}{\alpha_{j+1}} + \left(\frac{B_j}{\alpha_{j+1}} + R_j - \frac{\varphi_j\alpha_{j+1}}{8}\right)^2 + p\alpha^2 = 0.
\end{aligned} \qquad (3.4)$$

Here $j = 0,\ldots,n-1$.

4.Circular plates with piece-wise constant thickness

Let us consider a circular plate with piece-wise constant thickness. In this case

$$\gamma = \gamma_j, \quad \gamma_j \neq 1$$

for $\rho \in (\alpha_j,\alpha_{j+1})$ where $j = 0,\ldots,n$ and $\alpha_0 = 0$, $\alpha_{n+1}=1$. Here γ, γ_j ($j = 0,\ldots,n$) stand for the non-dimensional thickness in the region $\rho \in D_j$.

The plasticity condition may be written as

$$n_2^2 + m_2 = \gamma_j^2, \qquad j = 0,\dots,n \tag{4.1}$$

for the region $\rho \in D_j$ and as

$$n_1^2 + m_1 = \gamma_j^2 \tag{4.2}$$

at the boundaries $\rho = \alpha_j$.

The deflection distribution among plastic hinge circles will not change, e.g. the relations (2.1)-(2.5) remain valid. Instead of (2.6) we have now

$$m_1(\alpha_j) = \gamma_j^2 - n_1^2(\alpha_j), \tag{4.3}$$

where $j = 1,\dots,n$.

It should be mentioned that by the assumptions made in the present paper about the yield surface and deformation law, the non-dimensional membrane forces n_1, n_2 do not depend explicitly on the quantities γ_j.

Integrating the second equation of the equilibrium equations and taking into account the expressions (1.7), (2.1), (2.2), (2.11), (2.14), (2.15), (4.1) one obtains

$$m_1 = \gamma_j^2 - \frac{\varphi_j^2}{48\rho}(\rho - \alpha_{j+1})^3 - \frac{\varphi_j R_j}{4\rho}(\rho - \alpha_{j+1})^2 - \tag{4.4}$$

$$- \frac{\varphi_j^2}{8}\left[\frac{\rho^2}{3} - \rho\alpha_{j+1}\right] - R_j^2 - R_j\varphi_j\frac{\rho}{2} - \frac{p}{3}\rho^2 - B_j\varphi_j + \frac{C_j}{\rho}$$

for $\rho \in D_j$; $j = 0,\dots,n$. Constants C_j can be determined by means of continuity requirements as follows:

$$C_0 = 0, \quad C_j = C_{j-1} + \alpha_j(\gamma_{j-1}^2 - \gamma_j^2) + \frac{\varphi_j^2}{48}(\alpha_j - \alpha_{j+1})^3 +$$

$$+ \frac{\varphi_j R_j}{4}(\alpha_j - \alpha_{j+1})^2 + \alpha_j(R_j^2 - R_{j-1}^2) + \frac{\varphi_j^2}{8}\alpha_j^2\left[\frac{\alpha_j}{3} - \alpha_{j+1}\right] +$$

$$+ \frac{\varphi_{j-1}^2}{12}\alpha_j^3 + \frac{\alpha_j^2}{2}(\varphi_j R_j - \varphi_{j-1}R_{j-1}) - \alpha_j(\varphi_j B_j - \varphi_{j-1}B_{j-1}), \tag{4.5}$$

where $j = 1,\dots,n$.

First one of the relations for determination parameters w_j obtains the form

$$\gamma_n^2 + \frac{\varphi_n^2}{12} - \varphi_n B_n + C_n - \frac{p}{3} = 0, \tag{4.6}$$

whereas the other n relations coincide with (2.18).

5. Annular plates with piece-wise constant thickness

The previous analysis may be accommodated for the annular plates with piece-wise constant thickness. The membrane force n_1 may be expressed as

$$n_1 = \frac{\varphi_j}{4}\left[\frac{\rho}{2} - \alpha_{j+1}\right] + R_j + \frac{B_j}{\rho}$$

for $j = 0,\ldots,n$, where

$$B_0 = -\frac{\varphi_0}{4}\left[\frac{\alpha^2}{2} - \alpha_1\alpha\right] - R_0\alpha,$$

$$B_j = B_{j-1} - \frac{\alpha_j^2}{8}(\varphi_{j-1} + \varphi_j) + \frac{\varphi_j}{4}\alpha_j\alpha_{j+1} + \alpha_j(R_{j-1} - R_j).$$

The bending moment takes the form

$$m_1 = \gamma_j^2 - \frac{\varphi_j^2}{48\rho}(\rho - \alpha_{j+1})^3 - \frac{\varphi_j R_j}{4\rho}(\rho - \alpha_{j+1})^2 - \frac{\varphi_j^2}{8}\left[\frac{\rho^2}{3} - \right.$$

$$\left. - \rho\alpha_{j+1}\right) - R_j^2 - R_j\varphi_j\frac{\rho}{2} - \frac{p}{2}\rho^2 - B_j\varphi_j + \frac{C_j}{\rho} + p\alpha^2,$$

where $j = 0,\ldots,n$ and the integration constants may be expressed as

$$C_0 = -\alpha\gamma_0^2 + \frac{\varphi_0^2}{48}(\alpha - \alpha_1)^3 + \frac{\varphi_0 R_0}{4}(\alpha - \alpha_1)^2 + \frac{\varphi_0^2\alpha^2}{8}\left[\frac{\alpha}{3} - \right.$$

$$\left. - \alpha_1\right) + R_0^2\alpha + R_0\varphi_0\frac{\alpha^2}{2} - \frac{2}{3}p\alpha^3 + \varphi_0 B_0\alpha,$$

$$C_j = C_{j-1} + \alpha_j(\gamma_{j-1}^2 - \gamma_j^2) + \frac{\varphi_j^2}{48}(\alpha_j - \alpha_{j+1})^3 +$$

$$+ \frac{\varphi_j R_j}{4}(\alpha_j - \alpha_{j+1})^2 + \frac{\varphi_j^2}{8}\left[\frac{\alpha_j^2}{3} - \alpha_j\alpha_{j+1}\right] + \alpha_j(R_j^2 - R_{j-1}^2) +$$

$$+ \frac{\varphi_{j-1}^2}{8}\alpha_j^3 + \frac{\alpha_j^2}{2}(\varphi_j R_j - \varphi_{j-1}R_{j-1}) + \alpha_j(\varphi_j B_j - \varphi_{j-1}B_{j-1}).$$

The boundary condition $m_1(1) = 0$ gives

$$\gamma_n^2 + \frac{\varphi_n^2}{12} - \frac{p}{3} - B_n\varphi_n + C_n + p\alpha^2 = 0$$

and from the requirements (4.3) follow n other relations which coincide with (3.4).

6. Discussion

The results of calculations are presented in Fig. 3-8. Fig. 3 shows the load-deflection relation for a simply supported circular plate of constant thickness. In Fig.3 the curves signed by 1 and 3 represent the upper and lower bounds developed by Erkhov and Kislova [7]. Lines 2 and 4 correspond to the solutions obtained by Lepik [9], Onat and Haythornthwaite [5], respectively, for the plates whose material obeys the Tresca yield condition. Erkhov and Kislova used the approximation of the yield surface for the Tresca materials, which corresponds to the method of limited interaction between forces and moments.

Curve 5 in Fig.3 is obtained by the method suggested in the present paper. It corresponds to the kinematically admissible displacement field with one hinge in the center of the plate. The shaded region in Fig.3 presents the region of admissible solutions with two hinges (one of them is located at the center of the plate). It is worth emphasizing that the location of the hinges is not unique. However, the coordinate α_1 is not arbitrary in the present case. Restrictions to the values of α_1 are imposed obliquely; they are the consequences of the requirement of statical admissibility of the solution under consideration. The bounds to the location of the hinge circle off the center of the plate are presented in Fig.6 for different values of the maximal deflection w_0. The continuous lines in Fig.6 correspond to the circular plate, the discontinuous ones to the annular plate with inner radii $\alpha_0 = 0{,}1$.

Although the quantity α_1 may vary in quite a wide range as shown in Fig.6, the possible of location region of the corresponding load-deflection curve is comparatively narrow. Moreover, on the basis of Fig.6 one may draw a conclusion that the method suggested in the present paper leads to the load-deflection relation which is comparatively close to the results obtained by other authors. At the same time the solution associated with one hinge is very simple.

The moment distributions for solutions with one hinge are presented in Fig.4. The curves 1, 2, 3 and 4 correspond to the values of maximal deflection $w_0 = 0{,}5$; $w_0 = 2$; $w_0 = 3$ and $w_0 = 4$, respectively. The tendency of the bending moment to vanish at the center of the plate in case the deflection increases appears to be natural because the stress state tends to the membrane state, as shown by Lepik [9].

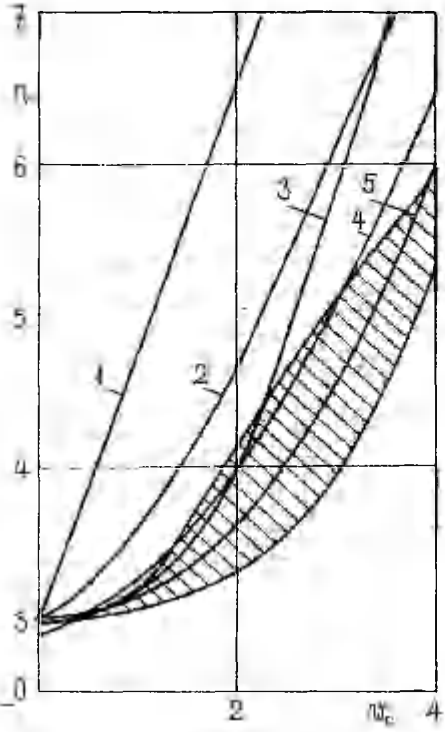

Fig. 3

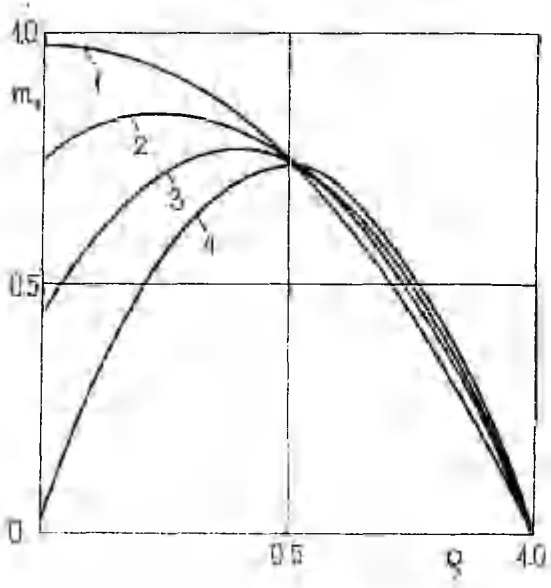

Fig. 4

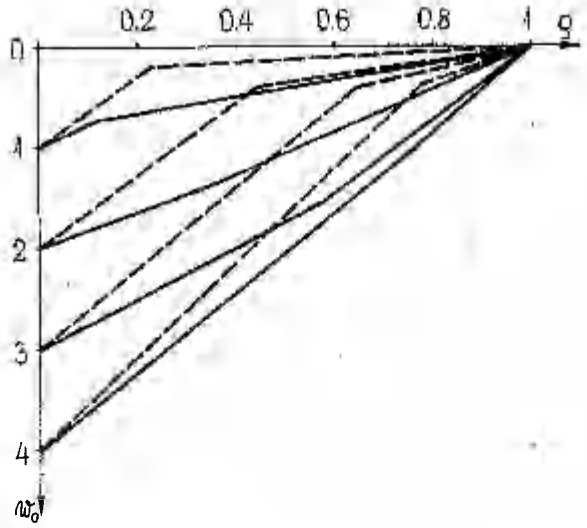

Fig. 5

Deflections of the circular plate corresponding to the solutions with two hinges are shown in Fig.5. Continuous and

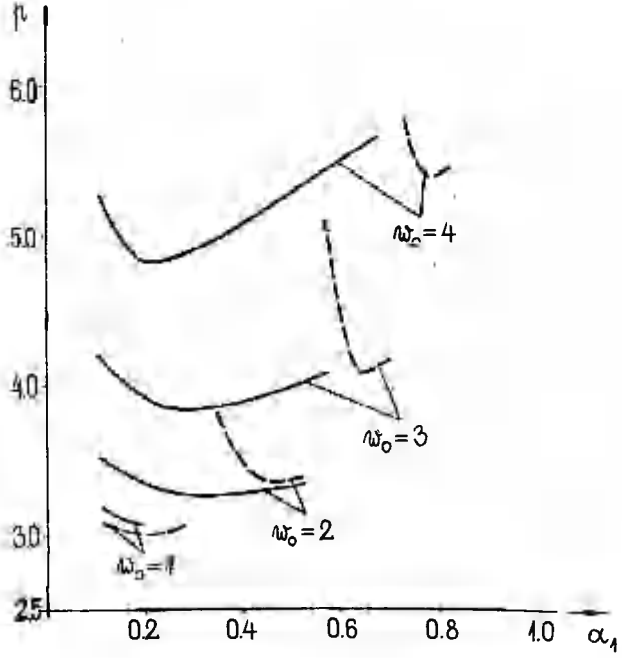

Fig. 6

dotted lines in Fig.5 correspond to the lower and upper bound, respectively, for fixed maximal deflection.

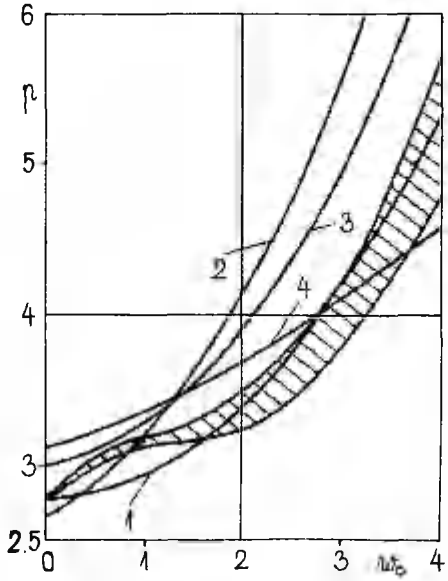

Fig. 7

Similar results obtained for annular plates are presented in Fig.6-8. Here the inner radii of the plate is $\alpha_0 = 0.1$. In Fig.7 there is shown the load-deflection relation obtained

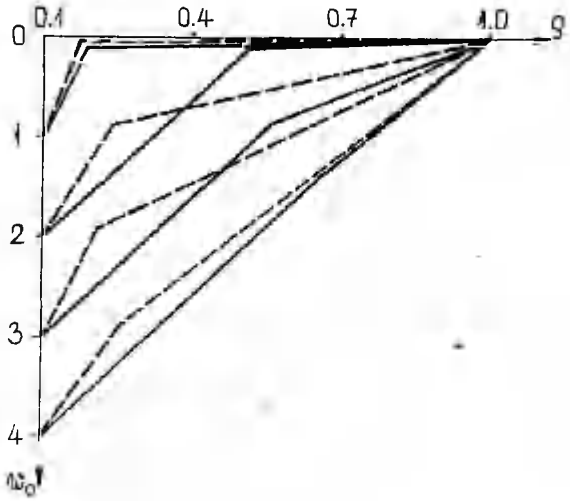

Fig. 8

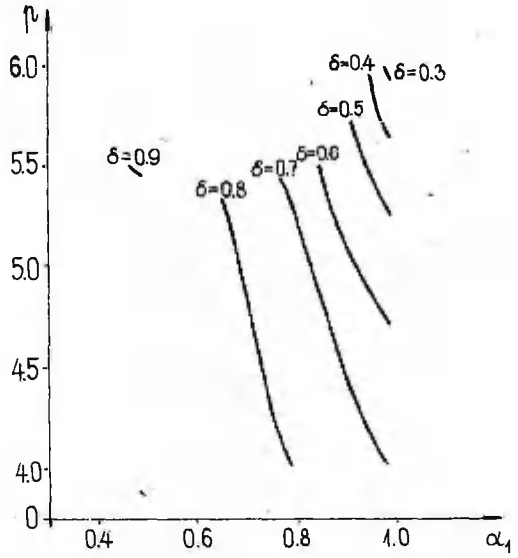

Fig. 9

from the solution without one hinge (curve 1). Herein is presented the region of admissible p - w_0 diagrams also associated with the mechanism with one hinge. As in the case of the circular plate, the striped region is comparatively narrow and it is situated not far from the line which corresponds to the solution without hinges. Curves 2, 3, and 4 calculated in [8] present the load-deflection relations for annular plates, subjected to the lateral pressure and radial tension in the case of the material which obeys the Von Mises yield condition. Lines 2, 3 and 4 correspond to the radial tensions $0,5N_*$, $0,3N_*$ and $0,1N_*$, respectively.

The values of the quantity α_1 in the case of circular plates of piece-wise constant thickness corresponding to the load intensity are presented in Fig.9. The results are obtained for $w_0 = 0,5$. Here $\gamma_0 = 1$ and $\delta = \gamma_1$.

References

1.Calladine C.R., Simple ideas in the large-deflection plastic theory of plates and slabs. Engineering Plasticity (Ed. J. Heyman and F.A. Leckie). Cambridge University Press, 1968, 93-127.

2.Jones N., Combined distributed loads on rigid-plastic

circular plates with large deflections. Int. J. Solids and Struct., 1969, 5(1), 51-64.
3.Kondo K., Plan T. H. H., Large deformations of rigid-plastic circular plates. Int. J. Solids and Struct., 1981, 17(11), 1043-1055.
4.Kondo K., Plan T. H. H., Large deformations of rigid-plastic polygonal plates. J. Struct. Mech., 1981, 9(3), 271-293.
5.Onat E. T., Haythornthwalte R. M., Load carrying capacity of circular plates at large deflection. J. Appl. Mech., 1956, 23, 49-55.
6.Sawczuk A., Wprowadzenie do mechaniki konstrukcji plastycznych. Warszawa, PWN, 1982.
7.Ерхов М.И., Кислова Л.В., Большие прогибы жестко-пластических круглых пластинок с шарнирным опиранием края. В сб.: "Исслед. по строит. мех. и методам расчета ". М., 1981, 4-12.
8.Леллеп Я., Маяк Ю., Большие прогибы жестко-пластических кольцевых пластин. Уч. зап. Тартуск. ун-та, 1987, 772, 33-43.
9.Лепик Ю. Р., Пластическое течение гибких круглых пластинок из жестко-пластического материала. Изв. АН СССР. Мех. и машиностр., 1960, 2, 78-87.

ПРИБЛИЖЕННЫЙ АНАЛИЗ БОЛЬШИХ ПЛАСТИЧЕСКИХ ДЕФОРМАЦИЙ КРУГЛЫХ И КОЛЬЦЕВЫХ ПЛАСТИН

Ян Леллеп, Хелле Хейн
Тартуский университет

Резюме

Исследуется задача деформирования круглых и кольцевых пластин при больших прогибах. Материал пластины жестко-пластический, подчиняющийся условию пластичности Треска и ассоциированному закону деформирования. Предполагается, что пластина приобретает форму пересекающихся конусов, разделенных шарнирными окружностями. Найдены решения для круглых и кольцевых пластин при постоянной и кусочно-постоянной толщине.

Acta Et Commentationes Universitatis Tartuensis. 939. 1992

OPTIMAL LOCATIONS OF RIGID STIFFENERS FOR A GEOMETRICALLY NON-LINEAR PLASTIC CYLINDRICAL SHELL

Jaan Lellep and Sander Hannus
Tartu University

Abstract. An optimal design method is developed for plastic cylindrical shells with stiffeners. The optimal location of the stiffeners is determined for a shell of the Von Mises material. Geometrical non-linearity is taken into account.

The problem is transformed into a boundary-value problem, which is solved numerically. The numerical results are presented for the case when the shell is strengthened with the aid of one rigid hoop stiffener.

Introduction

One of the possibilities to increase the compliance or load carrying capacity of sructures is to furnish them with additional rigid supports. With regard to the cylindrical tubes subjected to the internal pressure loading this implies the use of the rigid hoop stiffeners. It is reasonable to determine the position of the additional supports or stiffeners so that the optimality criterion attains the minimum value.

The early works devoted to the determination of the optimal positions of additional supports by Mróz and Rozvany [3,4], also by Lepik [8]. Cinquini and Kouam [1] studied the plastic cylindrical shells with stiffeners in the case of the Tresca material, whereas in [7] a shell of maximal load carrying capacity of the Von Mises material was examined. Geometrical non-linearity is taken into account in [2,6] assuming that the material obeys the Tresca yield condition.

1. Basic equations and preliminaries

The behaviour of a rigid-plastic circular cylindrical shell of radii R and length 2l is studied in the present paper. The internal loading is assumed to consist of two components - of the lateral pressure of intensity P and of axial tension N_1. The left-hand end of the shell is built in, whereas the right end is simply supported.

Moreover, at the positions $x = S_j$, where $j = 1,\ldots,n$ there are located absolutely rigid ring supports (rigid hoop stiffeners).

The problem consists in the determination of the optimal positions for additional supports. The optimality of the solution is meant in the sense of the minimum of the criterion

$$J = \int_0^{2l} W^k dx, \tag{1.1}$$

where W is the lateral deflection, k stands for a fixed number ($k \geq 1$). Optimality criterion (1.1) may be interpreted as an approximation of the criterion

$$J_1 = \max_{x \in [0,2l]} |W(x)| \tag{1.2}$$

as shown by Banichuk [5].

Since the use of the optimality criterion (1.2) is quite complicated due to the non-differentiability of (1.2) in the present paper (1.1) will be employed.

The posed problem will be handled as a problem of the optimal control theory, provided S_j ($j = 1,\ldots,n$) are preliminarily unknown parameters. The equations which have to be met by state variables and a control are the corollaries of the constitutive and equilibrium equations of the large deflection theory of cylindrical shells.

Material of the shell is assumed to be rigid-plastic one and obey the Von Mises yield condition in the approximated form

$$n_1^2 - n_1 n_2 + n_2^2 + \frac{3}{4} m^2 - 1 = 0, \tag{1.3}$$

where $n_{1,2} = N_{1,2}/N_0$, $m = M/M_0$, N_0 and M_0 being the yield load and yield moment, respectively.

Using the equilibrium equations and employing the associated deformation law (the law of gradientality in the deformation-type theory of plasticity) one obtains the following set of equations (the variables q and z may be referred to as additional state variables and u stands for the non-dimensional axial displacement):

$$m' = q, \qquad q' = \frac{3\omega w n_1 m}{2(2n_2 - n_1)} + \omega(p - n_2),$$

$$w' = z, \qquad z' = \frac{3\omega w m}{2(2n_2 - n_1)}, \tag{1.4}$$

$$u^* = -\frac{1}{2}z^2 + \frac{\omega w(2n_1 - n_2)}{2n_2 - n_1}.$$

In (1.4) primes denote differentiation with respect to the non-dimensional coordinate ξ and

$$\xi = \frac{x}{l}, \quad \omega = \frac{N_0 l^2}{RM_0}, \quad p = \frac{RP}{N_0},$$
$$w = \frac{N_0 W}{M_0}, \quad u = \frac{Ul N_0^2}{M_0^2}, \quad s_j = \frac{S_j}{l}. \tag{1.5}$$

Since each part of the shell has to operate in the plastic stage we have to take into account the restrictions

$$p - p_j \geq 0, \qquad j = 0,\ldots,n, \tag{1.6}$$

where p_j stands for the limit load for this part of the shell which is located among the supports at $\xi = s_j$ and $\xi = s_{j+1}$. Here $s_0 = 0$ and $s_{n+1} = 2$. Evidently, the load carrying capacity of a cylindrical shell depends upon the internal loading as well as on the parameters s_j and s_{j+1}. For fixed values s_j and s_{j+1} it will be calculated numerically.

Thus, the posed problem consists in the minimization of the functional (1.1) accounting for the differential restrictions (1.4) as well as the algebraic restriction (1.3) and inequalities (1.6). It appears to be convenient to transform (1.6) into

$$p - p_j - \theta_j^2 = 0, \qquad j = 0,\ldots,n, \tag{1.7}$$

where the quantities θ_j will be handled as preliminarily unknown constant parameters.

It is reasonable to assume that the stationary plastic hinges are located at $\xi = s_j$ $(j = 0,\ldots,n)$. Therefore, the corresponding boundary and intermediate conditions may be written as

$$m(s_j) = m_*, \qquad w(s_j) = 0, \qquad j = 0,\ldots,n, \tag{1.8}$$

$$m(s_{n+1}) = w(s_{n+1}) = 0. \tag{1.9}$$

The hypothesis about plastic hinge circles introduces the need for discontinuites of variables q and z at $\xi = s_j$ $(j = 1,\ldots,n)$.

2. Optimality conditions

In order to obtain necessary optimality conditions let us

introduce Lagrangeian multipliers φ, ν_j $(j = 0,\ldots,n)$ and adjoint variables ϕ_i $(i = 1,\ldots,5)$. Using the Lagrangeian multipliers the functional (1.1) may be presented as

$$J_* = \sum_{j=0}^{n} \int_{s_j}^{s_{j+1}} \Big[w^k + \phi_1(m' - q) + \phi_2\Big(q' - \frac{3\omega n_1 mw}{z(2n_2 - n_1)} - \omega(p - n_2)\Big) +$$

$$+ \phi_3(w' - z) + \phi_4\Big(z' - \frac{3\omega mw}{z(2n_2 - n_1)}\Big) + \phi_5\Big(\frac{\omega w(n_2 - 2n_1)}{2n_2 - n_1} +$$

$$+ u' + \frac{z^2}{2}\Big) + \varphi\Big(n_1^2 - n_1 n_2 + n_2^2 + \frac{3}{4} m^2 - 1\Big)\Big] d\xi +$$

$$+ \sum_{j=0}^{n} \nu_j(p - p_j - \theta_j^2). \qquad (2.1)$$

Let us calculate the variation of the functional (2.1) denoting the variations of state variables by δm, δq, δw, δz, δu, respectively. At the same time one has to take into account that the state variables q, z, and u as well as the control ones may have discontinuites at $\xi = s_j$ $(j = 1,\ldots,n)$. Moreover, the parameters s_j $(j = 1,\ldots,n)$ as well as p_j and θ_j are not preliminarily fixed. Therefore, one has to distinguish between the values of weak variation δy and full variation Δy of a state variable y at $\xi = s_j$. They are related to each other as follows:

$$\Delta y(s_j \pm) = \delta y(s_j \pm) + y'(s_j \pm)\Delta s_j. \qquad (2.2)$$

Here the signs plus and minus denote the right and left hand limits at $\xi = s_j$, respectively.

Determining the full variation of the functional (2.1) one obtains the equation

$$\sum_{j=0}^{n} \int_{s_j}^{s_{j+1}} \Big[kw^{k-1}\delta w + \phi_1 \delta m' - \phi_1 \delta q + \phi_2 \delta q' + \omega\phi_2 \delta n_2 - \frac{3\omega}{2}(\phi_4 +$$

$$+ n_1\phi_2)\Big(\frac{w\delta m + m\delta w}{2n_2 - n_1} - \frac{2mw\delta n_2}{(2n_2 - n_1)z}\Big) + \phi_3 \delta w' - \phi_3 dz + \phi_4 \delta z' +$$

$$+ \phi_5 \delta u' + \phi_5 z \delta z - \frac{\omega\phi_5(2n_1 - n_2)\delta w}{2n_2 - n_1} + \omega\phi_5 w \frac{3n_1 \delta n_2}{(2n_2 - n_1)^2} + \qquad (2.3)$$

$$- \varphi(n_1 \delta n_2 - 2n_2 \delta n_2 - \frac{3}{2} m\delta m)\Big] d\xi - \sum_{j=0}^{n} \nu_j(\Delta p_j + 2\theta_j \delta\theta_j) = 0.$$

According to (2.3) the adjoint set has the form

$$\phi_1' = -\frac{3\omega}{2} w \frac{(\phi_4 + n_1)}{2n_2 - n} + \frac{3}{2} \varphi m,$$

$$\phi_2' = -\phi_1,$$

$$\phi_3' = kw^{k-1} + \frac{\omega}{2n_2 - n_1}\left[-\frac{3}{2}(\phi_4 + n_1\phi_2)m + \phi_5(2n_1 - n_2)\right], \qquad (2.4)$$

$$\phi_4' = -\phi_3 + \phi_5 z,$$

$$\phi_5' = 0.$$

Since the variable n_2 is a control variable and p_j, θ_j - parameters one obtains from (2.3)

$$\omega\phi_2 + \frac{\omega w}{(2n_2 - n_1)z}\left[3m(\phi_4 + n_1\phi_2) + 3n_1\phi_5\right] + \varphi(2n_2 - n_1) = 0 \qquad (2.5)$$

and

$$\nu_j\theta_j = 0, \qquad j = 0,\ldots,n. \qquad (2.6)$$

Taking into account (2.4)-(2.6) one can present (2.3) as

$$\sum_{j=1}^{n}\left\{\left[\phi_1\delta_m + \phi_2\delta q + \phi_3\delta w + \phi_4\delta z\ \phi_5\delta u\right]_{\xi=s_j} - \nu_j\Delta p_j\right\} +$$

$$+ \phi_2(2)\,\Delta q(2) + \phi_4(2)\Delta z(2) + \phi_5(2)\Delta u(2) - \qquad (2.7)$$

$$- \phi_2(0)\Delta q(0) - \phi_4(0)\delta z(0) - \phi_5(0)\Delta u(0) = 0,$$

where quadratic brackets denote the jumps of the corresponding quantities and the requirements for m and w are met.

Evidently the limit loads p_j depend on s_j and s_{j+1}. Therefore

$$\Delta p_j = \frac{\partial p_j}{\partial s_j}\Delta s_j + \frac{\partial p_j}{\partial s_{j+1}}\Delta s_{j+1}. \qquad (2.8)$$

The weak variations of state variables in (2.7) are related to the full variations as shown in (2.2). Considering the variations $\Delta q(s_j\pm)$, $\Delta z(s_j\pm)$, $\Delta u(s_j\pm)$ as independent quantities (similarly Δq, Δz and Δu are free at the both ends of the optimal trajectory) (2.7) yields

$$\phi_2(s_j) = \phi_4(s_j) = \phi_5(s_j) = 0, \qquad j = 0,\ldots,n+1. \qquad (2.9)$$

Using the boundary and intermediate conditions (2.2) for the adjoint variables as well as the relations

$$\delta m(s_j\pm) = -\,q(s_j\pm)\Delta s_j, \quad \delta w(s_j\pm) = -\,z(s_j\pm)\Delta s_j, \qquad (2.10)$$

which are the natural consequences of requirements (1.8) the

equation (2.7) may be transformed into the form

$$\sum_{j=1}^{n}\left[\phi_1(s_j)q(s_j) + \phi_3(s_j)z(s_j)\right]\Delta s_j + \sum_{j=0}^{n}\nu_j\Delta p_j = 0. \qquad (2.11)$$

Making use of (2.8) one obtains from (2.11)

$$\left[\phi_1(s_j)q(s_j) + \phi_3(s_j)z(s_j)\right] + \sum_{i=0}^{n}\frac{\partial}{\partial s_j}(\nu_i p_i) = 0, \qquad (2.12)$$

$$j = 1,\ldots,n.$$

3. Optimal solution

In order to solve the set (2.12) we have to integrate equations (1.4) and (2.4) making use of the boundary and intermediate conditions (1.8), (1.9), (2.9) as well as the requirements (1.3), (1.6), (2.5), (2.6). The numerical solution procedure may be simplified, since according to (2.4) and (2.9)

$$\phi_5 = 0. \qquad (3.1)$$

Substitution of (3.1) into (2.5) gives the relation

$$\varphi = \frac{-\omega\phi_2}{2n_2 - n_1} - \omega w\,\frac{3m(\phi_4 + n_1\phi_2)}{(2n_2 - n_1)^3}, \qquad (3.2)$$

which should be applied in the right-hand side of the set (2.4).

The use of (2.12) is complicated as for as the Lagrange'lan multipliers $\nu_j (j = 0,\ldots,n)$ are not specified.It follows from (2.6) that either $\nu_j = 0$ or $\theta_j = 0$. The latter version implies that according to (1.7) $p_j = p$. In other words the stress state in the correspodlng part of the shell is associated with the limit load. However, the problems of the optimal design of cylindrical shells with additional supports were studied in [7], assuming that the load intensity equals the load carrying capacity of the shell. In the present study the attention is focused on the post-yield behaviour of the shell under consideration.

Thus, it is reasonable to examine the cases, when $p_j \neq p$ e.g. $\theta \neq 0$. Therefore, now $\nu_j = 0$ and equations (2.12) can be converted into

$$\left[\phi_1(s_j)q(s_j) + \phi_3(s_j)z(s_j)\right] = 0, \qquad j = 1,\ldots,n\ . \qquad (3.3)$$

However, one has to take into account that the possibility may be realized when a part of the shell, say region

(s_{j-1}, s_j) is in the limit state, but (s_j, s_{j+1}) is associated with finite deflections. In this case $\nu_{j-1} \neq 0$ and $\nu_j = 0$. Thus, we must employ equation (2.12) for determination of the corresponding Lagrangian multiplier ν_{j-1}.

The problem is completely solved numerically using the Runge-Kutta fourth-order method for integration of equations (1.4) and (2.4). Specifying $s_j (j = 1,\ldots,n)$, (1.4) can be solved substituting, according to (1.3)

$$n_2 = \frac{n_1}{2} + \sqrt{1 - \frac{3}{4}(m^2 + n_1^2)}. \qquad (3.4)$$

Substituting the values of state variables as well as φ and n_2 from (3.2) and (3.4) into (2.4) one can integrate these equations. Finally the improvements for coordinates s_j $(j = 1,\ldots,n)$ are calculated making use of (2.12) and (3.3), respectively.

4. Discussion

The results are presented for the case $n = 1$ in Fig.1 and Fig.2. In Fig.1 distributions of the transverse displacements are given. In this example the following values of the non-dimensional parameters are chosen: $\omega = 8$, $p = 1.96$, $n_1 = 0.2$. Curves 1, 2 and 3 correspond to $s = s_a$, $s = s_c$, respectively. These values are defined as follows:

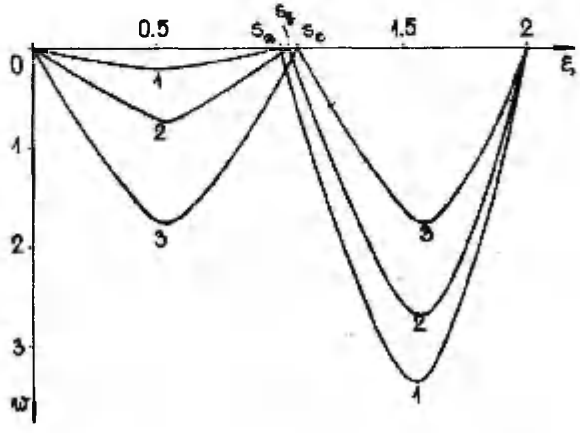

Fig. 1

a)the support is located in the center of the shell $(s = s_a = 1.0)$; b)the location of the support coincides with the optimal position associated with the mean deflection, i.e. taking into account criterion (1.1)$(s = s_b = 1.03054)$;

c)the optimal location of the support is determined by means of the minimum of the maximal deflection of the shell ($s = s_c = 1.07291$).

Distributions of the bending moments are given in Fig.2. Here, curves 1,2 and 3 correspond to the cases a), b) and c), respectively.

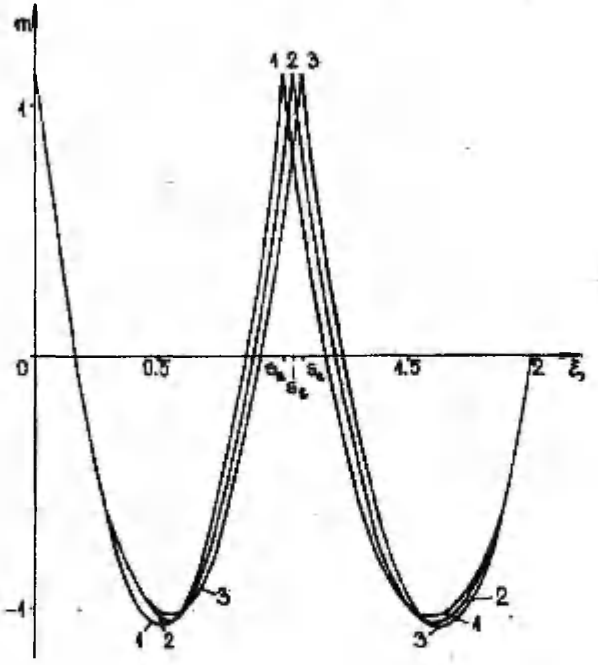

Fig. 2

References

1.Cinquini C., Kouam M., Optimal plastic design of stiffened shells. Int. J. Solids and Struct., 1983, 19(9), 773-783.

2.Lellep J., Parametrical optimization of plastic cylindrical shells in the post-yield range. Int. J. Eng. Sci., 1985, 23(12), 1289-1303.

3.Mróz Z., Rozvany G.I.N., Optimal design of structures with variable support conditions. J.Optimiz. Theory and Appl., 1975, 15(1), 85-101.

4.Rozvany G.I.N., Optimal design of flexural systems. Pergamon Press, 1976.

5. Баничук Н.В., Оптимизация форм упругих тел. М., Наука, 1980.
6. Леллеп Я.А., Оптимальное расположение дополнительных опор к геометрически нелинейной пластической цилиндрической оболочке. Прикл. мех., 1985, 1, 60-66.
7. Леллеп Я., Ханнус С., Оптимизация расположения дополнительных опор к пластической цилиндрической оболочке. Уч. зап. Тартуск. ун-та, 1988, 799, 21-26.
8. Лепик Ю., Оптимальное проектирование конструкций в случае динамического нагружения. Таллинн, Валгус, 1982.

ОПТИМАЛЬНОЕ РАСПОЛОЖЕНИЕ ЖЕСТКИХ КРУГОВЫХ ОПОР К ГЕОМЕТРИЧЕСКИ НЕЛИНЕЙНЫМ ПЛАСТИЧЕСКИМ ЦИЛИНДРИЧЕСКИМ ОБОЛОЧКАМ

Ян Леллеп, Сандер Ханнус
Тартуский университет

Резюме

В работе выработан метод определения оптимального расположения дополнительных круговых опор к пластическим цилиндрическим оболочкам. Предполагается, что материал оболочки подчиняется условию пластичности Мизеса. Учитываются умеренно большие прогибы. Поставленная проблема сводится к граничной задаче, которая решается численно. Результаты вычислений приводятся в случае одной дополнительной опоры.

Acta Et Commentationes Universitatis Tartuensis, 939, 1992

THE ONE-DIMENSIONAL EQUI-STRENGTH PROBLEM FOR NONHOMOGENEOUS SPHERICAL VESSELS, CYLINDRICAL TUBES AND ANNULAR DISCS RELATIVE TO ARBITRARY YIELD POLYGON

Kalle Hein and Mati Heinloo
Tartu University

Abstract. The design of nonhomogeneous equi-strength spherical vessels, cylindrical tubes and annular discs, subjected to quasistatic loads upon the internal and external radii is presented. The rotation of the tubes and disks around their axis and the dependence of their physical and mechanical qualities on radial coordinate is assumed. The statically allowed limit stress states, determined by the sides of the arbitrary yield polygon, are analyzed in detail. The equations for determination of the rational distributions of the Young modulus which guarantee the change from the elastic state to the plastic one simultaneously at all points of the examined constructions, when their quasistatic loads get the limit values have been obtained.

Notation

p_1 – internal pressure;
p_2 – external pressure;
$\sigma_r^\circ, \sigma_\theta^\circ$ – radial and hoop stresses;
σ_z° – axial stress component for tube;
u – radial displacement;
ρ – radial coordinate;
a – inner radius;
b – outer radius;
σ° – yield stress;
ν – the Poisson ratio;
E° – the Young modulus;
h° – disk thickness;
ω° – angular velocity for rotating discs and tubes;
T_1° – inner temperature;
T_2° – outer temperature;
η – linear thermal expansion coefficient;
γ – density;
$\varepsilon_r, \varepsilon_\theta$ – radial and hoop strain components;
ε_z – axial strain component for tube;

T_* - temperature in the natural state, when the stress and strain components are equal to zero;

It is convenient to introduce the following dimensionless quantities:

$$r = \frac{\rho}{b};\ \alpha = \frac{a}{b};\ \sigma_r = \frac{\sigma_r^\circ}{\sigma^\circ};\ \sigma_\theta = \frac{\sigma_\theta^\circ}{\sigma^\circ};\ \sigma_z = \frac{\sigma_z^\circ}{\sigma^\circ};\ \nu;\ \varepsilon_r;$$

$$E = \frac{E^\circ}{\sigma^\circ};\ u = \frac{u^\circ}{b};\ h = \frac{h^\circ}{b};\ \omega = \frac{\gamma(\omega^\circ b)^2}{\sigma^\circ};\ \varepsilon_\theta;\ \varepsilon_z;$$

$$T = \frac{T^\circ}{T_*};\ T_2 = \frac{T_2^\circ}{T_*} - 1;\ T_1 = \frac{T_1^\circ}{T_*} - 1;\ \eta = \eta^\circ T_*;$$

$$p_1 = \frac{p_1^\circ}{\sigma^\circ};\ p_2 = \frac{p_2^\circ}{\sigma^\circ}.$$

1. Introduction

Many of modern methods of regulation of the stress state of nonhomogeneous bodies by special distribution of the qualities of the materials open an important trend in the optimal design of nonhomogeneous constructions. In the first investigations [7, 16] distributions of the material's qualities that give prescribed statically allowed stresses in the nonhomogeneous constructions has been obtained by means of the reciprocal method. Some of papers [1, 3-6, 8-10, 12, 14, 15, 17] had determined distributions of the qualities for materials that guarantee the extreme for set parameter. In a few of the papers on the stresses lay some additional requirements in the optimal design of the nonhomogeneity. For example E. P. Kondakov [13] found the distribution of the Young modulus, that guarantees the constant hoop stresses in cylindrical tube, loaded by internal pressure. K. Hein and M. Heinloo solved the elasticity problem with the additional requirement that the stresses satisfy the Tresca [2, 18-21, 23, 24] or Von Mises [21, 22, 25] yield conditions simultaneously at all points. This requirement guarantee the change of the construction from the elastic state to the plastic one simultaneously at all points while the quasi-static loads get their limit values. Constructions permitting such changes are called equi-strength constructions. The equi-strength rotating discs with regard to the Von Mises yield criterion were obtained by Yhe Kai-Yuan and Liu Ping

[11] by an appropriate choice of thickness distribution. The investigations in papers [2, 18-25] show, that the equi--strength annular discs, spherical vessels and cylindrical tubes have obvious advantages over analogous homogeneous constructions. The aim of this paper is to generalize the results of papers [2, 18-21, 23, 24] to the arbitrary piecewise linear yield polygon.

2. Basic equations

Let us assume that the spherical vessels, cylindrical tubes and annular discs are made of an isotropic nonhomogeneous linearly elastic material which obeys the linear yield criterion, corresponding to the sides of arbitrary yield polygon. We also suppose, that the discs and tubes are rotating with constant angular velocity. These constructions are subjected to normal quasistatic loads upon their internal and external radii in the stationary temperature field. The physical and mechanical quantities depend on radial coordinate r.

Under such assumptions the stresses σ_r and σ_θ must satisfy the following equilibrium equation:

$$\sigma_r' - \frac{q}{r}(\sigma_\theta - \sigma_r) + \frac{h'}{h}\sigma_r + \omega r = 0, \tag{1}$$

where for cylinder $h' = 0$, $q = 1$, for disc $q = 1$ and for sphere $h' = 0$, $q = 2$, $\omega = 0$. Here and further the prime denotes the derivative on coordinate r.

We have the following compatibility equation:

$$\varepsilon_\theta - \varepsilon_r + r\varepsilon_\theta' = 0 \tag{2}$$

and the Hooke's law

$$\begin{aligned}
\varepsilon_r &= \frac{1}{E}\left[\sigma_r - \nu(\sigma_\theta + \sigma_z)\right] + \eta T, \\
\varepsilon_\theta &= \frac{1}{E}\left[\sigma_\theta - \nu(\sigma_r + \sigma_z)\right] + \eta T, \\
\varepsilon_z &= \frac{1}{E}\left[\sigma_z - \nu(\sigma_r + \sigma_\theta)\right] + \eta T.
\end{aligned} \tag{3}$$

In the case of spherical vessel we must take $\varepsilon_z = \varepsilon_\theta$, $\sigma_z = \sigma_\theta$.

We assume, that the cylindrical tube is in plane strain state and annular disk in plane stress state. It means, that we have $\sigma_z = 0$ for the disc and $\varepsilon_z = 0$ for the tube. The latter condition gives

$$\sigma_z = \nu(\sigma_r + \sigma_\theta) - E\eta T. \qquad (4)$$

The function T(r) may be determined from the heat conduction equation

$$\frac{d}{dr_1}\left[r_1^q\, k\, \frac{dT_1}{dr_1}\right] = 0$$

for stationary temperature field which solution has the form

$$T(r) = T_2 - (T_2 - T_1)\frac{\ln r}{\ln \alpha} \qquad (5)$$

for tube and disc and

$$T(r) = \frac{1}{r(1-\alpha)}\left[T_1\alpha(1-r) + T_2(r-\alpha)\right] \qquad (6)$$

for sphere, when the heat conduction coefficient k does not depend from r.

Let us formulate now the next problem: **To find such distributions of the qualities for the material that guarantee the change from the elastic state to plastic one simultaneously at all points of the construction, while the quasistatic stresses achieve their limit values.**

According to the statement of the problem the stresses must satisfy the prescribed yield condition

$$f(\sigma_r, \sigma_\theta, \sigma_z) = 0 \qquad (7)$$

at all values of coordinate r at the moment of change from the elastic to the plastic state.

Taking into account (4) and substitute ε_r and ε_θ from (3) into (2) we get the following equation:

$$(1+\nu^*)(\sigma_\theta - \sigma_r) + r\left[\frac{\varkappa'}{\varkappa} - \frac{E'}{E}\right]\left[(1+\nu^* - q\nu'^*)\sigma_\theta - \nu^*\sigma_r\right] +$$
$$+ r\left[(1+\nu^* - q\nu^*)\sigma_\theta' - \nu^*\sigma_r' - \nu^{*\prime}(\sigma_r - (1-q)\sigma_\theta)\right] + \qquad (8)$$
$$+ \frac{E}{\varkappa}(\eta^{*\prime}T + \eta^*T') = 0,$$

where $\varkappa = 1$, $q = 2$, $\nu^* = \nu$, $\eta^* = \eta$ for sphere, $\varkappa = 1$, $q = 1$, $\nu^* = \nu$, $\eta^* = \eta$, for disk and $\varkappa = 1 - \nu^2$, $\nu^* = \nu/(1-\nu)$, $q = 1$, $\eta^* = (1+\nu)\eta$ for tube.

Thus, for solution of the set problem we have the system of equations (1), (7) and (8). This system connect eight functions $\sigma_r = \sigma_r(r)$, $\sigma_\theta = \sigma_\theta(r)$, $\sigma = \sigma(r)$, $h = h(r)$, $\omega = \omega(r)$, $E = E(r)$, $\nu = \nu(r)$, $\eta = \eta(r)$ five of which must be described and three functions can be determined.

For determination of the displacement u(r) we can use the following formula:

$$u(r) = r\varepsilon_0(r). \tag{9}$$

It is noteworthy that in several cases we can first solve the system of equations (1), (7) and then using the solution of this system also equation (8). It means that the solving of the set problem can be split up into the problems of determination of the statically allowed stress states satisfying the prescribed yield condition, and of determination of the rational distributions of material qualities. Notice that the splitting, pointed out above, take place for tubes only if, $T(r) \equiv 0$. For getting the united solution to tubes, discs and spheres we shall assume that $T(r) \equiv 0$ for a tube.

We consider further, that σ, ω, η, ν are constants $h(r)$ - the prescribed function and we shall find the functions $\sigma_r = \sigma_r(r)$, $\sigma_\theta = \sigma_\theta(r)$, $E = E(r)$.

3. Analysis of statically allowed stress states

Modern materials, which are used in building up constructions, possess a wide spectrum of plastic properties for description of which various yield conditions are applied. In connect with that we shall investigate the problem, set for arbitrary yield polygon with the tops in the points $A_i(x_i, y_i)$ $(i=1,2,\ldots,n)$ on the plane σ_r, σ_θ (Fig.). Then the yield condition, corresponding to the side A_kA_{k+1}, where $x_{k+1} \neq x_k$, of yield polygon, has the following form:

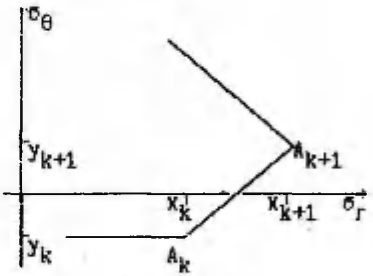

Fig.

$$\sigma_\theta^k = a_k\sigma_r^k + b_k, \tag{10}$$

and

$$\min(x_k, x_{k+1}) \leq \sigma_r^k \leq \max(x_k, x_{k+1}). \tag{11}$$

Here σ_r^k and σ_θ^k are the stresses on the side A_kA_{k+1} of yield polygon, and

$$a_k = \frac{y_{k+1} - y_k}{x_{k+1} - x_k}, \qquad b_k = \frac{y_k x_{k+1} - x_k y_{k+1}}{x_{k+1} - x_k}.$$

For $x_{k+1} = x_k$, the yield condition has the form

$$\sigma_r^k = x_k, \tag{12}$$

and

$$\min(y_k, y_{k+1}) \le \sigma_\theta^k \le \max(y_k, y_{k+1}). \tag{13}$$

According to the set problem we suppose that (10), (11) takes place at the certain region for r. Then substitution (10) to (1) give

$$\sigma_r^{k\cdot} + \frac{qf_k}{r}\sigma_r^k = \frac{qb_k}{r} - \omega r, \tag{14}$$

where

$$f_k = 1 - a_k + \frac{h'r}{hq}.$$

The solution of the differential equation (14) may be written as follows:

$$\sigma_r^k = \frac{1}{f_1^k}\left[\int_\alpha^r \left(\frac{qb_k}{r} - \omega r\right) f_1^k dr + \sigma_r^k(\alpha)\right], \tag{15}$$

where

$$f_1^k = \exp\left[q\int_\alpha^r \frac{f_k(\xi)}{\xi}\, d\xi\right].$$

Let us assume that inequalities (11) take place at $r = \alpha$ and $r_1 = \min(r_1^*, r_1^{**})$, where r_1^* $(r_1^* \ge \alpha)$ the minimum positive solution of equation $\sigma_r^k(r) = \max(x_k, x_{k+1})$ and r_1^{**} $(r_1^{**} \ge \alpha)$ the minimum positive solution of equation $\sigma_r^k(r) = \min(x_k, x_{k+1})$. If $r_1 \ge 1$, then the yield condition (10), (11) is satisfied $\forall$ r, $r \in [\alpha, 1]$ and from (15) we get the next connection between boundary values $\sigma_r^k(\alpha)$ and $\sigma_r^k(1)$:

$$\sigma_r^k(1) f_1(1) = \int_\alpha^1 \left(\frac{qb_k}{r} - \omega r\right) f_1^k dr + \sigma_r^k(\alpha). \tag{16}$$

If $r_1 \le 1$, then the yield condition (10),(11) will be satisfied only for $\forall$ r, $r \in [\alpha, r_1]$, and (15) will yield

$$\sigma_r^k(r_1) f_1^k(r_1) = \int_\alpha^{r_1} \left(\frac{qb_k}{r} - \omega r\right) f_1^k dr + \sigma_r^k(\alpha). \tag{17}$$

For $r > r_1$ one can suppose, that

$$\sigma_\theta^{k+1} = a_{k+1}\sigma_r^{k+1} + b_{k+1}, \tag{18}$$

and

$$\min(x_{k+1},x_{k+2}) \le \sigma_r^{k+1} \le \max(x_{k+1},x_{k+2}), \qquad (19)$$

when $\sigma_r^k(r_1) = \max(x_k,x_{k+1})$ or

$$\sigma_\theta^{k-1} = a_{k-1}\sigma_r^{k-1} + b_{k-1},$$

and

$$\min(x_{k-1},x_k) \le \sigma_r^{k-1} \le \max(x_{k-1},x_k),$$

when $\sigma_r^k(r_1) = \min(x_k,x_{k+1})$.
For example, for yield condition (18), (19) one can have

$$\sigma_r^{k+1} = \frac{1}{f_1^{k+1}}\left[\int_{r_1}^{r}\left(\frac{qb_{k+1}}{r} - \omega r\right)f_1^{k+1}dr + \sigma_r^k(r_1)\right], \qquad (20)$$

where

$$f_1^{k+1} = \exp\left[q\int_{r_1}^{r}\frac{f_{k+1}(\xi)}{\xi}d\xi\right].$$

In (20) we used the condition, that

$$\sigma_r^k(r_1) = \sigma_r^{k+1}(r_1).$$

The yield condition (18),(19) takes place for $\forall\, r$, $r\in[r_1,r_2]$, where $r_2 = \min(r_2^*,r_2^{**})$, r_2^* $(r_2^* \ge r_1)$ - the minimum positive solution of equation $\sigma_r^{k+1}(r) = \max(x_{k+1},x_{k+2})$, r_2^{**} $(r_2^{**} \ge r_1)$ - the minimum positive solution of equation $\sigma_r^{k+1}(r) = \min(x_{k+1},x_{k+2})$.

If $r_2 \ge 1$, then the yield condition (10), (11) is satisfied for $\forall\, r$, $r\in[\alpha,r_1]$ and the yield condition (18), (19) for $\forall\, r$, $r\in[r_1,1]$ and (17), (20) give the following connection between $\sigma_r^k(\alpha)$ and $\sigma_r^{k+1}(1)$:

$$\sigma_r^{k+1}(1)f_1^{k+1}(1) = \int_{r_1}^{1}\left(\frac{qb_{k+1}}{r} - \omega r\right)f_1^{k+1}dr + \qquad (21)$$

$$+ \frac{1}{f_1^k(r_1)}\left[\int_{\alpha}^{r_1}\left(\frac{qb_k}{r} - \omega r\right)f_1^k dr + \sigma_r^k(\alpha)\right].$$

Notice that (21) gives the nonlinear relation between $\sigma_r^{k+1}(1)$ and $\sigma_r^k(\alpha)$, because r_1 depends on $\sigma_r^k(\alpha)$.

If $r_2 \le 1$, then the yield condition (18), (19) is satisfied for $\forall\, r$, $r\in[r_1, r_2]$. For $r > r_2$ one can assume, that

$$\sigma_\theta^{k+1} = a_{k+2}\sigma_r^{k+2} + b_{k+2},$$

and

$$\min(x_{k+2}, x_{k+3}) \le \sigma_r^{k+2} \le \max(x_{k+2}, x_{k+3}),$$

if $\sigma_r^{r+1}(r_2) = \max(x_{k+1}, x_{k+2})$ or (10), (11) if $\sigma_r^{k+1}(r_2) = \min(x_{k+1}, x_{k+2})$.

So, we can build up the statically allowed stress states, which satisfy the yield condition corresponding to the sides of arbitrary yield polygon, where $x_k \neq x_{k+1}$, for the above mentioned constructions.

Let us consider now the case, when $x_k = x_{k+1}$. Then the yield condition has the form (12), (13). Substitution of (12) into (1) gives

$$\sigma_\theta^k(r) = x_k\left(1 + \frac{h'r}{hq}\right) + \frac{\omega r^2}{q}. \qquad (22)$$

For spherical vessels, cylindrical tubes and circular disks with constant thickness ($h' \equiv 0$) under pressures ($\omega \equiv 0$), equations (12), (13) and (22) give, that the yield condition (12), (13) is possible only, if

$$\sigma_\theta^k(r) = \sigma_r^k(r) = x_k = y_k = y_{k+1}. \qquad (23)$$

Notice, that yield condition (10), (11) contains the case of (23).

If $h' \neq 0$ or (and) $\omega \neq 0$, then, as above, it is possible to find the segment for coordinate r, where the inequalities (13) are correct and continue the building up of the statically allowed stress state, when this segment does not cover the segment $[\alpha,1]$.

Papers [2, 20] contain the best examples on building up the statically allowed stress states relative to the yield condition, which corresponds to the sides of the Tresca yield polygon.

4.Determination of rational distributions of the Young modulus

For determination of the rational distribution we can use the equation (8) and the displacement continuity condition

$$u^k(r_k) = u^{k+1}(r_k). \qquad (24)$$

In the region of change of coordinate r where there is sat-

isfied yield condition (10), (11) or (12), (13) equation (8) give $E_k^{*}E_k^{-1}=$

$$= \frac{(1+\nu^{*})(\sigma_\theta^k-\sigma_r^k)+r[(1+\nu^{*}-q\nu^{*})\sigma_\theta^{k\prime}+\nu^{*}\sigma_r^{k\prime}]+E_k\alpha^{-1}\eta^{*}T'}{r[(1+\nu^{*}-q\nu^{*})\sigma_\theta^{k}-\nu^{*}\sigma_r^{k}]}. \quad (25)$$

According to (9) the displacement continuity condition (24) has the form

$$\varepsilon_\theta^k(r_k)=\varepsilon_\theta^{k+1}(r_k). \quad (26)$$

By substitution of ε_θ^k from (3) to (25) we get

$$E_{k+1}(r_k)E_k^{-1}(r_k)=\frac{(1+\nu)\sigma_\theta^k(r_k)-\nu\sigma_r^k(r_k)+\eta T(r_k)}{(1+\nu)\sigma_\theta^{k+1}(r_k)-\sigma_r^{k+1}(r_k)+\eta T(r_k)} \quad (27)$$

for the sphere;

$$E_{k+1}(r_k)E_k^{-1}(r_k)=\frac{\sigma_\theta^k(r_k)-\nu\sigma_r^k(r_k)+\eta T(r_k)}{\sigma_\theta^{k+1}(r_k)-\nu\sigma_r^{k+1}(r_k)+\eta T(r_k)} \quad (28)$$

for the disk and

$$E_{k+1}(r_k)E_k^{-1}(r_k)=\frac{(1+\nu)\sigma_\theta^k(r_k)-\sigma_r^k(r_k)}{(1+\nu)\sigma_\theta^{k+1}(r_k)-\sigma_r^{k+1}(r_k)} \quad (29)$$

for the tube ($T(r)\equiv 0$).

Stresses σ_θ^k and σ_r^k are determined by (10), (15) or (22), (12) in the formulas (25)-(29). The formulas (26)-(29) determine the jump in the values of the Young modulus by crossing the border of change of the yield condition.

Thus, if the value $E_1(\alpha)$ were known it would be possible by using formulas (25)-(29) to find the rational distributions of the Young modulus, which guarantee the above given statically allowed stress states when the loads have reached their limit values.

Many good examples for the rational distributions of the Young modulus can be found in papers (2),(18) - (21),(23), (24) the Tresca yield polygon has been used.

References

1. Faulkner M.G., Mioduchowski A., Hong D.P., Optimal jump nonhomogeneity of prismatic bars in torsion. Trans. ASME, J. Vibr., Acoust. Stress and Reliab. Des., 1984, 106(4), 897-901.

2.Hein K., Heinloo M., The design of nonhomogeneous equi-strength annular discs of variable thickness under internal and external pressures. Int. J. Solids Struct., 1990, 26(5-6), 617-630.
3.Klosowicz B., Transient thermal stress in bimodulos sphere with orthotropic temperature-dependent properties. Rozpr. Inz., 1986, 16(7), 557-568.
4.Klosowicz B., Sur la nonhomogeneity optimale d'une barre tordue. Bull. Acad. Polon. Sci. ser. sci. techn., 1970, 18(8), 611-615.
5.Klosowicz B., Lurie K.A., On the optimal nonhomogeneity of a torsional elastic bar. Arch. mech. stosow., 1972, 24(2) , 239-249.
6.Klosowicz B., Lurie K.A., On the optimal distribution of elastic moduli of a nonhomogeneous body. J.Optimiz. Theory and Appl., 1973, 12(1), 32-42.
7.Olszak W., Rychlewsky J., Nichthomogenitats - Problem im elastischen und vorplastischen Bereich. Österr. Ing. Arch., 1961, 15, 130-152.
8.Rammerstorfer F.G., On the optimal distribution of the Young's modulus of a vibrating, prestressed beam. J. Sound and Vibr., 1974, 37(1), 140-145.
9.Sarp A., Optimal shape and nonhomogeneity of a nonuniformly compressed column. Int. J. Solids Struct., 1979, 15(12), 935-949.
10.Sarp A., Ibrahim S., Optimal shape and nonhomogeneity of a Timoshenko beam for maximum load. J. Ship. res. 1979, 23(4), 229-234.
11.Yhe Kal-yuan, Liu Ping, Equi-strength design of nonhomogeneous variable thickness high speed rotating disk under steady temperature field. Appl. Math. and Mech., 1986, 7(9), 769-778.
12.Альтенбах Х., Определение модулей упругости для пластин, изготовленных из неоднородного по толщине анизотропного материала. Изв. АН СССР, Мех. тверд. тела, 1987, 1, 139-146.
13.Кондаков Э.П., Расчет оптимальной зависимости модуля упругости от радиуса для трубы, нагруженной внутренним давлением, с целью повышения допустимых давлений. Тр. Моск. гидромелиор. ин -та, 1981, 69, 179-186.

14. Кунташев П.А. Немировский Ю.В., О некоторых свойствах оптимальных термоупругих проектов при фиксированных полях напряжений или деформаций. ПММ, 1985, 49(3), 476-484.
15. Кунташев П.А., Немировский Ю.В., Оптимизация напряженного состояния распределением упругих параметров в термоупругих телах. Мех. неоднор. структур. Тез. докл. 2 всес. конф.,Львов, 1987, 1, 158-159.
16. Лехницкий С.Г., Радиальное распределение напряжений в клине и полуплоскости с переменным модулем упругости. ПММ, 1962, 26(1), 146-151.
17. Расторгуев Г.И., Оптимизация жесткостей тонких ребер расположенных вдоль концентрических окружностей, в растянутой пластине. Динам. и прочн. элем. авиац. констр., 1987, 34-43.
18. Хейн К., Хейнлоо М. Оптимальная неоднородность сферического сосуда под давлением. Tartu Ülk. Toim., 1985, 721, 43-51.
19. Хейн К., Хейн М., Хейнлоо М., Оптимальная непрерывная неоднородность вращающегося диска в стационарном поле температуры. Tartu Ülk. Toim., 1987, 772, 60-69.
20. Хейн К., Хейнлоо М., Оптимизация непрерывной неоднородности цилиндрических труб под воздействием давлений. Tartu Ülk. Toim., 1987, 772, 44-59.
21. Хейн К., Хейнлоо М., Оптимизация неоднородности вращающихся дисков. Мех. неоднор. структур. Тез. докл. 2 всес. конф., Львов, 1987, 2, 284-285.
22. Хейн К., Хейнлоо М., Автоматизированный расчет оптимальной непрерывной неоднородности цилиндрических труб и круглых дисков, равнопрочных относительно условия пластичности Мизеса. Tartu Ülk. Toim., 1988, 799, 52-61.
23. Хейн К., Хейнлоо М., Оптимальная неоднородность вращающегося диска переменной толщины в стационарном поле температуры. Пробл. прочн., 1988, 7, 121. (Рукоп. деп. в ВИНИТИ, № 2635-В88).
24. Хейн К.Э., Хейнлоо М.Л., Оптимальная непрерывная неоднородность вращающихся равнопрочных дисков, насаженных на жесткий вал. В сб. Прикл. пробл. прочности и пластичности. Анализ и оптим. деформируемых систем, 1988, 61-67.
25. Хейн К., Хейнлоо М., Проектирование непрерывной неоднородности для равнопрочных цилиндрических труб с подвижными

торцами в условиях стационарного нагрева. Tartu Ülik. Toim., 1989, 853, 93-100.

ОДНОМЕРНАЯ ПРОБЛЕМА РАВНОПРОЧНОСТИ ДЛЯ НЕОДНОРОДНЫХ СФЕРИЧЕСКИХ СОСУДОВ, ЦИЛИНДРИЧЕСКИХ ТРУБ И КРУГЛЫХ ДИСКОВ ОТНОСИТЕЛЬНО ПРОИЗВОЛЬНОГО МНОГОУГОЛЬНИКА ПЛАСТИЧНОСТИ

Калле Хейн и Мати Хейнлоо
Тартуский университет

Резюме

Для неоднородных сферических сосудов, вращающихся цилиндрических труб и круглых дисков, подверженных квазистатическому давлению на внутреннем и внешнем радиусах решается задача об определении такого распределения модуля Юнга, которое гарантирует выполнение сразу во всех точках предельного напряженного состояния, соответствующего сторонам произвольного многоугольника пластичности.

Acta et Commentationes Universitatis Tartuensis. 939. 1992

DESIGN OF NONHOMOGENEOUS EQUI-STRENGTH CYLINDRICAL TUBES UNDER PRESSURES WITH REGARD TO THE CONDITION OF MAXIMAL APPLIED STRESSES

Kalle Hein

Tartu University

Abstract. A solution is found to the problem of determining the optimal distribution of the Young's modulus of cylindrical tubes, which guaranties the satisfaction of the condition of maximal applied stresses simultaneously at all points while pressures achieve their limit values.

Notation

σ_r^0, σ_θ^0 – radial and hoop stress components;

p_1^0 – inner pressure;

p_2^0 – external pressure;

a – inner radius;

b – outer radius;

r – radial coordinate;

σ_0 – yield stress;

ν – Poisson's ratio;

E^0 – Young's modulus distribution.

It is convenient to introduce the following dimensionless variables

$$\rho = \frac{r}{a}; \quad \alpha = \frac{a}{b}; \quad \sigma_\theta = \frac{\sigma_\theta^0}{\sigma_0}; \quad \sigma_r = \frac{\sigma_r^0}{\sigma_0};$$

$$p_1 = \frac{p_1^0}{\sigma_0}; \quad p_2 = \frac{p_2^0}{\sigma_0}; \quad E = \frac{E^0}{E_0}.$$

Introduction

Techniques to determine the limit pressures and the corresponding distributions of Young's modulus for nonhomogeneous equi-strength cylindrical tubes under inner and external pressures have been studied by Hein and Heinloo [1,2]. The method used in these papers has been based on the solutions of the elasticity problem with the additional requirement that the cylindrical tubes should change from elastic to plastic states simultaneously at all points after quasistatic pressures have achieved their limit values.

The optimal distributions of Young's modulus which guarantee the satisfaction of the Tresca yield criterion simultaneously at all points in the material of the cylindrical tubes and the relations between the limit values of the pressures were presented analytically in [1]. The equistrength state for tubes with regard to the Von Mises yield criterion has been examined numerically in [2].

The use of a concrete yield criterion depends on the treatment of the problem. Solving the problem in the case of various conditions is also of theoretical interest. So, in this paper the above mentioned problem has been solved with regard to the condition of maximal applied stresses.

1. Basic equations

Let us assume that the cylindrical tubes are made of an isotropic linearly elastic material which obeys the condition of maximal applied stresses. The Poisson ratio and the yield stress are constants whereas Young's modulus is the function of the radial coordinate.

For nonhomogeneous cylindrical tubes under quasistatic pressures the stresses must satisfy the basic equations of the elasticity theory: Hooke's law, the equilibrium equation

$$r\sigma_r' + \sigma_r - \sigma_\theta = 0 \tag{1}$$

and the compatibility equation

$$q' = \frac{r((1-\nu)\sigma_\theta' - \nu\sigma_r') - (\sigma_r - \sigma_\theta)}{r((1-\nu)\rho_\theta - \nu\sigma_r)}, \tag{2}$$

where $q = \ln E(r)$. In the present paper in eqs (1),(2) and in all other formulae the primes denote differentiation with respect to r. We consider the limit state of the tubes under uniformly distributed pressures. Therefore, the boundary conditions are

$$\sigma_r(\alpha) = -p_1, \tag{3}$$

$$\sigma_r(1) = -p_2. \tag{4}$$

The analysis is based on the condition of maximal applied stresses from which we obtain the following restrictions

$$|(2-\nu)\sigma_r - (1+\nu)\sigma_\theta| \le 2, \tag{5}$$

$$|(2-\nu)\sigma_\theta - (1+\nu)\sigma_r| \le 2, \tag{6}$$

$$|(1-2\nu)(\sigma_\theta + \sigma_r)| \le 2. \tag{7}$$

These conditions establish that all possible stress states lie either within or on yield surface of the maximal applied

stresses. If in one or two of the conditions (5)-(7) the sign of equality is valid for all radial coordinates r, the stress state lies on the yield surface and the tube is fully plastic.

2. Statically admissible limit pressures

At first, let us assume that condition

$$(2 - \nu)\sigma_r - (1 - \nu)\sigma_\theta = -2 \tag{8}$$

holds good for all radial coordinates r. On the basis of this assumption and making use of boundary condition (4), the equilibrium equation (1) has the following solution

$$\sigma_r = (2s - p_2)r^m - 2s, \tag{9}$$

where $s = 1/(1 - 2\nu)$ and $m = (1 - 2\nu)/(1 + \nu)$. The boundary condition (3) and eq (9) yield us the following relation between the static limit inner and external pressures

$$p_1 = 2s + (p_2 - 2s)\alpha^m. \tag{10}$$

To ensure the admission of the solution, it is necessary to require that conditions (6), (7) should be fulfilled. It is easy to show that they are valid if

$$-\frac{2}{3}(s + n) \le \sigma_r \le -\frac{2}{3}, \tag{11}$$

where $n = (1 - \nu)s$. Using expression (9) for radial stress, we can write (11) as

$$\frac{2}{3} \le p_2 \le 2s - \frac{2}{3m}\alpha^{-m}, \tag{12}$$

that gives the bounds of limit external pressures.

If we examine all possible regime in yield condition (θ)-(8) analogous to this, we obtain, that the problem does not have a statically admissible solution for the regimes

$$(2 - \nu)\sigma_r - (1 + \nu)\sigma_\theta = 2, \quad (1 - 2\nu)(\sigma_r + \sigma_\theta) = 2. \tag{13}$$

All other statically admissible solutions can be written as

$$p_1 = \begin{cases} \alpha^{-\frac{1}{n+s}}(p_2 + 2s) - 2s, & \\ \qquad \text{when } 0 \le p_2 \le \frac{4}{3}(n + s)\alpha^{\frac{1}{n+s}} - 2s, & (14) \\ 2s + \alpha^m(p_2 - 2s), & \\ \qquad \text{when } \frac{2}{3} \le p_2 \le 2s - \frac{2}{3m}\alpha^{-m} & (15) \end{cases}$$

and

$$p_1 = \begin{cases} 2s + \alpha^{-\frac{1}{n+s}}(p_2 - 2s), & \text{when } 2s(1 - \alpha^{\frac{1}{n+s}}) \le p_2 \le \frac{2}{3m}, \quad (16) \\ s + (p_2 - s)\alpha^{-2}, & \text{when } s - \frac{\alpha^2}{3} \le p_2 \le s + \frac{\alpha^2}{3}. \quad (17) \end{cases}$$

As we see, the problem can not be solved, if

$$\frac{4}{3}(n + s)\alpha^{\frac{1}{n+s}} - 2s \le p_2 \le \frac{2}{3} \quad \text{for } p_1 > p_2 \quad (18)$$

and

$$\frac{2}{3m} < p_2 < s - \frac{\alpha^2}{3} \quad \text{for } p_1 < p_2. \quad (19)$$

Now we can note on the basic of (14) that, if

$$p_2 = \frac{4}{3}(n + s)\alpha^{\frac{1}{n+s}} - 2s, \text{ then } p_1 = \frac{2}{3}$$

and if

$$p_2 = \frac{2}{3}, \text{ then } p_1 = 2[s + \frac{\alpha^m}{3}(1 - 3s)].$$

Therefore, let us consider the tube as a multilayer tube and assume in one layer there is satisfied one equation of yield criterion and in the other layer the other one with equality sign for all coordinates r.

The radius of surface x, which separate two different regime, is determined from condition .

$$p^* = \frac{2}{3}, \quad (20)$$

where p^* - limit contact pressure of layers. Hence, using the relation between limit pressures (14), we get

$$x = \left[\frac{p_2 + 2s}{\frac{2}{3} + 2s}\right]^{n+s}. \quad (21)$$

Now, taking into account $p_2 = p^*$ and (21), equation (15) gives the following relation

$$p_1 = 2s + \left[\frac{\alpha(\frac{2}{3} + 2s)^{n+s}}{(p_2 + 2s)^{n+s}}\right]^m (p_2 - 2s) \quad (22)$$

for p_2 determined by (18).

Similarly, making use of the previous analysis, we get the

solution for interval (19)

$$p_1 = 2\left[\frac{\alpha}{\sqrt{3}(s - p_2)}\right]^{-\frac{1}{s+n}}\left(\frac{1}{3m} - s\right) + 2s. \qquad (23)$$

The dependence of p_1 on p_2, calculated by the formulas (14)-(17), (22), (23) are shown in Fig.1 by curves 2-2. Curves 1-1 which have been presented previously in [1] correspond to the case of the Tresca yield criterion. All calculations have been done for ν = = 0.33, α = 0.5. As we see in Fig.1, there is a region in the case of which there cannot exist any equl-strength stress state. Such an interval was discovered already in [2]. This analytical result confirms the plausibility of the solutions that were got numerically in [2].

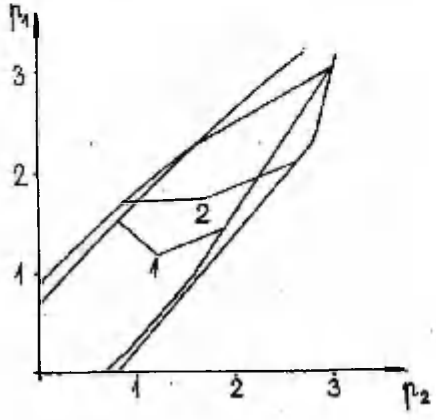

Fig. 1

3. Distributions of Young's modulus

We are interested in determining of the distribution of the nonhomogeneity - of Young's modulus, which guarantees the satisfaction of the yield criterion simultaneously at all points under the above determined limit pressures. For this purpose the compatibility equation (2) will be used. Adding to differential equation (2) the initial condition $q(1) = 0$ and solving the equation, we get the Young modulus distributions from the following equation:

$$\frac{E(r)}{E(1)} = \exp q(r). \qquad (24)$$

The variation of Young modulus with r is shown in Fig.2. Curve 1 corresponds to the case $p_1 = 3.17$, $p_2 = 3.00$; curve 2 - $p_1 = 0.03$, $p_2 = 0.80$, curve 3 - $p_1 = 1.18$, $p_2 = 1.80$; curve 4 - $p_1 = 1.99$, $p_2 = 2.50$.

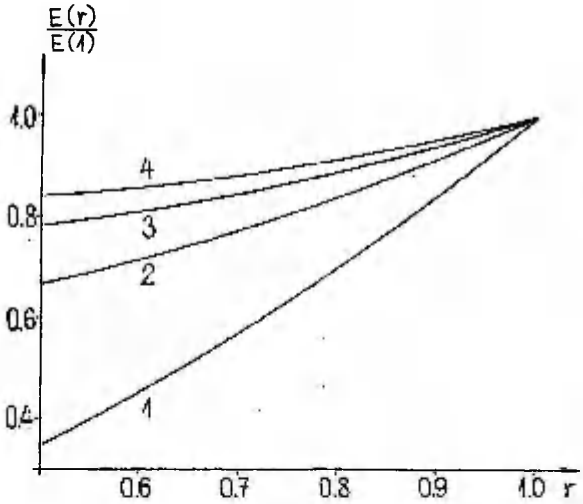

Fig. 2

References

1.Heln K., Heinloo M., Optimization of the continuous nonhomogenelty of a cylindrical tube under pressures (in Russian). Tartu Ülik. Toim., 1987, 772, 44-59.

2.Hein K., Heinloo M., Automatic calculation of the optimal non-homogeneity for cylindrical tubes and circular disks of uniform strength with regard to the Mises yield condition (in Russian). Tartu Ülik. Toim., 1988, 799, 52-61.

ПРОЕКТИРОВАНИЕ НЕОДНОРОДНЫХ ЦИЛИНДРИЧЕСКИХ ТРУБ ПОД ДАВЛЕНИЯМИ, РАВНОПРОЧНЫХ ОТНОСИТЕЛЬНО УСЛОВИЯ НАИБОЛЬШЕГО ПРИВЕДЕННОГО НАПРЯЖЕНИЯ

Калле Хейн

Тартуский университет

Решена задача об определении непрерывных распределений модуля Юнга, гарантирующих при предельных значениях давлений выполнение условия наибольшего приведенного напряжения сразу во всех точках трубы. На фигурах приведены для иллюстрации графики зависимостей между предельными давлениями и некоторыми распределениями модуля Юнга.

Acta Et Commentationes Universitatis Tartuensis, 939, 1992

ABOUT INTEGRAL CONSTRAINTS

Heino Relvik
Tallinn Technical University

Abstract. In the present paper, the analogues of kinetic energy will be used for forming differential equations of movement of non-holonomic mechanical systems. An example of considering the integral constraints between the generalised coordinates has been solved.

Let us have the analogue of kinetic energy [4]

$$H^{(-2),1} = \sum m_i \overset{(-2)}{\vec{v}}_i \cdot \vec{a}_i = \sum m_i \vec{r}_i \cdot \vec{a}_i, \tag{1}$$

where

$$\vec{r}_i = \vec{r}_i(0) + \int_0^t \vec{r}_i dt$$

and, consequently,

$$\frac{d\vec{r}_i}{dt} = \vec{r}_i.$$

Suppose we have succeeded in forming the radius-vectors

$$\vec{r}_i = q_j \vec{u}_{ij} \tag{2}$$

by means of the generalized coordinates q_j and the velocity base $\vec{u}_{ij}$. Then the main parts

$$\vec{r}^{\,*} = q_j \vec{u}_{ij}$$

of the integrals

$$\vec{r}_i = \int_0^t q_j \vec{u}_{ij} dt = q_j \vec{u}_{ij}\Big|_0^t - \int_0^t q_j \dot{\vec{u}}_{ij} dt$$

will give us the main part of the function (1):

$$H^{*-2,1} = \sum m_i \vec{a}_i \cdot q_j \vec{u}_{ij}, \tag{3}$$

where $\vec{a}_i$ as the second derivatives from (2) do not depend on q_j and the partial derivatives

$$\frac{\partial H^{*-2,1}}{\partial q_j} = \sum m_i \vec{a}_i \cdot \vec{u}_{ij}$$

will present the sum $\sum m_i \vec{a}_i \cdot \vec{u}_{ij}$. Thus we shall get the equations

$$\frac{\partial H^{*-2,1}}{\partial q_j} = Q_j, \ (j = 1,2,\ldots, s), \tag{4}$$

where Q_j are the generalized forces

$$Q_j = \sum \vec{F}_1 \cdot \vec{u}_{1j}.$$

Analogously to (3), putting

$$D^{*-2} = \sum \vec{F}_1 \cdot q_j \vec{u}_{1j}$$

and

$$K^{*-2,1} = H^{*-2,1} - D^{*-2}$$

we shall have the equations

$$\frac{\partial H^{*-2,1}}{\partial q_j} = \frac{\partial D^{*-2}}{\partial q_j}, \qquad \frac{\partial K^{*-2,1}}{\partial \dot{q}_j} = 0. \tag{5}$$

Let the integrals q_j of generalized coordinates q_j be connected by means of a linear equation of constraints

$$a_0 + a_1 q_1 + \ldots + a_s q_s = 0,$$

where $a_0, \ldots, a_s$ do not depend on q_k. Then anyone of the q_k can be expressed by the others and the result be substituted into (4). So the number of equations (4) will be s-1. (Besides this method of direct substitution, there will also exist other ones, for example, the method of Lagrange's multipliers.)

In practice, the radius-vectors (2) cannot always be completely formed. For example, in case of a simple pendulum

$$\vec{r} = r\vec{u}_r$$

by r = const all the information about movement is hidden in $\vec{u}_r$ and the generalized coordinate φ (angle of direction of the pendulum) is implicit. Then we shall turn to the velocity in order to get more information, as it will be shown in next example.

In order to demonstrate the idea of the equations (4) by means of a possibly simple example, let the deformable body be devided into only two parts (Fig. 1) with concentrated masses m_1 and m_2. So the body will be presented by a double pendulum.

Example. Double pendulum.

Let us find the forces F_1, F_2 and F_3 which will give the pendulum such a movement that

$$\varphi = \Phi + 0.2t. \tag{6}$$

We can see that $\vec{F}_1 = -F_1\vec{u}_r$, $\vec{F}_2 = -\vec{F}_2' = F_2\vec{u}_1$, $\vec{F} = F_3\vec{u}_\Phi$, $\vec{r}_A^{**} = \ddot{r}\vec{u}_r + r\dot{\varphi}\dot{\vec{u}}_\varphi$, $\vec{r}_A = r\vec{u}_r$, $\vec{v}_A = r\dot{\varphi}\vec{u}_\varphi$, $\vec{a}_A = r\ddot{\varphi}\vec{u}_\varphi - r\dot{\varphi}^2\vec{u}_r$, $\vec{r}_B^{**} = \ddot{r}\vec{u}_r +$

$+ r\dot{\varphi}\vec{u}_\varphi + l\dot{\vec{u}}_1 + l\dot{\varphi}\vec{u}_\varphi)$, $\vec{r}_B = r\vec{u}_r + l\vec{u}_1$, $\vec{v}_B = r\dot{\varphi}\vec{u}_\varphi + l\dot{\varphi}\vec{u}_\varphi$, $\vec{a}_B = r\ddot{\varphi}\vec{u}_\varphi - r\dot{\varphi}^2\vec{u}_r + l\ddot{\varphi}\vec{u}_\varphi - l\dot{\varphi}^2\vec{u}_1$.

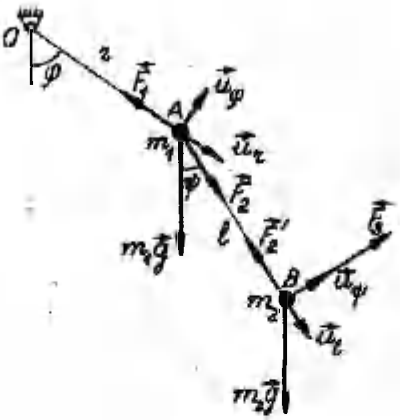

Fig. 1

The equation (5) will take the form

$$\frac{\partial}{\partial \dot{q}_j}\left[m_1\vec{a}_A.(\dot{r}\vec{u}_r + r\dot{\varphi}\vec{u}_\varphi) + m_2\vec{a}_B.(\dot{r}\vec{u}_r + r\dot{\varphi}\vec{u}_\varphi + \dot{l}\vec{u}_1 + l\dot{\varphi}\vec{u}_\varphi)\right] =$$

$$= \frac{\partial}{\partial \dot{q}_j}\left[(m_1\vec{g} + \vec{F}_1 + \vec{F}_2).(\dot{r}\vec{u}_r + r\dot{\varphi}\vec{u}_\varphi) + \right.$$

$$\left. + (m_2\vec{g} + \vec{F}_2' + \vec{F}_3).(\dot{r}\vec{u}_r + r\dot{\varphi}\vec{u}_\varphi + \dot{l}\vec{u}_1 + l\dot{\varphi}\vec{u}_\varphi)\right],$$

where $q_1 = r$, $q_2 = \varphi$, $q_3 = l$ and $q_4 = \psi$.

Substituting the equality (6) here ($\varepsilon = -0.2t$), we shall get

$$\frac{\partial}{\partial \dot{q}_j}\left[(m_1\vec{a}_A + m_2\vec{a}_B).(\dot{r}\vec{u}_r + r\dot{\varphi}\vec{u}_\varphi) + m_2\vec{a}_B.(\dot{l}\vec{u}_1 + l\dot{\varphi}\vec{u}_\varphi + l\varepsilon\vec{u}_\varphi)\right] -$$

$$- \frac{\partial}{\partial \dot{q}_j}\left[(m_1\vec{g} + m_2\vec{g} + \vec{F}_1 + \vec{F}_3).(\dot{r}\vec{u}_r + r\dot{\varphi}\vec{u}_\varphi) + \right. \qquad (7)$$

$$\left. + (m_2\vec{g} + \vec{F}_2' + \vec{F}_3).(\dot{l}\vec{u}_1 + l\dot{\varphi}\vec{u}_\varphi + l\varepsilon\vec{u}_\varphi)\right]$$

(see also [1,2,3]).

The necessary partial derivatives of (7) will give us the

$$\frac{\partial}{\partial r} \rightarrow \quad (m_1\vec{a}_A + m_2\vec{a}_B).\vec{u}_r = [(m_1 + m_2)\vec{g} + \vec{F}_1 + \vec{F}_3].\vec{u}_r; \tag{8}$$

$$\frac{\partial}{\partial l} \rightarrow \quad m_2\vec{a}_B.\vec{u}_1 = (m_2\vec{g} + \vec{F}_2 + \vec{F}_3).\vec{u}_1; \tag{9}$$

$$\frac{\partial}{\partial \varphi} \rightarrow \quad (m_1\vec{a}_A + m_2\vec{a}_B).r\vec{u}_\varphi + m_2\vec{a}_B.l\vec{u}_\psi =$$

$$= [(m_1 + m_2)\vec{g} + \vec{F}_1 + \vec{F}_3].r\vec{u}_\varphi + (m_2\vec{g} + \vec{F}_2 + \vec{F}_3).l\vec{u}_\psi; \tag{10}$$

$$\frac{\partial}{\partial \varepsilon} \rightarrow \quad m_2\vec{a}_B.l\vec{u}_\psi = (m_2\vec{g} + \vec{F}_2 + \vec{F}_3).l\vec{u}_\psi. \tag{11}$$

With the aid of (11) the equation (10) will be simplified and we shall have

$$(m_1\vec{a}_A + m_2\vec{a}_B).\vec{u}_\varphi = [(m_1 + m_2)\vec{g} + \vec{F}_1 + \vec{F}_3].\vec{u}_\varphi. \tag{12}$$

Now the equations (8), (9), (11) and (12) will give us a system with four unknown quantities φ, F_1, F_2 and F_3.

When taken $m_1 = 2$ kg, $m_2 = 1$ kg, $r = 1$ m, $l = 0.5$ m, $\varphi_0 = \pi/3$ and $\dot{\varphi}_0 = 0$, the equations (8), (9), (10) and (11) will give us:

$$[2 + \sin^2(0.2)]\ddot{\varphi} + 0.5\dot{\varphi}^2\sin(0.2) + \ddot{\varphi}^2\sin(0.2)\cos(0.2) =$$

$$= -3g\sin\varphi + g\sin(\varphi - 0.2)\cos(0.2);$$

$$F_3 = [0.5 + \cos(0.2)]\ddot{\varphi} - \dot{\varphi}^2\sin(0.2) + g\sin(\varphi - 0.2);$$

$$F_2 = \ddot{\varphi}\sin(0.2) + [0.5 + \cos(0.2)]\dot{\varphi}^2 + g\cos(\varphi - 0.2);$$

$$F_1 = [3 + 0.5\cos(0.2)]\dot{\varphi}^2 - 0.5\ddot{\varphi}\sin(0.2) + 3g\cos(0.2) +$$

$$+ 0.1987\,F_3,$$

from where

$$\ddot{\varphi} = -0.1442\,\dot{\varphi}^2 - 9.8066\sin\varphi - 0.9362\cos\varphi;$$

$$F_3 = 1.4801\,\ddot{\varphi} - 0.1987\,\dot{\varphi}^2 + 9.8066\sin(\varphi - 0.2);$$

$$F_2 = 0.1987\,\ddot{\varphi} + 1.4801\,\dot{\varphi}^2 + 9.8066\cos(\varphi - 0.2);$$

$$F_1 = 3.4900\,\dot{\varphi}^2 - 0.0993\,\ddot{\varphi} + 29.4200\cos\varphi + 0.1987\,F_3.$$

The solution to this system is given on Fig. 2.

For control, one can observe the masspoints A and B separately with the aid of the forces F_1, F_2 and F_3. Then

$$\sin\psi = \frac{1}{F_2}(2\dot{\varphi}\cos\varphi - 2\dot{\varphi}^2\sin\varphi + F_1\sin\varphi);$$

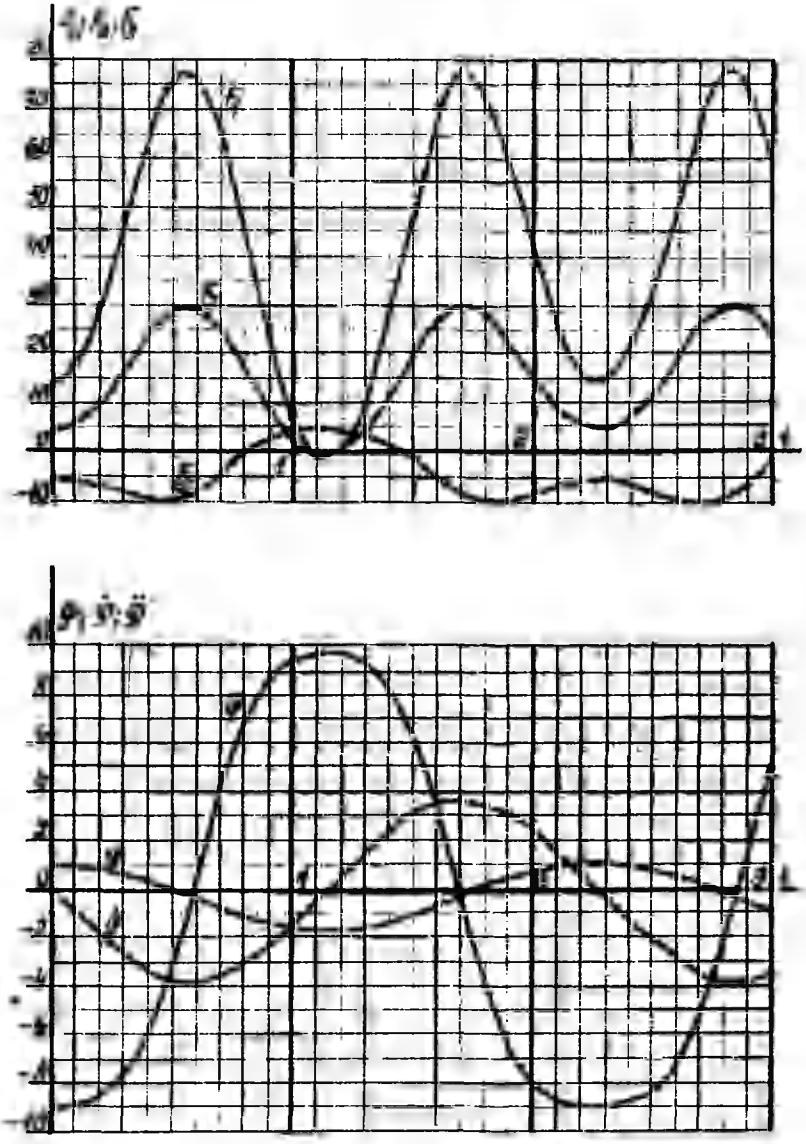

Рис. 3

$$\cos\Phi = \frac{1}{F_2}\,(F_1\cos\varphi - 2\dot{\varphi}\sin\varphi - 2\dot{\varphi}^2\cos\varphi - 2g);$$

$$\ddot{\Phi} = 2[\dot{\varphi}^2\sin(\varphi - \Phi) - \ddot{\varphi}\cos(\varphi - \Phi) - m_2 g\,\sin\Phi + F_3];$$

$$\dot{\Phi}^2 = 2[-\ddot{\varphi}\sin(\varphi - \Phi) - \dot{\varphi}^2\cos(\varphi - \Phi) - g\,\cos\Phi + F_2].$$

The control will give a good result for the angles φ and Φ: $\varphi = \Phi + 0.2$. In general cases, the integral $\varphi = \Phi + 0.2t + C$, where C will depend on the initial value of φ and Φ. In the present example, one can agree that $C = 0$ and therefore $\varphi = \Phi + 0.2t$.

References

1. Relvik H., On Mangeron's Generalized Equations of Analytical Dynamics and Some Related Problems. Memorille sectillor stilntifice Acad. Rep. Soc. Romania, 1987, ser. IV t. X, Nr. 1, 57-81.
2. Гольст Г., Рельвик Х., Сильде О., Уравнение возможной мощности в аналитической механике. ТПИ, Таллин, 1978.
3. Гольст Г., Рельвик Х., Сильде О., Основные вопросы аналитической механики. Уравнение возможной мощности. "Валгус", Таллин, 1979.
4. Рельвик Х., Составление дифференциальных уравнений движения при помощи аналогов кинетической энергии. Труды ТПИ, 1973, 345, 53-62.

ОБ ИНТЕГРАЛЬНЫХ СВЯЗЯХ

Хейно Рельвик

Таллиннский технический университет

Резюме

В статье составлены дифференциальные уравнения движения при помощи аналогов кинетической энергии. Дан пример, где учтены интегральные связи между обобщенными координатами.

Acta Et Commentationes Universitatis Tartuenaia. 939, 1992

ОБ ОДНОЙ ПОСТАНОВКЕ ЗАДАЧИ УСТОЙЧИВОСТИ ДВИЖЕНИЯ НА ОСНОВЕ УРАВНЕНИЯ ВОЗМОЖНОЙ МОЩНОСТИ

Ариэл Хяйтин
Таллиннский технический университет

В статье рассматривается устойчивость установившихся движений (УД) механических систем.

Для получения уравнений движения и уравнений возмущенного движения (УВД) используется уравнение возможной мощности (УВМ). Даются примеры, иллюстрирующие полученные результаты.

Рассмотрим задачу, в которой необходимо исследовать устойчивость установившихся движений механической системы в случае, когда УВД имеют постоянные коэффициенты. Одним из немаловажных обстоятельств ее решения является вывод УВД из УВМ. Оно заключается в том, что в основе метода УВМ лежит выбор независимых скоростей, число которых равно числу степеней свободы механической системы. Это позволяет, в случае неголономной системы, не вводить уравнения неголономных связей, которые оказываются автоматически учтёнными. В уравнения движения будут входить только независимые скорости, а в УВД их возмущения.

В статье вводится определённо-положительная функция возмущений скоростей и координат W, производная которой по времени равняется выражению, полученному в результате преобразования УВД. Определение устойчивости рассматриваемых УД здесь принимается в виде ограниченности функции W во времени. Это определение эквивалентно требованию ограниченности возмущений, входящих в эту функцию. Если найдены эти возмущения как функции времени, удовлетворяющие исходным УВД, тогда можно найти условия устойчивости рассматриваемых движений.

Отметим, что при таком подходе, задача об устойчивости установившихся движений сводится к исследованию устойчивости движения системы по отношению к части переменных [5].

1. Уравнения движения механической системы запишем в виде, полученном из УВМ [1], краткий вид которого

$$\{\dot{T}\} = \{N\}. \qquad (1.1)$$

Далее по повторяющимся индексам производится суммирование, пределы изменения которых, как правило, даются один раз.

В (1.1) имеем:

$$\{\dot{T}\} = (g_{\alpha\nu}\dot{v}^{\alpha} + \Gamma_{\alpha\beta,\nu}v^{\alpha}v^{\beta})\{v^{\nu}\};\quad \{N\} = Q_{\nu}\{v^{\nu}\},$$

v^{α}, $\{v^{\alpha}\}$ – соответственно, действительные и возможные независимые параметры скорости;

$g_{\alpha\nu} = \sum_{i=1}^{N} m_i \vec{u}_{i\alpha} \cdot \vec{u}_{i\nu}$ – метрический тензор; $Q_{\nu} = \sum_{i=1}^{N} \vec{F}_i \frac{\partial \vec{r}_i}{\partial \pi^{\nu}}$ – обобщенная сила; $\Gamma_{\alpha\beta,\nu} = \sum_{i=1}^{N} \frac{\partial \vec{u}_{i\beta}}{\partial \pi^{\alpha}} \cdot \vec{u}_{i\nu}$ – символ Кристоффеля; m_i, $\vec{r}_i$, $\vec{F}_i$ – соответственно, масса i-ой точки, ее радиус-вектор и приложенная к ней сила; $\vec{u}_{i\alpha}$ – базисный вектор, соответствующий скорости v^{α}; π^{α} – в общем случае квазикоордината; $\alpha, \beta, \nu = 1, 2, \ldots, S$; $S = n - m$; n – число обобщенных координат; m – число уравнений неголономных связей; S – число степеней свободы системы.

Развернутый вид (1.1) будет:

$$(g_{\alpha\nu}\dot{v}^{\alpha} + \Gamma_{\alpha\beta,\nu}v^{\alpha}v^{\beta} - Q_{\nu})\{v^{\nu}\} = 0. \qquad (1.2)$$

Учтя независимость $\{v^{\nu}\}$, получим уравнения движения системы

$$g_{\alpha\nu}\dot{v}^{\alpha} + \Gamma_{\alpha\beta,\nu}v^{\alpha}v^{\beta} - Q_{\nu} = 0. \qquad (1.3)$$

Уравнения установившихся движений получаются из (1.3), если учесть постоянство циклических скоростей и позиционных координат в этом движении [2], имеем:

$$\Gamma_{\alpha\beta,\nu}v^{\alpha}v^{\beta} - Q_{\nu} = 0, \qquad (1.4)$$

причем в каждой конкретной задаче следует еще принять во внимание (2.19), (2.21) статьи [7].

Рассматриваемая здесь задача состоит в определении условий устойчивости установившихся движений (1.4). Сначала, однако, необходимо записать УВД для более общей задачи.

Пусть частным решением уравнений (1.3) будут следующие функции времени:

$$v^{\alpha} = v^{\alpha}(t), \qquad (1.5) \qquad q^{j} = q^{j}(t),\ j = 1, 2, \ldots, n. \qquad (1.6)$$

Обобщенные скорости $\dot{q}^{j}$ выражаются через независимые (в общем случае квазискорости) скорости v^{α} линейно:

$$\dot{q}^{j} = A^{j}_{\alpha}v^{\alpha}, \qquad (1.7)$$

где $A^{j}_{\alpha} = A^{j}_{\alpha}(q^{\beta})$ [7].

Более общая задача заключается в исследовании устойчивости движения системы, определяемого уравнениями (1.5) и (1.6). Обозначим Δ отклонения величин v^{α} и q^{j} в действительном движении системы от решений (1.5) и (1.6) следующим образом:

$$\delta v^{\alpha} = v^{\alpha} - v^{\alpha}(t), \qquad (1.8) \qquad \delta q^{j} = q^{j} - q^{j}(t). \qquad (1.9)$$

Отклонения δv^{α} и δq^{j} являются возмущениями, соответственно, скоростей и координат. В дальнейшем будут использоваться возмущения не обобщенных координат δq^{j}, а, в общем случае, квазикоординат. Связь между этими возмущениями осуществляется аналогично зависимости (1.7) в виде:

$$\delta q^{j} = A^{j}_{\alpha}\, \delta\pi^{\alpha}. \qquad (1.10)$$

2. Подставив (1.8) и (1.10) в (1.1) или (1.2), получим:

$$\delta(\{\dot{T}\} - \{N\}) = 0(\{\dot{T}\} - \{N\}), \qquad (2.1)$$

где

$$\delta(\{\dot{T}\} - \{N\}) = [g_{\alpha\nu}\delta\dot{v}^{\alpha} + v^{\alpha}v^{\beta}\delta\Gamma_{\alpha\beta.\nu} + \\ + (\Gamma_{\alpha\beta.\nu} + \Gamma_{\beta\alpha.\nu})v^{\alpha}\delta v^{\beta} + \dot{v}^{\alpha}\delta g_{\alpha\nu} - \delta Q_{\nu}]\{v^{\nu}\} \qquad (2.2)$$

является совокупностью линейных членов в УВМ в возмущенном движении.

Правая же часть (2.1)

$$0(\{\dot{T}\} - \{N\}) = (\delta\dot{v}^{\alpha}\delta g_{\alpha\nu} + \delta(\Gamma_{\alpha\beta.\nu} + \Gamma_{\beta\alpha.\nu})v^{\alpha}\delta v^{\beta} + \\ + \Gamma_{\alpha\beta.\nu}\delta v^{\alpha}\delta v^{\beta} + 0^{*}(\Gamma_{\alpha\beta.\nu})v^{\alpha}v^{\beta} - 0^{*}(Q_{\nu}) + 0^{**}_{\nu})\{v^{\nu}\} \qquad (2.3)$$

содержит члены выше первого порядка малости. В (2.2) и (2.3) применяются следующие обозначения малых величин. Например: $\delta\Gamma_{\alpha\beta.\nu}$, $0^{*}(\Gamma_{\alpha\beta.\nu})$ – величины соответственно, первого и второго порядка малости при разложении $\Gamma_{\alpha\beta.\nu}$ в ряд (подразумевается, что $\Gamma_{\alpha\beta.\nu} = \Gamma_{\alpha\beta.\nu}(q^{\gamma})$, $\gamma = 1, 2, \ldots, S$, или $\gamma = a$, см. (2.19) в [7]), 0^{**}_{ν} – все остальные члены более высокого порядка малости.

Уравнения линейного приближения в статьях [6,7] получаются из (2.1) путем отбрасывания правой части и учета независимости $\{v^{\nu}\}$. Подставим теперь в левую часть (2.1) вместо (2.2) его выражение в виде (6.1) статьи [7], учтя независимость возможных скоростей $\{v^{\nu}\}$, получим УВД, содержащие члены высшего порядка малости:

$$g_{\alpha\nu}(\delta\pi^{\alpha})^{\cdot\cdot} + C_{\alpha\nu}(\delta\pi^{\alpha})^{\cdot} + S_{\alpha\nu}\delta\pi^{\alpha} = 0_{\nu}, \qquad (2.4)$$

где

$$C_{\alpha\nu} = 2\Gamma_{\beta\alpha.\nu}v^{\beta}, \qquad (2.5)$$

$$S_{\alpha\nu} = ((\Gamma_{\beta\nu.\lambda} - \Gamma_{\lambda\beta.\nu})\gamma^{\lambda}_{\alpha\eta} + \frac{\partial(\Gamma_{\beta\alpha.\nu} - \Gamma_{\alpha\beta.\nu})}{\partial\pi^{\eta}} + \frac{\partial\Gamma_{\beta\eta.\nu}}{\partial\pi^{\alpha}})v^{\eta}v^{\beta} -$$

$$-\frac{\partial Q_\nu}{\partial \pi^\alpha};\ \lambda,\ \eta = 1,\ 2,\ldots,\ S, \qquad (2.6)$$

O_ν – означает совокупность членов второго и выше порядка малости, представленных в (2.3).

Вернемся теперь к решению исходной задачи, т.е. исследованию устойчивости установившихся движений (1.4) в случае, когда коэффициенты в (2.4) являются постоянными величинами.

Запишем коэффициенты $G_{\omega\nu}$ и $S_{\omega\nu}$ уравнений (2.4) в виде:

$$G_{\omega\nu} = G'_{\omega\nu} + G''_{\omega\nu}, \qquad (2.7) \qquad S_{\omega\nu} = S'_{\omega\nu} + S''_{\omega\nu}, \qquad (2.8)$$

где

$$G'_{\omega\nu} = G'_{\nu\alpha} = (G_{\omega\nu} + G_{\nu\alpha})/2, \qquad (2.9)$$

$$G''_{\omega\nu} = -G''_{\nu\alpha} = (O_{\omega\nu} - G_{\nu\alpha})/2, \qquad (2.10)$$

$$S'_{\omega\nu} = S'_{\nu\alpha} = (S_{\omega\nu} + S_{\nu\alpha})/2, \qquad (2.11)$$

$$S''_{\omega\nu} = -S''_{\nu\alpha} = (S_{\omega\nu} - S_{\nu\alpha})/2. \qquad (2.12)$$

Умножив уравнение (2.4) на $(\delta\pi^\nu)^{\cdot}$, суммируя по ν и учтя (2.7) – (2.12), получим:

$$\dot{W} = O_\nu(\delta\pi^\nu)^{\cdot} - (G'_{\omega\nu}(\delta\pi^\alpha)^{\cdot} + S''_{\omega\nu}\delta\pi^\alpha)(\delta\pi^\nu)^{\cdot}/2, \qquad (2.13)$$

где

$$W = (g_{\omega\nu}(\delta\pi^\mu)^{\cdot}(\delta\pi^\nu)^{\cdot} + S'_{\omega\nu}\delta\pi^\alpha\delta\pi^\nu)/2, \qquad (2.14)$$

и $g_{\omega\nu} = g_{\nu\alpha}$, (см. п. 1).

3. Пусть W в (2.14) будет определенно-положительной функцией в некоторой области D изменения своих переменных:

$$W((\delta\pi^\alpha)^{\cdot}, \delta\pi^\alpha, v^\alpha) > 0, \qquad (3.1)$$

и, как видно из (2.14), обращается в ноль при $(\delta\pi^\alpha)^{\cdot} = \delta\pi^\alpha = 0$:

$$W(0, 0, v^\alpha) = 0. \qquad (3.2)$$

Введем следующее определение устойчивости установившихся движений (1.4).

Движения (1.4) будем называть устойчивыми в некоторой области D изменения переменных функции W, если в этой области для любого наперед заданного положительного числа ε, как бы мало оно ни было, можно найти другое положительное число $\eta(\varepsilon)$, такое, что для всех возмущенных движений, отличающихся от (1.4), для которых в начальный момент времени $t = t_0$ выполняется неравенство

$$W(t_0) \leqslant \eta, \qquad (3.3)$$

будет при всех $t > t_0$ выполняться неравенство

$$W(t) < \varepsilon; \qquad (3.4)$$

в противном случае оно неустойчиво.

На основании предложенного определения можно сформулировать следующее утверждение.

Пусть установившееся движение (1.4) устойчиво в области D, в которой выполняются условия (3.1) и (3.2). Покажем, что об устойчивости этих движений можно судить по решению уравнений

$$g_{\alpha\beta}(\delta\pi^{\alpha})^{\cdot\cdot} + G_{\alpha\beta}(\delta\pi^{\alpha})^{\cdot} + S_{\alpha\beta}\delta\pi^{\alpha} = 0, \qquad (3.5)$$

полученных из (2.4) путем отбрасывания правой части.

Действительно, интегрируя (2.13) имеем:

$$W(t) - W(t_0) = \int(0_{\nu} - (G_{\alpha\beta}(\delta\pi^{\alpha})^{\cdot} + S_{\alpha\beta}\delta\pi^{\alpha})/2)\,d(\delta\pi^{\nu}). \qquad (3.6)$$

Поскольку движение устойчиво, то всегда можно выбрать ε из (3.4) настолько малым, что получающееся η из (3.3) и, соответственно, разность

$$W(t) - W(t_0) \Rightarrow 0. \qquad (3.7)$$

Из определённой положительности функции W в (2.14), выбора ε в (3.4) и учета (3.2), следует, что возмущения $(\delta\pi^{\alpha})^{\cdot} \Rightarrow 0$ и $\delta\pi^{\alpha} \Rightarrow 0$. Поэтому, принимая еще во внимание (3.7), можно в (3.6) отбросить члены высшего порядка малости 0_{ν}. Но это эквивалентно их отбрасыванию в уравнениях (2.4), что и требовалось.

Обратно, если составленная на основе уравнений (3.5) функция W содержит только те возмущения $(\delta\pi^{\alpha})^{\cdot}$ и $\delta\pi^{\alpha}$ (являющиеся решениями уравнений (3.5)), которые ограничены во времени, то в этом случае движение (1.4) будет устойчивым. Действительно, выбором начальных возмущений $\delta\pi^{\alpha}_0$ и $(\delta\pi^{\alpha})^{\cdot}_0$ можно добиться выполнения условий (3.3) и (3.4).

Таким образом, в рассматриваемом случае, поставленная задача решается с помощью уравнений (3.5). Проверка этого решения может быть осуществлена путем подстановки найденных из (3.5) возмущений в (2.4) или (2.13).

Проиллюстрируем полученные результаты следующими примерами.

4. Движение тела вокруг закрепленной точки. Случай Эйлера.

Уравнения линейного приближения для данной задачи соответствующие уравнениям (3.5) уже найдены в статье [6]. Отметим, что в названной статье возмущения обозначены в виде π^{α} и $\dot{\pi}^{\alpha}$, здесь же они имеют, соответственно, вид $\delta\pi^{\alpha}$ и $(\delta\pi^{\alpha})^{\cdot}$. Тогда уравнение (2.13) в этом случае будет:

$$\dot{W} = v^1(\delta\pi^1)^{\cdot}(((I_2 - I_1)(\delta\pi^2)^2 + (I_3 - I_1)(\delta\pi^3)^2)^{\cdot}/2 + (I_3 - I_2)v^1\delta\pi^2\delta\pi^3) + O_v, \tag{4.1}$$

где O_v – члены более высокого порядка малости и

$$2W = I_1(\delta\pi^1)^{\cdot 2} + I_2(\delta\pi^2)^{\cdot 2} + I_3(\delta\pi^3)^{\cdot 2} + (v^1)^2((I_1 - I_3)(\delta\pi^2)^2 + (I_1 - I_2)(\delta\pi^3)^2). \tag{4.2}$$

Общее решение уравнений линейного приближения (из этой же статьи) имеет вид:

$$\delta\pi^1 = C_1^1 + C_2^1 t;\ \delta\pi^2 = C_\mu^2 e^{\lambda_\mu t};\ \delta\pi^3 = C_\mu^3 e^{\lambda_\mu t}, \tag{4.3}$$

$\mu = 3, 4, 5, 6$, а корни характеристического уравнения принимают следующие значения:

$$\lambda_{1,2} = 0;\ \lambda_{3,4} = v^1 i;\ i = \sqrt{-1};$$
$$\lambda_{5,6} = v^1\sqrt{(I_1-I_2)(I_3-I_1)/I_2I_3}\ . \tag{4.4}$$

Наконец, возмущения скоростей найдутся по формуле (4.5) статьи [6]:

$$\delta v^1 = (\delta\pi^1)^{\cdot};\ \delta v^2 = (\delta\pi^2)^{\cdot} - v^1\delta\pi^3;\ \delta v^3 = (\delta\pi^3)^{\cdot} + v^1\delta\pi^2. \tag{4.5}$$

Как известно, в этой задаче исследуется устойчивость вращения тела вокруг одной из его главных осей инерции. Для оси с моментом инерции I_1 уравнение установившегося движения будет: $v^1 = \text{const}$, $v^2 = v^3 = 0$.

При вращении вокруг средней оси инерции $I_2 > I_1 > I_3$, один корень в (4.4) будет с положительной действительной частью. Возмущения (4.3) и (4.5) будут со временем расти, а следовательно и функция W из (4.2). Имеет место неустойчивость такого движения.

Рассматривая же вращение вокруг большой или малой оси инерции, из (4.4) получаем два нулевых и четыре мнимых корня. Среди возмущений (4.3) только $\delta\pi^1$ возрастает со временем, но оно не входит в функцию W в (4.2). Следовательно, в этом случае W удовлетворяет условиям (3.3) и (3.4), и движение является устойчивым. Отметим, что как видно из (4.2), область устойчивости этих двух движений будет различной.

5. Качение однородного эллипсоида вращения по горизонтальной плоскости.

В задаче рассматривается качение без проскальзывания однородного эллипсоида вращения по горизонтальной плоскости без учета сопротивления качению и вращению. Определяются условия устойчивости его установившихся движений.

Пусть параметрами эллипсоида будут масса M и полуоси a, b = c, причем их отношение k = a/b > 1. Введем полуподвижную систему отсчета CXYZ с ортами $\vec{I}$, $\vec{J}$, $\vec{k}$, угловая скорость которой

$$\vec{\Omega} = \dot{\lambda}\,\vec{I} + \dot{\phi}\,(\vec{J}\sin\lambda + \vec{k}\cos\lambda), \qquad (5.1)$$

где (фиг.1) неподвижный вертикальный орт

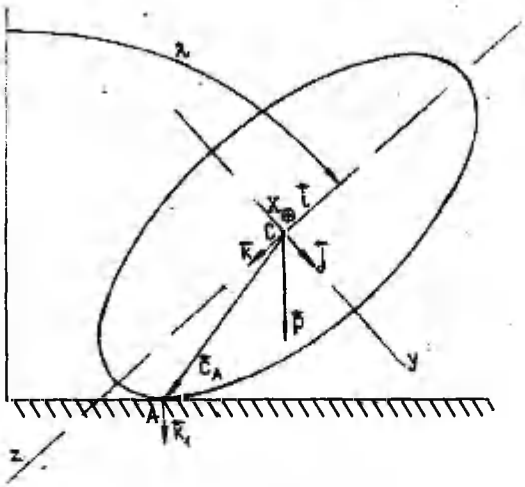

фиг.1

$$\vec{k}_1 = \vec{J}\sin\lambda + \vec{k}\cos\lambda. \qquad (5.2)$$

По отношению к введенной системе отсчета эллипсоид имеет угловую скорость $\dot{\varphi}$, так что вектор его полной угловой скорости будет:

$$\vec{\omega} = \vec{\Omega} + \dot{\varphi}\,\vec{k} = \dot{\lambda}\,\vec{I} + \dot{\phi}\,\vec{J}\sin\lambda + (\dot{\varphi} + \dot{\phi}\cos\lambda)\,\vec{k}. \qquad (5.3)$$

За независимые параметры скорости выберем проекции вектора $\vec{\omega}$ на оси CXYZ, тогда:

$$\vec{\omega} = \omega_1\vec{I} + \omega_2\vec{J} + \omega_3\vec{k}. \qquad (5.4)$$

Из сравнения (5.3) и (5.4) имеем следующее преобразование скоростей:

$$\omega_1 = \dot{\lambda};\ \omega_2 = \dot{\phi}\sin\lambda,\ \omega_3 = \dot{\varphi} + \dot{\phi}\cos\lambda;$$
$$\dot{\lambda} = \omega_1,\ \dot{\phi} = \omega_2/\sin\lambda,\ \dot{\varphi} = \omega_3 - \omega_2\operatorname{ctg}\lambda. \qquad (5.5)$$

Уравнения движения эллипсоида найдем с помощью УВМ [1]:

$$(I_x + M(y_A^2 + z_A^2))\dot{\omega}_1 + M(y_A\cos\lambda - z_A\sin\lambda)\rho_A\omega_1^2 -$$
$$-(I_x + Ma^2)\omega_2^2\operatorname{ctg}\lambda + (I_z + Mb^2)\omega_2\omega_3 = Mg(z_A\sin\lambda - y_A\cos\lambda),$$

$$(I_y + Mz_A^2)\dot{\omega}_2 - My_Az_A\dot{\omega}_3 + ((I_y + Ma^2)ctg\lambda - Mz_A\rho_A sin\lambda)\omega_1\omega_2 -$$

$$- (I_z + Mz_A\rho_A cos\lambda)\omega_1\omega_3 = 0, \qquad (5.6)$$

$$(I_z + My_A^2)\dot{\omega}_3 - My_Az_A\dot{\omega}_2 + M(y_A\rho_A sin\lambda - b^2)\omega_1\omega_2 + My_A\rho_A\omega_1\omega_3 cos\lambda = 0,$$

где входящие в уравнения величины выражаются в виде:

$$I_x = I_y = 0.2M(a^2 + b^2) = 0.2Mb^2(k^2 + 1);\ k = a/b;\ I_z = 0.4Mb^2;$$

$$y_A = bsin\lambda(1 + (k^2 - 1)cos^2\lambda)^{-0.5};\ z_A = bk^2cos\lambda(1 + (k^2 - 1) \times$$

$$\times cos^2\lambda)^{-0.5};\ \rho_A = bk^2(1 + (k^2 - 1)cos^2\lambda)^{-1.5}, \qquad (5.7)$$

здесь ρ_A - радиус кривизны эллипса в плоскости CYZ в точке A.

Необходимые для дальнейших расчетов выражения коэффициентов метрического тензора $g_{\alpha\beta}$ и символов Кристоффеля $\Gamma_{\alpha\beta,\nu}$, у которых индексы α, β, $\nu = 1, 2, 3$, имеют вид:

$$g_{11} = I_x + M(y_A^2 + z_A^2);\ g_{22} = I_y + Mz_A^2;\ g_{33} = I_z + My_A^2;\ g_{23} = g_{32} =$$

$$= -My_Az_A;\ \Gamma_{11.1} = M\rho_A(y_Acos\lambda - z_Asin\lambda);\ \Gamma_{22.1} = -(I_x + Ma^2)ctg\lambda;$$

$$\Gamma_{32.1} = 0.5I_z;\ \Gamma_{23.1} = Mb^2 + 0.5I_z;\ \Gamma_{12.2} = -Mz_A\rho_A sin\lambda;\ \Gamma_{21.2} =$$

$$= (I_y + Ma^2)ctg\lambda;\ \Gamma_{31.2} = -0.5I_z;\ \Gamma_{13.2} = -(Mz_A\rho_A cos\lambda + 0.5I_z);$$

$$\Gamma_{21.3} = -(Mb^2 + 0.5I_z);\ \Gamma_{12.3} = My_A\rho_A sin\lambda + 0.5I_z;\ \Gamma_{13.3} =$$

$$= My_A\rho_A cos\lambda. \qquad (5.8)$$

С учетом постоянства циклических скоростей ω_2, ω_3 и позиционной координаты λ (т.е. $\dot{\omega}_1 = \omega_1 = \dot{\omega}_2 = \dot{\omega}_3 = 0$), из (5.6) получим уравнение установившегося движения эллипсоида:

$$(I_z + Mb^2)\omega_2\omega_3 - (I_x + Ma^2)\omega_2^2 ctg\lambda = Mg(z_Asin\lambda - y_Acos\lambda). \qquad (5.9)$$

Уравнение (5.9) представляет двухмерное многообразие движений эллипсоида в пространстве параметров ω_2, ω_3, λ. Отметим следующие возможные случаи этих движений:

1) $\lambda = 0$, $\omega_2 = 0$, $\omega_3 \neq 0$ - эллипсоид вращается вокруг вертикальной оси CZ;

2) $\lambda = 0.5\pi$, $\omega_3 = 0$, $\omega_2 \neq 0$ - эллипсоид вращается вокруг вертикальной оси CY;

3) $\lambda = 0.5\pi$, $\omega_2 = 0$, $\omega_3 \neq 0$ - эллипсоид катится по плоскости, ось CZ - горизонтальна;

4) при промежуточном значении угла λ, центр C эллипсоида описывает окружность (в плоскости, которая параллельна опорной) радиусом $\rho_C = (\omega_3 y_A - \omega_2 z_A)sin\lambda/\omega_2$. Такой же результат получается из опубликованной в [3], более общей задачи качения тела вращения по горизонтальной шероховатой плоскости.

Целью данной задачи является определение условий устойчивости движений (5.9) и в частности в случаях 1) и 4) при $\lambda = 45^{\circ}$.

Для достижения поставленной цели воспользуемся уравнениями линейного приближения [7]. Применив (6.3) указанной статьи, с учетом (5.8) в данной задаче, получим два уравнения, которые после элементарного интегрирования дадут:

$$(\delta\pi^2)^{\cdot} = (-2\omega_2 ctg\lambda + I_z(g_{33}\omega_3 + g_{23}\omega_2)/\Delta)\delta\pi^1, \qquad (5.10)$$

$$(\delta\pi^3)^{\cdot} = ((g_{22}(I_z + 2Mb^2) + 2g_{23}(I_y + Ma^2)ctg\lambda)\omega_2 - g_{23}I_z\omega_3)\delta\pi^1/\Delta,$$

где введено обозначение: $\Delta = g_{22}g_{33} - g_{23}g_{32}$.

Применив (6.2) той же статьи [7], получим еще одно УВД в рассматриваемой задаче:

$$g_{11}(\delta\pi)^{\cdot\cdot} - 2(I_x + Ma^2)\omega_2 ctg\lambda(\delta\pi^2)^{\cdot} + (I_z + Mb^2)(\omega_2(\delta\pi^3)^{\cdot} +$$

$$+ \omega_3(\delta\pi^2)^{\cdot}) + \delta\pi^1(((I_z + Mb^2)\omega_3 - 2(I_x + Ma^2)\omega_2 ctg\lambda)(\omega_2 ctg\lambda +$$

$$+ I_z Mz_A\rho_A(\omega_2 sin\lambda + \omega_3 cos\lambda)/\Delta) - (I_z + Mb^2)(\omega_2^2 + \qquad (5.11)$$

$$+ I_y My_A\rho_A(\omega_2 sin\lambda + \omega_3 cos\lambda)\omega_2/\Delta) + \omega_2^2(I_x + Ma^2)/sin^2\lambda -$$

$$- Mg(z_A cos\lambda + y_A sin\lambda - \rho_A)) = 0,$$

куда необходимо подставить выражение для $(\delta\pi^2)^{\cdot}$ из (5.10) и

$$\omega_2(\delta\pi^3)^{\cdot} + \omega_3(\delta\pi^2)^{\cdot} = ((1 + I_y My_A^2/\Delta)\omega_2^2 + \omega_3^2 I_z g_{33}/\Delta -$$

$$- 2\omega_2\omega_3 ctg\lambda)\delta\pi^1;$$

тогда получится дифференциальное уравнение второго порядка относительно возмущения $\delta\pi^1 = \delta\lambda$. Условие устойчивости движения (5.9) получим из выражения при $\delta\pi^1$, которое должно быть в этом случае положительным. Ввиду его громоздкости, вычисления удобнее производить численно. Так для вертикального вращения вокруг оси CZ ($\lambda = 0$) эллипсоида, у которого $k = 2$, условие устойчивости такого движения получится в виде $\omega_3^2 > 15.3g/b$, (здесь $g = 9.81 м/с^2$), а для угла $\lambda = 45^{\circ}$ аналогичное условие будет: $18.9\omega_2^2 + 0.56\omega_3^2 - 5.26\omega_2\omega_3 > 0.57g/b$. Такие условия можно вычислить для любого угла λ. Функция W в данном случае будет:

$$2W = g_{11}(\delta\pi^1)^{\cdot 2} + S_{11}(\delta\pi^1)^2,$$

где ввиду (5.10) исключены возмущения $(\delta\pi^2)^{\cdot}$ и $(\delta\pi^3)^{\cdot}$, а S_{11} выражение, получающееся при $\delta\pi^1$ в (5.11). Таким образом, условие устойчивости движения (5.9) можно представить в виде

$S_{11} > 0$.

Автор выражает благодарность И.С. Емельяновой за критические замечания.

Литература

1. Гольст Г., Рельвик Х., Сильде О., Основные вопросы аналитической механики. Таллинн, "Валгус", 1979.
2. Емельянова И.С., К определению циклических координат и стационарных движений механических систем. В сб. Динамика систем. Горький, изд-во Горьковск. ун-та, 1974, 3, 117-130.
3. Карапетян А.В., Об устойчивости стационарных движений систем некоторого вида. Изв. АН СССР. Мех. тверд. тела, 1983, 2, 45-52.
4. Малкин И.Г., Теория устойчивости движения. "Наука", 1966.
5. Румянцев В.В., Озиранер А.С., Устойчивость и стабилизация движения по отношению к части переменных. "Наука", 1987.
6. Хайтин А., Применение уравнения возможной мощности к исследованию устойчивости движения механических систем. Уч.зап. Тартуск. ун-та, 1985, 721, 109-117.
7. Хайтин А., К вопросу переставимости операций дифференцирования и варьирования и ее применения в теории устойчивости движения. Уч. зап. Тартуск. ун-та, 1989, 853, 144-156.

ABOUT THE SETTING UP OP MOTION STABILITY TASK ON THE BASIS OF POSSIBLE POWER EQUATION

Ariel Haitin
Tallinn Technical University

Summary

The equations of perturbed motion are dealt with in the present paper. These equations have been derived on the basis of the possible power equation. Linear approximations of these equations have been obtained in articles [6,7]. A somewhat different solution as compared to the traditional one has been obtained for the task, which deals with the stability determination of the stationary motion of a mechanical system.

Acta Et Commentationes Universitatis Tartuensis, 939, 1992

ПРИМЕНЕНИЕ ОБОБЩЕННЫХ ФУНКЦИЙ ДЛЯ РАСЧЕТА СОСТАВНЫХ БАЛОК НА УПРУГОМ ОСНОВАНИИ

Геннадий Арясов, Александр Снитко, Евгений Соколов
Таллиннский технический университет

Обычно для максимального сокращения числа вычислительных операций при расчете балок, подвергающихся действию нагрузок различного вида, а также в случае изменения жесткости балки по ее длине используется метод начальных параметров. Однако, для его реализации необходимо удовлетворить ряду условий, которые в значительной степени снижают эффективность этого метода. В данной статье рассматривается метод, свободный от указанных недостатков - метод обобщенных функций [1,3,6].

При исследовании изгиба балок переменной жесткости использование обобщенных функций дает возможность производить процесс интегрирования исходного дифференциального уравнения практически теми же способами, что и для балок постоянной жесткости. Что касается составных балок на упругом основании, то и для них новые методы теории обобщенных функций позволяют предельно упростить процесс решения.

Покажем это на конкретных примерах. Однако, предварительно приведем правила интегрирования функций, содержащих единичную функцию и дельта-функцию. Известно из [7] формула (3)

$$\int \varphi(x)\delta(x-a)dx = \eta(x-a)\varphi(a); \qquad (1)$$

где $\varphi(x)$ - некоторая непрерывная на рассматриваемом промежутке функция; $\delta(x-a)$ и $\eta(x-a)$ - дельта - функция и единичная функция. Кроме того, с помощью непосредственного дифференцирования и учета фильтрующего свойства дельта-функции $\varphi(x)\cdot\delta(x-a) = \varphi(a)\cdot\delta(x-a)$ легко доказать справедливость следующей формулы:

$$\int \varphi(x)\cdot\eta(x)dx = \eta(x-a)\int_a^x \varphi(x)dx. \qquad (2)$$

Используя формулы (1) и (2), можно интегрировать уравнение упругой линии балки, не накладывая на нагрузку и ее жесткость никаких ограничений. При этом, как и в методе начальных параметров, общий интеграл задачи будет содержать число произвольных постоянных, равное порядку исходного дифференциального уравнения.

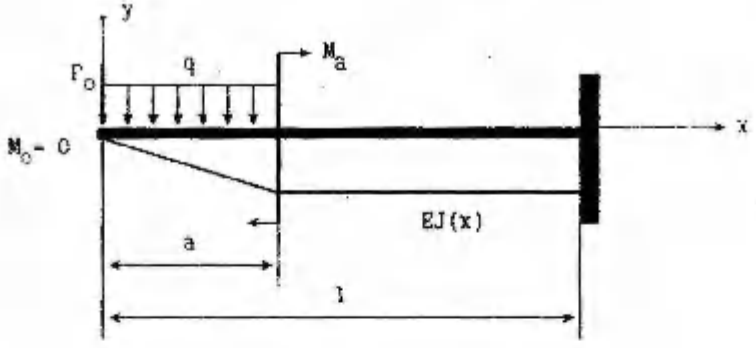

Фиг.1

Рассмотрим решение на примере консольной балки (фиг.1). Как известно, дифференциальное уравнение изгиба балки записывается в форме:

$$EJ(x)\cdot y'' = M. \tag{3}$$

Помещая начало отсчета на свободном конце балки, изгибающий момент и жесткость можно записать в таком виде:

$$M(x) = -P_0 - [1 - \eta(x - a)]q\frac{x^2}{2} + \eta(x - a)[M_0 - qa(x - \frac{a}{2})];$$

$$EJ(x) = [1 - \eta(x - a)]\cdot EJ(a)[\alpha + (1 - \alpha)\frac{x}{a}] + \eta(x - a)\cdot EJ(a);$$

где $\alpha = \frac{J(0)}{J(a)}$; $\eta(x - 0) = 1$.

Таким образом, исходное дифференциальное уравнение (3) можно представить следующим образом:

$$EJ(a)y''(x) = -\left[1 - \eta(x - a)\right]\left[\frac{P_0x + qx^2/2}{\alpha + (1 - \alpha)x/a}\right] + \eta(x - a)\left[M_0 - P_0x - qa(x - a/2)\right]. \tag{4}$$

Его непосредственное интегрирование с учетом (2) дает:

$$EJ(a)y(x) = -\left[1 - \eta(x - a)\right]\frac{a}{1 - \alpha}\left\{\frac{qx^3}{12} + \left[P_0 - \frac{\alpha qa}{2(1 - \alpha)}\right]\frac{x^2}{2} - \frac{\alpha a}{1 - \alpha}\left[P_0 - \frac{\alpha qa}{2(1 - \alpha)}\right]\left\{\frac{a}{1 - \alpha}\left[(1 - \alpha)\frac{x}{a} + \alpha\right]\ln\left|(1 - \alpha)\frac{x}{a} + \alpha\right| - x\right\}\right\} + \eta(x - a)\left\{\frac{(2\alpha^2 + 5a - 1)^4}{12(1 - \alpha)^3} - \frac{(1 + \alpha)P_0a^3}{2(1 - \alpha)^2} - \right. \tag{5}$$

$$- \left[P_0 \frac{a^2}{1-\alpha} + \frac{(1-3\alpha)qa^3}{4(1-\alpha)^2}\right](x-a) - \frac{qa}{6}(x-a)^2\left(x-\frac{a}{2}\right) -$$

$$- \frac{P_0}{2}\left[\frac{x^3-a^3}{3} - a^2(x-a)\right] - M_0\frac{x-a}{2}\Bigg\} + C_1x^2 + C_2,$$

где

$$C_1 = P_0a^2\left[\frac{1}{1-\alpha} + \frac{1}{2}\left[\frac{1}{\alpha}^2 - 1\right]\right] + \frac{qa^3}{2}\left[\frac{1-3\alpha}{2(1-\alpha)^2} + \right.$$

$$\left. + \frac{1}{\alpha}\left(\frac{1}{\alpha} - 1\right)\right] - M_0a\left(\frac{1}{\alpha} - 1\right);$$

$$C_2 = P_0a^3\left\{\frac{1-\alpha}{2(1-\alpha)^2} + \frac{1}{1-\alpha}\left(\frac{1}{\alpha} - 1\right) + \frac{1}{2}\left[\frac{1}{3}\left[\frac{1}{\alpha}^3 - 1\right] - \right.\right.$$

$$\left.\left. - \left(\frac{1}{\alpha} - 1\right)\right]\right\} + \frac{qa^4}{4}\left[\frac{1-5\alpha+2\alpha^2}{3(1-\alpha)^2} + \frac{1-3\alpha}{(1-\alpha)^2}\left(\frac{1}{\alpha} - 1\right) + \right.$$

$$\left. + \frac{1}{3}\left(\frac{1}{\alpha} - 1\right)^2\left(2\frac{1}{\alpha} + 1\right)\right] - \frac{M_0a^2}{2}\left(\frac{1}{\alpha} - 1\right) - C_1l$$

постоянные интегрирования, определенные из начальных условий при $x = l$ $y = 0$, $y' = 0$.

На фиг.2 приведены результаты вычисления прогиба балки при $l = 2a$, $\alpha = 1/2$, $P_0 = qa$, $M_0 = qa^2/2$. Здесь же для сравнения пунктиром приведены результаты для случая $\alpha = 1$.

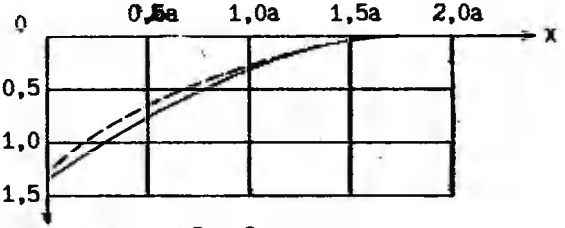

Фиг.2

$$\bar{y}(x) = \frac{EJ(a)}{qa^4}\bar{y}(x)$$

Такой же результат можно было бы получить, если вместо уравнения (4) воспользоваться дифференциальным уравнением :

$$\frac{d^2}{dx^2}\left[EJy''(x)\right] = q(x). \qquad (6)$$

При использовании уравнения (6) сила, приложенная в точке $x = 0$, вводится в уравнение с помощью выражения $P_0\delta(x-0)$, а изгибающий момент, действующий в точке $x = a$, с помощью выражения $M_0\delta(x-a)$. Тогда вместо (3) получим:

$$\frac{d^2}{dx^2}\left[EJy''(x)\right] = -\left[1-\eta(x-a)\right]q - P_0\delta(x) + M_0\delta'(x-a). \qquad (7)$$

Интегрируя данное дифференциальное уравнение, приходим к

$$EJ(x)y''(x) = -\left[1-\eta(x-a)\right]qx^2/2 -$$

$$-\eta(x-a)\left[qa(x-a/2) - M_0\right] - P_0x,$$

правая часть которого совпадает с выражением для изгибающего момента, входящего в дифференциальное уравнение (1). Здесь учтено, что $\eta(x) = \eta(x-0) = 1$. Постоянные $C_3 = 0$ и $C_4 = 0$, так как при $x = 0$ поперечная сила $Q(0) = -P_0$, а изгибающий момент $M(0) = 0$.

Покажем теперь, как можно использовать обобщенные функции при расчете балки на упругом основании со ступенчато меняющейся жесткостью. Будем предполагать, что балка состоит из участков, в пределах которых жесткость постоянна.

Тогда исходное дифференциальное уравнение изгиба балки запишется в такой форме:

$$\sum_{i=1}^{N}\left[\eta(x-a_{i-1}) - \eta(x-a_i)\right]\left[y^{IV} + 4k_1y_1\right] = \sum_{i=1}^{N}\left[\eta(x-a_{i-1}) -\right.$$

$$\left.-\eta(x-a_i)\right]\frac{q(x)l^4}{EJ_1} + \sum_{i=1}^{N-1}\left[\delta'(x-a_i)\left[\frac{J_i}{J_{i+1}}y_i(a_i) - y_{i+1}(a_i)\right] -\right.$$

$$\left.-\delta(x-a_i)\left[\frac{J_i}{J_{i+1}}y_i'(a_i) - y_{i+1}'(a_i)\right]\right]; \qquad (8)$$

где x – безразмерная координата, представляющая собою отношение осевой координаты к ее длине,

a_i – безразмерная координата точек сопряжения соседних участков балки,

$$y_1(x) = C_1\theta_1(k_1x) + C_2\zeta_1(k_1x) + C_3\theta_2(k_1x) +$$

$$+ C_4\zeta_2(k_1x) + y_r(k_1x);$$

$$y_1'(x) = C_1k_1\Phi_1(k_1x) + C_2k_1\varphi_1(k_1x) + C_3k_1\varphi_2(k_1x) +$$

$$+ C_4k_1\Phi(k_1x) + y_r'(k_1x);$$

$4k_1^4 = \frac{\beta_1 l^4}{EJ_1}$, где β_1 – коэффициент жесткости основания;

$$\theta_{1,2} = e^{\pm k_1 x}\cos k_1 x; \qquad \zeta_{1,2} = e^{+k_1 x}\sin k_1 x;$$

$$\varphi_{1,2} = e^{\pm k_1 x}(\cos k_1 x + \sin k_1 x); \quad \Phi_{1,2} = e^{\pm k_1 x}(\cos k_1 x - \sin k_1 x);$$

если $q_1(x) = \text{const}$, то $y_r(k_1 x) = \frac{q_1 l^4}{4k_1 EJ_1}$.

Решение дифференциального уравнения (8) $y(x)$ вместе с его производными $y'(x)$, $y^{\cdot}(x)$ и $y^{-}(x)$ можно записать следующим образом:

$$\begin{bmatrix} y\ (x) \\ y'\ (x \\ y^{\cdot}\ (x) \\ y^{-}\ (x) \end{bmatrix} = \sum_{i=1}^{N}\left[\eta(x - a_{i-1}) - \eta(x - a_i)\right]\left\{\left[\Phi(k_1 x)\right]\begin{bmatrix} C_1 \\ C_2 \\ C_3 \\ C \end{bmatrix} + \right.$$

$$\left. + \frac{l^4}{4k_1^4 EJ_1}\begin{bmatrix} q_1\ (x) \\ q_1'\ (x) \\ q_1^{\cdot}\ (x) \\ q_1^{-}\ (x) \end{bmatrix}\right\} - \frac{1}{2}\sum_{i=1}^{N-1}\sum_{p=1}^{1}\left[\eta(x - a_i) - \eta(x - a_1)\right] \times$$

$$\times \left[\Phi_{i+1} x)\right]\left[F(k_{i+1} x)\right]\left\{\left[\left[H(a_p)\right] + \left[G(a_p)\right]\right]\begin{bmatrix} C_1 \\ C_2 \\ C_3 \\ C_4 \end{bmatrix} + \right. \qquad (9)$$

$$\left. + \frac{l^4}{4Ek_{p+1}J_{p+1}}\begin{bmatrix} q_{p+1}^{-}(a_p) \\ q_{p+1}^{\cdot}(a_p) \\ q_{p+1}'(a_p) \\ q_{p+1}(a_p) \end{bmatrix} - \frac{l^4}{4Ek_p^4 J_p}\begin{bmatrix} q_p^{-}\ (a_p) \\ q_p^{\cdot}\ (a_p) \\ q_p'\ (a_p) \\ q_p\ (a_p) \end{bmatrix}\right\},$$

где $\eta(x - a_N) = 0$, $\eta(x - a_0) = 1$,

$$\left[\Phi(k_1 x)\right] = \begin{bmatrix} \theta_1 & \zeta_1 & \theta_2 & \zeta_2 \\ k_1\Phi_1 & k_1\varphi_1 & -k_1\varphi_2 & k_1\Phi_2 \\ -2k_1^2\zeta_1 & 2k_1^2\theta_1 & 2k_1^2\zeta_2 & -2k_1^2\theta_2 \\ -2k_1^3\varphi_1 & 2k_1^3\Phi_1 & 2k_1^3\Phi_2 & 2k_1^3\varphi_2 \end{bmatrix},$$

$$\left[\Phi(k_{i+1} x)\right] = \begin{bmatrix} \theta_1 & \zeta_1 & \theta_2 & \zeta_2 \\ k_{i+1}\Phi_1 & k_{i+1}\varphi_1 & -k_{i+1}\varphi_2 & k_{i+1}\Phi_2 \\ -2k_{i+1}^2\zeta_1 & 2k_{i+1}^2\theta_1 & 2k_{i+1}^2\zeta_2 & -2k_{i+1}^2\theta_2 \\ -2k_{i+1}^3\varphi_1 & 2k_{i+1}^3\Phi_1 & 2k_{i+1}^3\Phi_2 & 2k_{i+1}^3\varphi_2 \end{bmatrix}$$

$$\left[F(k_{p+1}a_p)\right] = \begin{bmatrix} -\varphi_2 & -2k_{p+1}\zeta_2 & 2k_{p+1}^2\Phi_2 & 4k_{p+1}^3\theta_2 \\ \Phi_2 & 2k_{p+1}\theta_2 & 2k_{p+1}^2\varphi_2 & 4k_{p+1}^3\zeta_2 \\ \Phi_1 & 2k_{p+1}\zeta_1 & -2k_{p+1}^2\varphi_1 & 4k_{p+1}^3\theta_1 \\ \varphi_1 & -2k_{p+1}\theta_1 & 2k_{p+1}^2\Phi_1 & 4k_{p+1}^3\zeta_1 \end{bmatrix},$$

$$\left[H(a_p)\right] = \begin{bmatrix} -2[]_{11} & 2[]_{12} & 2[]_{13} & 2[]_{14} \\ []_{21} & 2[]_{22} & 2[]_{23} & -2[]_{24} \\ []_{31} & []_{32} & -[]_{33} & []_{34} \\ -\tilde{\theta}_1 & \zeta_1-\tilde{\zeta}_1 & \theta_2-\tilde{\theta}_2 & \zeta_2-\tilde{\zeta}_2 \end{bmatrix},$$

$$[]_{11} = k_{p+1}^3\varphi_1 - k_p^{3\tilde{}}\varphi_1; \quad []_{12} = k_{p+1}^3\Phi_1 - k_p^{3\tilde{}}\Phi_1;$$

$$[]_{13} = k_{p+1}^3\Phi_2 - k_p^{3\tilde{}}\Phi_2; \quad []_{14} = k_{p+1}^3\varphi_2 - k_p^{3\tilde{}}\varphi_2;$$

$$[]_{21} = k_{p+1}^2\zeta_1 - k_p^{2\tilde{}}\zeta_1; \quad []_{22} = k_{p+1}^2\theta_1 - k_p^{2\tilde{}}\theta_1;$$

$$[]_{23} = k_{p+1}^2\zeta_2 - k_p^{2\tilde{}}\zeta_2; \quad []_{24} = k_{p+1}^2\theta_2 - k_p^{2\tilde{}}\theta_2;$$

$$[]_{31} = k_{p+1}\Phi_1 - k_p\tilde{\Phi}_1; \quad []_{32} = k_{p+1}\varphi_1 - k_p\tilde{\varphi}_1;$$

$$[]_{33} = k_{p+1}\varphi_2 - k_p\tilde{\varphi}_2; \quad []_{34} = k_{p+1}\Phi_2 - k_p\tilde{\Phi}_2;$$

$$\left[G(a_p)\right] = \begin{bmatrix} [\tilde{}]_{11} & [\tilde{}]_{12} & -[\tilde{}]_{13} & [\tilde{}]_{14} \\ \theta_1 - \frac{J_p}{J_{p+1}}\tilde{\theta}_1 & \zeta_1 - \frac{J_p}{J_{p+1}}\tilde{\zeta}_1 & \theta_2 - \frac{J_p}{J_{p+1}}\tilde{\theta}_2 & \zeta_2 - \frac{J_p}{J_{p+1}}\tilde{\zeta}_2 \\ 0 & 0 & 0 & 0 \\ 0 & 0 & 0 & 0 \end{bmatrix},$$

где

$$[\tilde{}]_{11} = k_{p+1}\Phi_1 - k_p\frac{J_p}{J_{p+1}}\tilde{\Phi}_1; \quad [\tilde{}]_{12} = k_{p+1}\varphi_1 - k_p\frac{J_p}{J_{p+1}}\tilde{\varphi}_1;$$

$$[\tilde{}]_{13} = k_{p+1}\varphi_2 - k_p\frac{J_p}{J_{p+1}}\tilde{\varphi}_2; \quad [\tilde{}]_{14} = k_{p+1}\Phi_2 - k_p\frac{J_p}{J_{p+1}}\tilde{\Phi}_2.$$

В матрицах $\left[H(a_p)\right]$ и $\left[G(a_p)\right]$ функции θ, ζ, φ и Φ

соответствуют аргументу $k_{p+1}a_p$, а функции $\tilde{\theta}$, $\tilde{\zeta}$, $\tilde{\varphi}$ и $\tilde{\Phi}$ - аргументу k_pa_p. Например, $\varphi_1 = \varphi_1(k_{p+1}a_p)$, $\tilde{\varphi}_1 = \varphi_1(k_pa_p)$.

Произвольные постоянные $C_1 - C_4$ определяются из граничных условий на краях балки.

Если балка симметрична, а также симметричны нагрузки и граничные условия, уравнение (9) может быть преобразовано к более простому виду. Для этого следует учесть, что функция (8) переписана следующим образом:

$$y_1(x) = C_1\bar{\theta}_1(k_1x) + C_2\bar{\zeta}_1(k_1x) + C_3\bar{\theta}_2(k_1x) + C_4\bar{\zeta}_2(k_1x) + y_r(k_1x), \tag{10}$$

где

$$\bar{\theta}_1(k_1x) = chk_1x\cdot cosk_1x, \quad \bar{\theta}_1' = k_1\bar{\Phi}_1(k_1x), \quad \bar{\Phi}_1(k_1x) = \bar{\theta}_2 - \bar{\zeta}_1,$$

$$\bar{\zeta}_1(k_1x) = chk_1x\cdot sink_1x, \quad \bar{\zeta}_1' = k_1\bar{\varphi}_1(k_1x), \quad \bar{\varphi}_1(k_1x) = \bar{\zeta}_2 - \bar{\theta}_1,$$

$$\bar{\theta}_2(k_1x) = shk_1x\cdot cosk_1x, \quad \bar{\theta}_2' = k_1\bar{\varphi}_2(k_1x), \quad \bar{\varphi}_2(k_1x) = \bar{\theta}_1 - \bar{\zeta}_2,$$

$$\bar{\zeta}_2(k_1x) = shk_1x\cdot cosk_1x, \quad \bar{\zeta}_2' = k_1\bar{\Phi}_2(k_1x), \quad \bar{\Phi}_2(k_1x) = \bar{\zeta}_1 - \bar{\theta}_2.$$

Поскольку функции $\bar{\theta}_1(k_1x)$ и $\bar{\zeta}_2(k_1x)$ - четные, а функции $\bar{\zeta}_1(k_1x)$ и $\bar{\theta}_2(k_1x)$ - нечетные, то в случае симметрии нагрузки и конструкции, выбирая начало отсчета в середине балки, необходимо в формуле (10) положить $C_2 = C_3 = 0$.

Тогда с учетом введенных обозначений уравнение (9) сохранит свой вид, а матрицы, входящие в это уравнение, запишутся в такой форме:

$$\left[\bar{\Phi}(k_1x)\right] = \begin{bmatrix} \bar{\theta}_1 & 0 & 0 & \bar{\zeta}_2 \\ k_1\bar{\Phi}_1 & 0 & 0 & k_1\bar{\Phi}_2 \\ -2k_1^2\bar{\zeta}_2 & 0 & 0 & 2k_1^2\bar{\theta}_1 \\ -2k_1^3\bar{\Phi}_2 & 0 & 0 & 2k_1^3\bar{\varphi}_1 \end{bmatrix},$$

$$\left[\bar{\Phi}(k_{i+1}x)\right] = \begin{bmatrix} \bar{\theta}_1 & \bar{\zeta}_1 & \bar{\theta}_2 & \bar{\zeta}_2 \\ k_{i+1}\bar{\Phi}_1 & k_{i+1}\bar{\varphi}_1 & k_{i+1}\bar{\varphi}_2 & k_{i+1}\bar{\Phi}_2 \\ -2k_{i+1}^2\bar{\zeta}_2 & 2k_{i+1}^2\bar{\theta}_2 & -2k_{i+1}^2\bar{\zeta}_1 & 2k_{i+1}^2\bar{\theta}_1 \\ -2k_{i+1}^3\bar{\Phi}_2 & 2k_{i+1}^3\bar{\varphi}_2 & -2k_{i+1}^3\bar{\varphi}_1 & 2k_{i+1}^3\bar{\Phi}_1 \end{bmatrix}.$$

$$\left[\bar{F}(k_{P+1}a_P)\right] = 2\begin{bmatrix} \bar{\Phi}_1 & 2_{P+1}\bar{\zeta}_2 & -2k^2_{P+1}\bar{\Phi}_2 & 4k^3_{P+1}\bar{\theta} \\ \bar{\varphi}_1 & 2_{P+1}\bar{\theta}_2 & 2k^2_{P+1}\bar{\varphi}_2 & 4k^3_{P+1}\bar{\zeta} \\ -\bar{\varphi}_2 & -2_{P+1}\bar{\zeta}_1 & 2k^2_{P+1}\bar{\varphi}_1 & -4k^3_{P+1}\bar{\theta} \\ -\bar{\Phi}_2 & 2_{P+1}\bar{\theta}_1 & -2k^2_{P+1}\bar{\Phi}_1 & -4k^3_{P+1}\bar{\zeta} \end{bmatrix},$$

$$\left[\bar{H}(a_P)\right] = \begin{bmatrix} -2[k^3_{P+1}\bar{\Phi}_2 - k^3_P\bar{\Phi}^*_2] & 0 & 0 & 2[k^3_{P+1}\bar{\Phi}_1 - k^3_P\bar{\Phi}^*_1] \\ -2[k^2_{P+1}\bar{\zeta}_2 - k^2_P\bar{\zeta}^*_2] & 0 & 0 & 2[k^2_{P+1}\bar{\theta}_1 - k^2_P\bar{\theta}^*_1] \\ k_{P+1}\bar{\Phi}_1 - k_P\bar{\Phi}^*_1 & 0 & 0 & k_{P+1}\bar{\Phi}_2 - \bar{\Phi}^*_2 \\ \bar{\theta}_1 - \bar{\theta}^*_1 & 0 & 0 & \bar{\zeta}_2 - \bar{\zeta}^*_2 \end{bmatrix}$$

$$\left[\bar{G}(a_P)\right] = \frac{1}{J_{P+1}}\begin{bmatrix} J_{P+1}k_{P+1}\bar{\Phi}_1 - k_PJ_P\bar{\Phi} & 0 & 0 & J_{P+1}k_{P+1}\bar{\Phi}_2 - k_PJ_P\bar{\Phi}^*_2 \\ J_{P+1}\bar{\theta}_1 - J_P\bar{\theta}^*_1 & 0 & 0 & J_{P+1}\bar{\zeta}_2 - J_P\bar{\zeta}^*_2 \\ 0 & 0 & 0 & 0 \\ 0 & 0 & 0 & 0 \end{bmatrix}.$$

Здесь без звездочки даются функции аргумента $k_{P+1}a_P$, а со звездочкой – аргумента k_Pa_P.

В качестве примера рассмотрим консольную балку (фиг.1) на упругом основании, состоящую из трех участков (фиг.3).

Результаты вычисления прогиба и изгибающего момента приведены на фиг.4.

Подобным же образом аппарат обобщенных функций применяется и при решении задач динамики и устойчивости сооружений, а также в теории пластин и оболочек [1–6].

Изложенный в статье метод расчета является первым этапом в формированиии новых подходов в преподавании курсов сопротивления материалов и строительной механики.

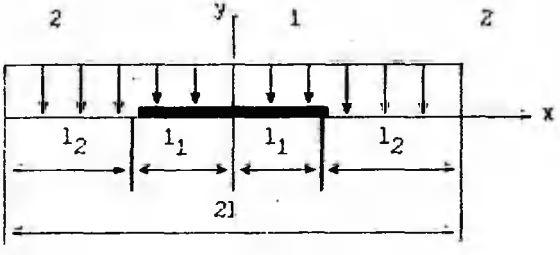

Фиг.3

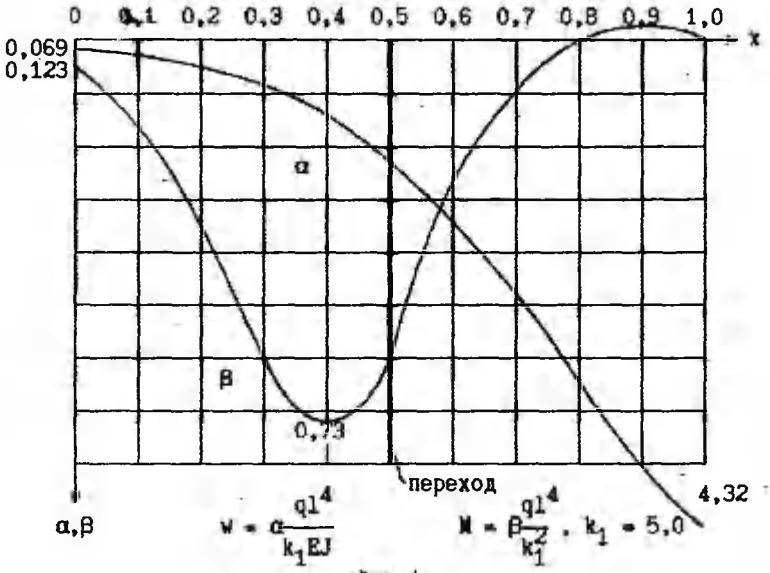

Фиг.4

ЛИТЕРАТУРА

1. Арясов Г.П, Снитко А.Н., Соколов Е.В., Расчет гофрированных оболочек типа сильфона методом обобщенных функций. Уч. зап. Тартуск. ун-та, 1983, 659, 88-94.
2. Арясов Г.П., Снитко А.Н., Соколов Е.В., Методы расчета слоистых гофрированных оболочек. Уч. зап. Тартуск. ун-та, 1985, 721, 94-101.
3. Арясов Г., Снитко А., Соколов Е., Расчет составных конструкций с помощью обобщенных функций. Уч. зап. Тартуск. ун-та, 1987, 772, 158-164.
4. Арясов Г.,Снитко А., Соколов Е., Метод дополнительных частных решений к расчету составных оболочек. Уч. зап. Тартуск. ун-та,1989, 853, 137-143.
5. Королев В.М., Слепов Б.Н., Соколов Е.В., Метод последовательного интегрирования дифференциальных уравнений пластин и оболочек. Строит. мех. и расчет сооружений. Межвуз. темат.сб.тр.,Л., ЛИСИ, 1980, 45-51.
6. Королев В.М., Слепов Б.Н., Соколов Е.В., Применение обобщенных функций к построению аналитических решений для составных оболочек и пластин. Строит .мех. сооружений. Межвуз.сб.тр., Л., ЛИСИ, 1981, 54-60.

7. Снитко А.Н., Соколов Е.В., Методы нахождения фундаментальных решений для дифференциальных уравнений теории оболочек вращения. Сб."Сопрот. матер.и теория сооружений", Киев, Будивельник, 1984, 44, 47-51.

APPLICATION OP GENERALIZED FUNCTIONS FOR THE CALCULATION OP COMPOUND BEAMS ON THE ELASTIC FOUNDATION

Gennadi Aryaeov, Aleksandr Snitko, Evgeni Sokolov
Tallinn Technical University

Summary

In this paper the calculation of compound beams on the elastic foundation is considered. Application of them will considerably simplify the solution of the problem. Numerical example has been given. Method of calculation, proposed in the present paper, will be the first stage in forming a new approach in mechanics of deforming bodies.

C O N T E N T S